Iranian Journal of Numerical Analysis and Optimization

Volume 7 , Number 2

Summer 2017

Serial Number: 12

Ferdowsi University of Mashhad, Iran

In the Name of God

Iranian Journal of Numerical Analysis and Optimization (IJNAO)

This journal is authorized under the registration No. 174/853 dated 1386/2/26, by the Ministry of Culture and Islamic Guidance.

Volume 7, Number 2, Summer 2017

ISSN: 2423-6977

Publisher: Faculty of Mathematical Sciences, Ferdowsi University of Mashhad

Published by: Ferdowsi University of Mashhad Press

Circulation: 100

Address: Iranian Journal of Numerical Analysis and Optimization

Faculty of Mathematical Sciences, Ferdowsi University of Mashhad

P.O. Box 1159, Mashhad 91775, Iran.

Tel. : +98-51-38806222 , **Fax:** +98-51-38807358

E-mail: mjms@um.ac.ir

Website: http://ijnao.um.ac.ir

This journal is indexed by:

- Zentralblatt
- ISC
- SID

به اطلاع کلیه محققان، پژوهشگران، اساتید ارجمند، دانشجویان تحصیلات تکمیلی و نویسندگان محترم می رساند که نشریه ایرانی آنالیز عددی و بهینه سازی - IJNAO - طبق مجوز شماره ۳/۱۸/۵۴۸۹۱۳/ مورخه ۱۳۹۲/۱۰/۲۵ مدیر کل محترم سیاست گذاری و برنامه ریزی امور پژوهشی وزارت علوم، تحقیقات و فناوری، علمی – پژوهشی میباشد.
بر اساس نامه شماره ۹۲/۱۵۳۶/پ مورخه ۱۳۹۲/۱۱/۲۱ سرپرست محترم معاونت پژوهشی وفناوری پایگاه استنادی علوم جهان اسلام، نشریه ایرانی آنالیز عددی و بهینه سازی در پایگاه ISC نیز نمایه می شود.

Iranian Journal of Numerical Analysis and Optimization

Volume 7, Number 2, Summer 2017

Ferdowsi University of Mashhad - Iran

Iranian Journal of Numerical Analysis and Optimization

This journal is published under the auspices of Ferdowsi University of Mashhad

---

* Full Professor

** Associate Professor

We would like to acknowledge the help of Narjes khatoon Zohorian in the preparation of this issue.

Letter from the Editor in Chief

I would like to welcome you to the Iranian Journal of Numerical Analysis and Optimization (IJNAO). This journal is published biannually and supported by the Faculty of Mathematical Sciences at the Ferdowsi University of Mashhad. Faculty of Mathematical Sciences with three centers of excellence and three research centers is well-known in mathematical communities in Iran.

The main aim of the journal is to facilitate discussions and collaborations between specialists in applied mathematics, especially in the fields of numerical analysis and optimization, in the region and worldwide.

Our vision is that scholars from different applied mathematical research disciplines, pool their insight, knowledge and efforts by communicating via this international journal.

In order to assure high quality of the journal, each article is reviewed by subject-qualified referees.

Our expectations for IJNAO are as high as any well-known applied mathematical journal in the world. We trust that by publishing quality research and creative work, the possibility of more collaborations between researchers would be provided. We invite all applied mathematicians especially in the fields of numerical analysis and optimization to join us by submitting their original work to the Iranian Journal of Numerical Analysis and Optimization.

Mohammad Hadi Farahi

Contents

Iranian Journal of Numerical Analysis and Optimization
Vol. 7, No. 2, (2017), pp 1–14
DOI:10.22067/ijnao.v7i2.52815

Image magnification by least squares surfaces

A.M. Esmaili Zaini, G.B. Loghmani*, and A.M. Latif

Abstract

Image magnification is one of the current issues of image processing in which keeping the quality and structure of images is the main concern. In image magnification, it is necessary to insert information in extra pixels. Adding information to an image should be compatible with the image structure without making artificial blocks. In this research, extra pixels are estimated using the surface of least squares, and all the pixels are reviewed according to the suggested edge-improving algorithm. The suggested method keeps the edges and minimizes the magnified image opacity and the artificial blocks. Numerical results are presented by using PSNR and SSIM fidelity measures and compared to some other methods. The average PSNR of the original image and image zooming is 32.79 which it shows that image zooming is very similar to the original image. Experimental results show that the proposed method has a better performance than others and provides good image quality.

Keywords: Image Magnification; Least Squares Surface; Interpolation.

1 Introduction

Image magnification is, indeed, image resolution increasing to achieve a higher- quality image. It plays an important role in image processing and

*Corresponding author
Received 1 June 2016; revised 14 August 2016; accepted 19 October 2016
A.M. Esmaili Zaini
Department of Applied Mathematics, Faculty of Mathematical Sciences, Yazd University, Yazd , Iran. e-mail: esmailizaini@stu.yazd.ac.ir

G.B. Loghmani
Department of Applied Mathematics, Faculty of Mathematical Sciences, Yazd University, Yazd , Iran. e-mail: loghmani@yazd.ac.ir

A.M. Latif
Department of Computer Engineering, Faculty of Engineering, Yazd University, Yazd , Iran. e-mail: alatif@yazd.ac.ir

machine vision. Image magnification has various applications in electronic publishing industries, digital cameras, medical imaging, images on the web, license plate recognition, and face recognition systems in law functions.

Recent studies indicate that the main emphasis is on the visual quality of images in many applications. Resolution edges and lack of blur and additional artifacts are two important factors in image quality. Many enlarging image algorithms use interpolation methods. Interpolation means to find a set of unknown pixel values in a set of known pixel values in the picture. In magnification, the following few basic parameters affect the image quality [11]:

1- An efficient magnification method should preserve the edges and boundaries.

2- The method should not produce undesirable constant piecewise or blocks of other regions.

3- The magnification method should be computationally efficient but not too dependent on the internal parameters of the image.

Traditional technologies in image magnification use linear interpolation for high-resolution samples. Pixel replication, bilinear interpolation, quadratic interpolation, bi-cubic interpolation, and spline interpolation are some of these methods [6, 8, 17]. These methods tend to smooth edges or produce blocky interpolated images with staircase edges. Therefore, the output of these methods produces blurred images. This indicates the inability of linear technologies to transfer new information to an image.

One of the features of the two linear interpolation methods is that, in the magnification ratio, artificial blocks and visual effects are undesirable, but edges are preserved at an acceptable level. In bi-cubic interpolation method with a high zoom ratio, artificial blocks and undesirable visual effects are lower, and the edges are preserved. Although determining the image quality is not easy in this method, for image magnification, the quadratic interpolation is better than bilinear interpolation, bi-cubic interpolation is better than quadratic interpolation, and spline interpolation is better than bi-cubic interpolation [16].

In recent years, nonlinear interpolation methods have been used to reform linear methods for improving image quality and solving the blur problem. The change of non-linear methods depends on the interpolation method. This means that the performance of these methods with sharp edges is different from their performance on soft tissues, while linear methods with all the pixels act in the same way [1, 3, 7]. In order to maintain the image quality and edges in non-linear methods, estimation methods of a subset of edge pixels [1], resampling and optimization parameters, implicit interpolation, and straight edges have been used [4, 14, 22].

In [22], a statistical method that tunes interpolation coefficients according to local edge structures is proposed. The technique of [4] uses a modified bilinear method, where the interpolation error theorem in an edge-adaptive fashion.

In [21], an edge-directed nonlinear interpolation technique is presented through directional filtering and data fusion. This algorithm interpolates a missing pixel in multiple directions, and then fuses the directional interpolation results by linear minimum mean square-error estimation.

In [2], the local adaptive magnification (LAZ) method uses the discontinuities information or sharp brightness changes, finds edges in different directions by taking two threshold values, and estimates the unknown pixels with respect to the edge pixels.

In [20], the artificial neural networks methods uses for doing zoom operations on digital images.

In [10], presents a nonlinear image interpolation algorithm that is based on the moving least squares technique. This methods ability to image zooming and preserving edge features.

In this paper, another least squares surface method is suggested, in which necessary pixels are obtained by calculating their coefficients using the least squares theory and edge-directed algorithms.

This paper continues as follows. In the second part, quadratic surfaces and the theory of least squares will be discussed. In the third part, the least square planes, suggested algorithms, and evaluation parameters will be proposed. The fourth section compares the results of implementation by other methods. In the last section, conclusions and recommendations will be presented.

2 Quadratic surfaces and least squares theory

The purpose of a quadratic surface in R^3 space composed of x, y and z is formed as equation (1), in which none of the coefficients A, B, C, D, E and F is zero. This equation called quadratic surfaces is an extension of a cone in R^2 space.

$$Ax^2 + By^2 + Cz^2 + Dxy + Exz + Fyz + Gx + Hy + Iz + J = 0. \tag{1}$$

Without losing any generality, the coefficients of product terms can be zero by a three-dimensional rotation, and convert equation (1) into a conventional or canonical form by a transfer, whose diagram is recognizable. The canonical equation for a quadratic surface is as in (2), the most famous sections of which are elliptical, hyperbolic, parabolic, and conic sections.
For example, the overall shape of an elliptical equation and parabolic surface are introduced according to equations (3) and (4), respectively:

$$Ax^2 + By^2 + Cz^2 + Gx + Hy + Iz + J = 0 \tag{2}$$
$$Ax^2 + By^2 + Cz^2 + Gx + Hy + Iz = 1 \tag{3}$$
$$Ax^2 + By^2 + +Gx + Hy = Iz \tag{4}$$

2.1 Least Squares Theory

Suppose $f(x)$ is a continuous function on the $[a, b]$ interval and $p(x)$ is a polynomial of the maximum degree n that is defined according to equation (5), in which c_i constants for $i = 0, 1, 2, \dots, n$ are real numbers.

$$p\left(x\right) = \sum_{i=0}^{n} c_i x^i. \tag{5}$$

The problem of approximating function f(x) by polynomial $p(x)$ can be considered by finding c_i constants for $i = 0, 1, 2, \dots, n$ to minimize $||f(x) - p(x)||$. The purpose of $||.||$ is Euclidean norms. To calculate the coefficients of c_i, Theorem 1 is used.

Theorem 1. *Let $f\left(x_1, x_2, \dots, x_n\right)$ be a function of n variables which has a local extremum at the point $(a_1, a_2, \dots, a_n)$. Then either f is non- differentiable at $(a_1, a_2, \dots, a_n)$, or it is differentiable at $(a_1, a_2, \dots, a_n)$ and $\nabla f(a_1, a_2, \dots, a_n) = 0$ or $\frac{\partial f}{\partial x_i}(a_1, a_2, \dots, a_n) = 0, \quad i = 0, 1, 2, \dots, n$*

If a set of data are in the form of $\{(x_i, y_i)\,|i = 1, 2, \dots, N\}$ and the suitable mathematical model for data relationship is a line, then the general problem is finding the best least squares line. A mathematical model for the relationship of the data is the polynomial of degree n in general for which $n < N.$, Then the problem is to find the least squares polynomial. Therefore, if the discrete data based on Euclidean norms are considered as in expression (6) according to Theorem 1, equation (7) should be established.

$$E = \sum_{i=1}^{N} \left(y_i - \left(c_0 + c_1 x_i + \ldots + c_n {x_i}^n\right)\right)^2 \tag{6}$$
$$\frac{\partial E}{\partial c_j} = 0, \quad j = 0, 1, 2, \dots, n. \tag{7}$$

After calculating the partial derivatives and simplifying them, the linear system of $(n + 1)$ equations called normal form is obtained as in (8) for distinct x_i, for $i = 1, 2, \dots, N$. This linear system of equations has a unique solution.

$$\begin{cases} c_0\sum_{i=1}^{N} x_i^0 + c_1\sum_{i=1}^{N} x_i^1 + \ldots + c_n\sum_{i=1}^{N} x_i^n = \sum_{i=1}^{N} y_i x_i^0 \\ c_0\sum_{i=1}^{N} x_i^1 + c_1\sum_{i=1}^{N} x_i^2 + \ldots + c_n\sum_{i=1}^{N} x_i^{n+1} = \sum_{i=1}^{N} y_i x_i^1 \\ \quad\vdots \qquad\qquad \vdots \qquad\qquad\qquad \vdots \qquad\qquad \vdots \\ c_0\sum_{i=1}^{N} x_i^n + c_1\sum_{i=1}^{N} x_i^{n+1} + \ldots + c_n\sum_{i=1}^{N} x_i^{2n} = \sum_{i=1}^{N} y_i x_i^n \end{cases} \tag{8}$$

If $f(x, y, z) = 0$ is a surface equation in the R^3 space, z depends on x and y. In addition, $\{(x_i, y_i, z_i)\,|i = 1, 2, \ldots, N\}$ is a set of discrete data obtained from the process of data collection, non of which lie on a known surface, either elliptical, or parabolic, or plane. Then according to 1 and the sum squares error, appropriate coefficients can be calculated.

Suppose $z = Ax + By + C$ is a surface equation in the R^3 space for $\{(x_i, y_i, z_i)\,|i = 1, 2, \ldots, N\}$ points. To obtain the surface of least squares Theorem 1 and error (9), the coefficients of A, B, C are calculated after solving normal equations (10).

$$E = \sum_{i=1}^{N} \left(Ax_i + By_i + C - z_i\right)^2 \tag{9}$$

$$\begin{cases} A\sum_{i=1}^{N} x_i^2 + B\sum_{i=1}^{N} x_i y_i + C\sum_{i=1}^{N} x_i = \sum_{i=1}^{N} z_i x_i \\ A\sum_{i=1}^{N} x_i y_i + B\sum_{i=1}^{N} y_i^2 + C\sum_{i=1}^{N} y_i = \sum_{i=1}^{N} y_i z \\ A\sum_{i=1}^{N} x_i + B\sum_{i=1}^{N} y_i + C\sum_{i=1}^{N} 1 = \sum_{i=1}^{N} z_i. \end{cases} \tag{10}$$

If $Ax^2 + By^2 + Cx + Dy = 1 - z^2$ is an elliptical surface in the space R^3 and $\{(x_i, y_i, z_i)\,|i = 1, 2, \ldots, N\}$ points are provided, calculation of the elliptical least-squares surface can be done according to Theorem 1 and deviation (11), with coefficients A, B, C, D achieved after solving linear device (12).

$$E = \sum_{i=1}^{N} \left(Ax_i^2 + By_i^2 + Cx_i + Dy_i + z_i^2 - 1\right)^2 \tag{11}$$

$$\begin{cases} A\sum\limits_{i=1}^{N} x_i^4 + B\sum\limits_{i=1}^{N} x_i^2y_i^2 + C\sum\limits_{i=1}^{N} x_i^3 + D\sum\limits_{i=1}^{N} y_ix_i^2 = \sum\limits_{i=1}^{N} x_i^2\left(1-z_i^2\right) \\ A\sum\limits_{i=1}^{N} x_i^2y_i^2 + B\sum\limits_{i=1}^{N} y_i^4 + C\sum\limits_{i=1}^{N} x_iy_i^2 + D\sum\limits_{i=1}^{N} y_i^3 = \sum\limits_{i=1}^{N} y_i^2\left(1-z_i^2\right) \\ A\sum\limits_{i=1}^{N} x_i^3 + B\sum\limits_{i=1}^{N} x_iy_i^2 + C\sum\limits_{i=1}^{N} x_i^2 + D\sum\limits_{i=1}^{N} y_ix_i = \sum\limits_{i=1}^{N} x_i\left(1-z_i^2\right) \\ A\sum\limits_{i=1}^{N} x_i^2y_i + B\sum\limits_{i=1}^{N} y_i^3 + C\sum\limits_{i=1}^{N} x_iy_i + D\sum\limits_{i=1}^{N} y_i^2 = \sum\limits_{i=1}^{N} y_i\left(1-z_i^2\right). \end{cases} \tag{12}$$

Similarly, if $Ax^2 + By^2 + Cx + Dy = z$ is parabolic surface in the space R^3 and $\{(x_i, y_i, z_i)\,|i = 1, 2, \ldots, N\}$ points are provided, calculation of the parabolic least-squares surface can be done according to Theorem 1 and deviation (13), with coefficients A, B, C, D achieved after solving linear device (14).

$$E = \sum_{i=1}^{N} \left(Ax_i^2 + By_i^2 + Cx_i + Dy_i - z_i\right)^2, \tag{13}$$

$$\begin{cases} A\sum\limits_{i=1}^{N} x_i^4 + B\sum\limits_{i=1}^{N} x_i^2y_i^2 + C\sum\limits_{i=1}^{N} x_i^3 + D\sum\limits_{i=1}^{N} y_ix_i^2 = \sum\limits_{i=1}^{N} x_i^2z_i \\ A\sum\limits_{i=1}^{N} x_i^2y_i^2 + B\sum\limits_{i=1}^{N} y_i^4 + C\sum\limits_{i=1}^{N} x_iy_i^2 + D\sum\limits_{i=1}^{N} y_i^3 = \sum\limits_{i=1}^{N} y_i^2z_i \\ A\sum\limits_{i=1}^{N} x_i^3 + B\sum\limits_{i=1}^{N} x_iy_i^2 + C\sum\limits_{i=1}^{N} x_i^2 + D\sum\limits_{i=1}^{N} y_ix_i = \sum\limits_{i=1}^{N} x_iz_i \\ A\sum\limits_{i=1}^{N} x_i^2y_i + B\sum\limits_{i=1}^{N} y_i^3 + C\sum\limits_{i=1}^{N} x_iy_i + D\sum\limits_{i=1}^{N} y_i^2 = \sum\limits_{i=1}^{N} y_iz_i. \end{cases} \tag{14}$$

Here, the linear equations system can be obtained for the quadratic surface.

3 Least Squares Surfaces and Image Magnification

In the image magnification, some new pixels are placed in the original pixels of the image. The purpose of magnification is to determine new pixels, which are determined based on their neighbouring pixels. There are two types of neighbourhood in two-dimensional images, which are known as the 4 and 8 cell. Neighbourhoods are shown in Figure 1.

In most of proposed methods, magnification rate is tried to be squared, or to a power of two, but it should be noted that the algorithm presented here is used for every magnification rate.

The first stage is the simplest one and requires expanding the source $n \times n$ pixels image onto a regular grid of size $(2n-1) \times (2n-1)$. More precisely, if

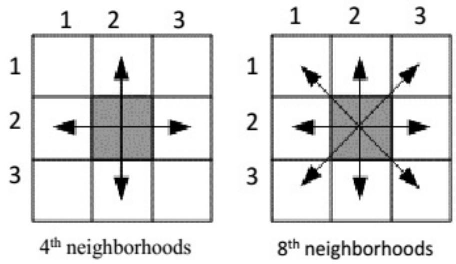

Figure 1: Types of neighbourhood.

$S(i,j)$ denotes the pixels in the i^{th} row and j^{th} column of the source image and $Z(l,k)$ denotes the magnified image pixel in the l^{th} row and k^{th} column in the zoomed picture, the f function [5] puts the original image pixel in the interlaced places of the new image:

$$\begin{aligned} &f : S \to Z \\ &f\left(S\left(i,j\right)\right) = Z\left(2i-1, 2j-1\right) \qquad i,j = 1,2,\ldots,n \end{aligned}$$

The result is shown in Figure 2. The original image pixel is indicated by symbol $\bullet$, and the other pixels which must be estimated have been identified by $11, 10$ and 01. To estimate the pixel values, the multi-stage least squares method is used along with a review of the surfaces.

In this algorithm, a new pixel value is estimated with its four neighbourhoods in the corner (pixel 11) by the proposed method. Since, all the neighbourhoods on the central pixels are equal in term of distance from the central pixel, all of them are attributed the same weight. The results are shown in Figure 3, and $\blacksquare$ is replaced by the estimated pixels. In the next stage, the pixels indicated by 1 are estimated by their four neighbourhoods. These pixels have two main pixels in the left and the right and two estimated pixels up and down the neighbourhoods. In estimation, pixels that are indicated with number 01 have the weight of 1, and the estimated pixels assigned with the weight of 0.5. Pixels with number 10 are estimated in the same manner. The results are shown in Figure (4), in which the symbols $\square$ and $\diamondsuit$ are replaced by the estimated pixels.

3.1 Least squares surface algorithm

In this algorithm, a point ($\bullet$) refers to the pixel coordinates of the image whose brightness and number of rows and columns are considered as a point in a three-dimensional space.

●	01	●	01	●
10	11	10	11	10
●	01	●	01	●
10	11	10	11	10
●	01	●	01	●

Figure 2: Copying value to the magnified image.

●	01	●	01	●
10	▪	10	▪	10
●	01	●	01	●
10	▪	10	▪	10
●	01	●	01	●

Figure 3: Estimation of neighbourhood pixels.

●	□	●	□	●
◇	▪	◇	▪	◇
●	□	●	□	●
◇	▪	◇	▪	◇
●	□	●	□	●

Figure 4: Estimation of neighbourhood pixels.

To estimate the required pixels in image magnification based on four neighbourhoods, initially by selection the four points and solving the linear least-squares surface equation, the desired pixel is estimated. It should be noted that, two adjacent pixels are used in the rows and columns of pixels to approximate the first and last of the average.

The proposed algorithm steps are as follows:

Step 1. Establish a linear system according to the chosen least-square surface.

Step 2. Solve linear equations and calculating surface coefficients.

Step 3. Estimate the desired pixel by replacing the number of rows and columns on the selective surface.
Step 4. Repeat steps 1 to 3 in three stages according to the zooming algorithm and estimating the required pixel
Step 5. Review all the estimated pixels based on the conducted sub-algorithm of the edge (3-2).

3.2 The modified sub-algorithm of the image edges

After estimating all the required image pixels, all estimated pixels are reviewed to improve the edges (Figure.5) based on the following conditions. A, B, C, and d are the main pixels, and $X, Y2, Y1, Z1$, and $Z2$ are the estimated pixels. The advantage of the sub-algorithm is the lack of any provinces for edges. The proposed algorithm steps are as follows:
Step 1. If $|A - D| > |B - C|$, then $X \leftarrow \frac{B+C}{2}$. In fact, the edge is in the northeast-southwest direction.
Step 2. If $|A - D| < |B - C|$, then $X \leftarrow \frac{A+D}{2}$. In fact, the edge is in the northwest-southeast direction.
Step 3. If $(A - D)(B - C) > 0$, then $Y1 \leftarrow \frac{A+B}{2}$ and $Y2 \leftarrow \frac{C+D}{2}$. In fact, the edge is in the north-south direction.
Step 4. If $(A - D)(B - C) < 0$, then $Z1 \leftarrow \frac{A+C}{2}$ and $Z2 \leftarrow \frac{B+D}{2}$. In fact, the edge is in the west-east direction.

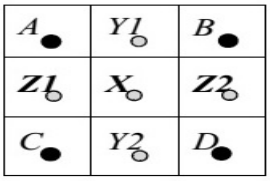

Figure 5: Design for modifying the image edge.

3.3 Assessment criteria

To compare two images in terms of their similarity, PSNR and SSIM criteria are used. The PSNR value is bigger and the SSIM is closer to 1, the images have more conformity [18, 19]. The PSNR criterion is calculated based on equation (15) and (16):

$$PSNR = 10 * Log_{10}\left(\frac{MAX_I^2}{MSE}\right)(dB) \tag{15}$$

$$MSE = \frac{1}{mn}\sum_{i=0}^{m-1}\sum_{j=0}^{n-1}\left[I(i,j) - K(i,j)\right]^2 \tag{16}$$

where $I(i,j)$ and $K(i,j)$ are the main image pixels and the estimated image, respectively, and MAX_I is the maximum image pixles.
SSIM criterion, which includes the image structural elements and measures the structural quality of the image as well as the similarity between the two images, has a value between 0 and 1. This means that 1 is the highest and 0 is the lowest similarity, which is calculated by equation (17).

$$SSIM(x,y) = \frac{(2\mu_x\mu_y + c_1)(2\sigma_{xy} + c_2)}{\left(\mu_x^2 + \mu_y^2 + c_1\right)\left(\sigma_x^2 + \sigma_y^2 + c_2\right)} \tag{17}$$

where μ , σ^2 and σ_{xy} are the average, variance, and covariance of the pixels in the image, respectively, and c_1 and c_2 are two unknown constants that prevent the fraction denominator from being zero.

4 Simulation results

To evaluate the proposed method, first, a digital image is considered as an original image, and then its size is reduced by removing alternative rows of columns by half, then, it is tried to make image size double using the proposed method and the other methods. As expected, the closer the degree of similarity is to the original image size, the algorithm has a better performance.

Implementation of the results of the suggested algorithm done in MATLAB. The results are presented in Tables 1 and 2. In Table 1, the PSNR criterion is used for zooming, and ten different and standard images [15] are applied according to Figure 6. Their dimensions all are 512×512. The results of the suggested least square plane (LSP) and least square ellipsoid (LSE) methods, bilinear interpolation (BIL) method, bi-cubic interpolation (BIC) method, and curvature interpolation (CIM) method [9] have been compared. The least difference of PSNR between LSP method and CIM method is 0.38, the most is 3.18, and its average is 1.71. Comparing LSE with CIM and PSNR scale, the minimum difference is 0.13, the maximum is 3.12, and the average is 1.52. With regard to each row and comparing the results, it can be concluded that the proposed method of LSP has a better performance than other methods on the selected image.

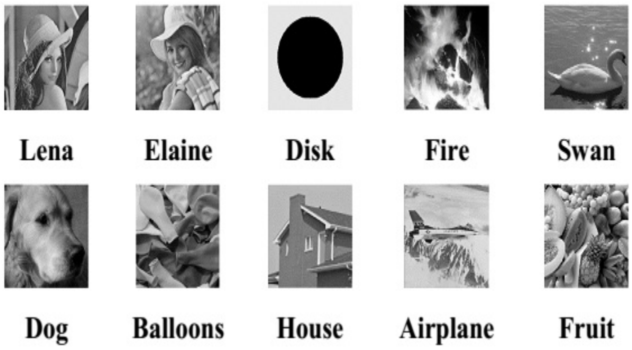

Figure 6: Different images and standards for image magnification.

Table 2 illustrates the results of comparing the suggested method and the other methods for the images in Figure 6, by SSIM criterion. The results show that the proposed method has a better performance than other methods with a good approximation. The minimum difference in SSIM for LSP by CIM is 0.0011, the maximum is 0.02, and the average is 0.0096. In a comparison of LSE method with CIM and SSIM criterion, the minimum difference is 0.001, the maximum is 0.099, and the average is 0.0095.

From a visual point of view, for example, the magnified image of Elaine is shown by LSP and LSE proposed methods, by BIL, BIC methods, as well as CIM method in Figure 7. Obviously, the images of the proposed method are more transparent and have less blur and good performance on the edges.

Figure 7: The results of Elaine's image magnification by the factor of 2 and using different methods.

Table 1: Comparison of the least square surface method and other methods by PSNR criterion.

Methods	BIL	BIC	CIM	Proposed method LSP	Proposed method LSE
lena	30.20	30.11	30.58	**33.47**	**33.34**
Elaine	31.26	31.08	31.49	**34.67**	**34.61**
Disk	30.94	30.82	31.56	**33.07**	**32.70**
Fire	31.66	31.71	31.82	**32.20**	**31.95**
Swan	31.19	30.74	31.44	**33.22**	**32.73**
Dog	31.83	31.37	32.05	**33.94**	**33.63**
Balloons	31.29	31.73	32.28	**33.52**	**34.07**
House	32.64	32.60	32.97	**34.00**	**33.83**
Airplane	29.70	29.59	30.12	**31.34**	**31.30**
Fruits	26.17	26.08	26.49	**28.44**	**28.20**
Average	30.69	30.58	31.08	**32.79**	**32.60**

Table 2: Comparison of the least square surface method and other methods by SSIM criterion.

Methods	BIL	BIC	CIM	Proposed method LSP	Proposed method LSE
lena	0.9504	0.9469	0.9514	**0.9714**	**0.9713**
Elaine	0.9536	0.9479	0.9578	**0.9589**	**0.9588**
Disk	0.9908	0.9908	0.9922	**0.9956**	**0.9953**
Fire	0.9770	0.9767	0.9779	**0.9857**	**0.9854**
Swan	0.9737	0.9727	0.9758	**0.98420**	**0.9841**
Dog	0.9701	0.9691	0.9708	**0.9814**	**0.9813**
Balloons	0.9815	0.9808	0.9856	**0.9893**	**0.9894**
House	0.9771	0.9763	0.9777	**0.9867**	**0.9866**
Airplane	0.9698	0.9696	0.9703	**0.9831**	**0.9831**
Fruits	0.9518	0.9513	0.9523	**0.9714**	**0.9712**
Average	0.9696	0.9682	0.9712	**0.9808**	**0.9807**

5 Conclusion

In this paper, a new method of the least squares surface has been used to enlarge images. Despite simple implementation and low computational complexity, this method provides more satisfactory results than bilinear interpolation methods, such as bicubic and curvature do. The study, has been conducted using one of the edge- improving techniques. The proposed method can be elaborated on in future studies through other edge- improving methods or nonlinear methods such as bivariate interpolation or radial basis functions interpolation with edge- shaving techniques.

References

1. Allebach, J. and Wong, P. W. *Edge-directed interpolation*, in Proc. IEEE Int. Conf. Image. Proc., 3 (1996), 707-710.

2. Battiato, S., Gallo, G. and Stanco, F. *A locally adaptive zooming algorithm for digital images,* Elsevier Science. Image and Vision Computing Journal, 20 (2002), 805-812.

3. Carrato, S. and Tenze, L. *A high quality 2X image interpolator*, IEEE Signal Process., 7 (2000),132-135.

4. Cha, Y. and Kim, S. *The error-amended sharp edge (ease) scheme for image magnification*, IEEE Trans. Image Process., 16 (2007), 1496-1505.

5. Gonzalez, R.C. and Woods, R.E., *Digital image processing,* Prentice Hall, 2008.

6. Hou, H.S. and Andrews, H.C. *Cubic splines for image interpolation and digital filtering,* IEEE Trans. Acoust., Speech, Signal Process., 26 (1978), 508-517.

7. Jensen, K. and Anastassion, D. *Subpixel edge localization and the interpolation of still images*, IEEE Trans. Image Process., 4 (1995), 285-295.

8. Keys, R.G. *Cubic convolution interpolation for digital image processing,* IEEE Trans. Acoust., Speech, Signal Process., 29 (1981), 1153-1160.

9. Kim, H., Cha, Y. and Kim, S. *Curvature interpolation method for image zooming,* IEEE Trans. Image Process., 20 (2011), 1895-1903.

10. Lee, Y.J. and Yoon, J. *Image zooming method using edge-directed moving least squares interpolation based on exponential polynomials,* Applied Mathematics and Computation, 269 (2015), 569-583.

11. Lee, Y.J. and Yoon, J. *Nonlinear image up-sampling method based on radial basis function interpolation,* IEEE Trans. Image Process., 19 (2010), 2682-2692.

12. Lehmann, T., Gnner, C. and Spitzer, K. *Survey: Interpolation methods in medical image processing,* IEEE Trans. Med. Imaging., 18 (1999), 1049-1075.

13. Li, M. and Nguyen, T.Q. *Markov random field model-based edge directed image interpolation,* IEEE Trans. Image Process., 17 (2008), 1121-1128.

14. Li, X. and Orchard, T. *New edge directed interpolation,* IEEE Trans. Image Process.,10 (2001), 1521-1527.

15. Online. Available:*www.freeimages.co.uk and sipi.usc.edu/database.*

16. Padmanabhan, S.A. and Chandramathi, S. *Image magnification using segmented polynomial interpolation in space*, European Journal of Scientific Research, 57 (2011), 447-453.

17. Thvenaz, P. , Blu, T. and Unser, M. *Interpolation revisited,* IEEE Trans. Med. Image., 19 (2000), 739-758.

18. Wang, Z. , Bovik, A.C., Sheikh H.R. and Simoncelli E.P. *Image quality assessment: From error visibility to structural similarity,* IEEE Trans. Image Process., 13 (2004), 600-612.

19. Wang, Z., Bovik, A.C., Sheikh, H.R., and Simoncelli, E.P. *The SSIM index for image quality assessment.* MATLAB implementation available online from: http://www. cns. nyu. edu/lcv/ssim, (2003), 23-66.

20. Youssef, D., Mohammed, B., Abdelmalek, A., Tarik, H. and El Miloud, J. *Zoom and Restoring of Digital Images with Artificial Neural Networks,* Computer Science and Engineering, 5 (2015),14-24.

21. Zhang, L. and Wu, X. *An edge-guided image interpolation algorithm via directional filtering and data fusion,* IEEE Trans. Image Process., 15 (2006), 2226-2238.

22. Zhang X. and Wu, X. *Image interpolation by adaptive 2-D autoregressive modeling and soft-decision estimation*, IEEE Trans. Image Process., 17 (2008), 887-896.

Iranian Journal of Numerical Analysis and Optimization
Vol. 7, No. 2, (2017), pp 15–37
DOI:10.22067/ijnao.v7i2.52085

Radial basis functions method for solving three-dimensional linear Fredholm integral equations on the cubic domains

M. Esmaeilbeigi*, F. Mirzaee and D. Moazami

Abstract

The main purpose of this article is to describe a numerical scheme for solving three-dimensional linear Fredholm integral equations of the second kind on the cubic domains. The method is based on interpolation by radial basis functions (RBFs) based on Gauss-Legendre nodes and weights. Error analysis is presented for this method. Finally, several examples are given and numerical examples are presented to demonstrate the validity and applicability of the method.

Keywords: Three-dimensional integral equation; Radial basis functions; Collocation method; Cubic domains.

1 Introduction

Consider the following three-dimensional linear Fredholm integral equation of the second kind

$$u(x,y,z) - \lambda \int_e^f \int_c^d \int_a^b K(x,y,z,r,s,t)u(r,s,t)drdsdt = h(x,y,z), (x,y,z) \in D, \quad (1)$$

*Corresponding author
Received 9 December 2015; revised 4 September 2016; accepted 16 November 2016
M. Esmaeilbeigi
Department of Mathematics, Faculty of Mathematical Sciences and Statistics, Malayer University, Malayer, Iran. e-mail: m.esmaeilbeigi@malayeru.ac.ir

F. Mirzaee
Department of Mathematics, Faculty of Mathematical Sciences and Statistics, Malayer University, Malayer, Iran. e-mail: f.mirzaee@malayeru.ac.ir

D. Moazami
Department of Mathematics, Faculty of Mathematical Sciences and Statistics, Malayer University, Malayer, Iran. e-mail: dmoazami@yahoo.com

where h and K are known functions, $u(x, y, z)$ is the unknown function to be determined, λ is a constant and D is an cubic domain.

Integral equations occur in a wide variety of physical applications. They are encountered in various fields of science and numerous applications such as: elasticity, plasticity, heat and mass transfer, oscillation theory, fluid dynamics, filtration theory, electrostatics, electrodynamics, game theory, control, queuing theory, electrical engineering, economics, medicine, etc. There are many different numerical methods for solving integral equations. Computational complexity of mathematical operations is the most important obstacle for solving integral equations in higher dimensions. The Nystrom method [15] and collocation method [5, 14, 29] are the most important approaches of the numerical solution of these integral equations.

To avoid the mesh generation, in recent years meshless techniques have attracted attention of researchers. In a meshless method, a set of scattered nodes are used instead of meshing the domain of the problem [6, 7, 26].

Among meshless methods, the radial basis functions (RBFs) method has become known as a powerful tool for the scattered data interpolation problem. The main advantage of radial basis functions is that they involve a single independent variable regardless of the dimension of the problem. One of the domain-type meshless methods, the so-called Kansa's method developed by Kansa in 1990 [20, 21], is obtained by directly collocating RBFs, particularly the multiquadric (MQ), for the numerical approximation of the solution. Kansa's method was recently extended to solve various ordinary and partial differential equations including the one-dimensional nonlinear Burgers equation [18] with shock wave, shallow water equations for tide and currents simulation [17], heat transfer problems [30], and free boundary problems [19,23].

Furthermore, the RBFs have been applied on the one-dimensional domains for solving linear second kind Fredholm and Volterra integral equations in [12], linear integro-differential equations in [13], nonlinear Volterra-Fredholm-Hammerstein integral equations in [25] and systems of nonlinear integral equations in [11]. Also, a numerical solution of two-dimensional Fredholm integral equations of the second kind on the square domains by Gaussian radial basis functions without the error analysis is introduced in [1].

In this paper, we will use the radial basis functions (RBFs) approximation for solving three-dimensional linear Fredholm integral equations of the second kind on cubic domains. The remainder of the paper is organized as follows: in Section 2, we show that how the radial basis functions are used to approximate the solution. In Section 3, we present a numerical method for solving the linear Fredholm integral equations of the second kind by the RBF approximation. In Section 4, error analysis for the proposed method is presented. Numerical examples are given in Section 5. Finally, we conclude the article in Section 6.

2 An outline of RBFs

The radial basis function (RBF) method for multivariate approximation is one of the most often applied tools in modern approximation theory due to spectral accuracy, flexibility with respect to geometry, dimensional independence and ease of implementation especially when the task is to interpolate scattered data in multi dimensions. The multiquadric (MQ) method was originally introduced by Hardy in 1968 for the interpolation of two dimensional scattered data to solve a problem from cartography [16]. The problem was to construct a continuous function from a set of sparse, scattered measurements from some source points on a topographic surface, which exactly fit to the given data and provides a good approximation of the features of the surface such as location of hilltops, saddles, breaks in slope, and drainage junctions. In fact the MQ method is a special version of the radial basis functions method. In 1982 Franke tested a large number of interpolation methods for two dimensional scattered data, and found that MQ method was one of the most impressive [10].

Table 1: Some well-known functions that generate RBFs.

Name of function	Definition
Multiquadrics (MQ)	$\phi(\mathbf{x}) = \sqrt{\|\mathbf{x}\|_2^2 + c^2}$
Inverse multiquadrics (IMQ)	$\phi(\mathbf{x}) = \left(\sqrt{\|\mathbf{x}\|_2^2 + c^2}\right)^{-1}$
Inverse quartics (IQ)	$\phi(\mathbf{x}) = \left(\|\mathbf{x}\|_2^2 + c^2\right)^{-1}$
Gaussian (GA)	$\phi(\mathbf{x}) = \exp\left(-c\|\mathbf{x}\|_2^2\right)$
Thin plate splines (TPS)	$\phi(\mathbf{x}) = (-1)^{k+1}\|\mathbf{x}\|_2^{2k}\log\|\mathbf{x}\|_2$
Conical splines (CS)	$\phi(\mathbf{x}) = \|\mathbf{x}\|_2^{2k-1}$

Definition 1. [28] A function $\phi : \mathbb{R}^s \longrightarrow \mathbb{R}$ is called radial basis provided there exists a univariate function $\varphi : [0, \infty) \longrightarrow \mathbb{R}$ such that

$$\phi(\mathbf{x}) = \varphi(r),$$

where $r = \|\mathbf{x}\|$ and $\|.\|$ is some norm on $\mathbb{R}^s$, usually the Euclidean norm.

Some well-known RBFs are listed in Table 1. Plots of some RBFs are presented in Figure (1).

The idea of radial basis function method for interpolation is derived from piecewise polynomial interpolation using a function of Euclidean distance and defined as follows:

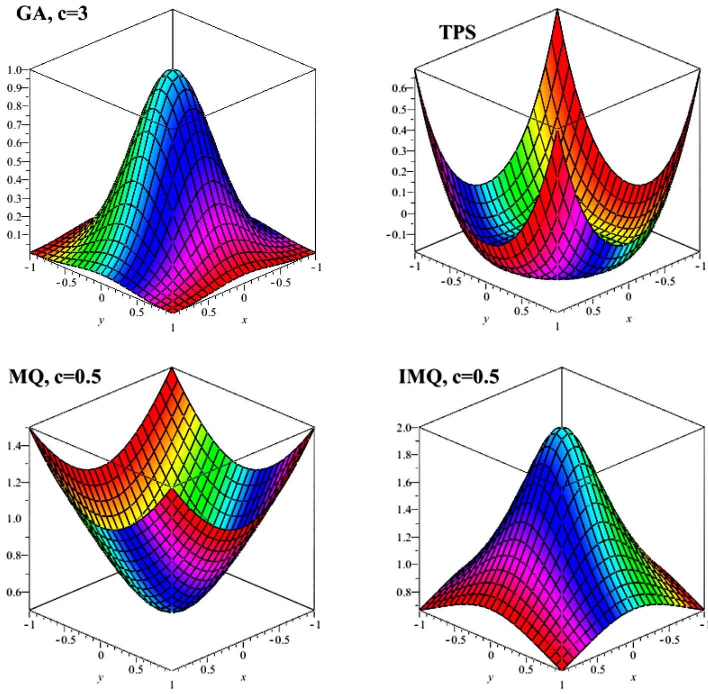

Figure 1: Plots of some radial basis functions.

2.1 Radial basis function interpolation

In the standard RBF interpolation problem, we are given generally scattered data sites $X = \{\mathbf{x}_1, \ldots, \mathbf{x}_N\} \subset D$ and associated real function values $u(\mathbf{x}_i), i = 1, \ldots, N$. Here D is usually some bounded domain in $\mathbb{R}^s$. It is our goal to find a (continuous) function $\mathscr{P}_N u : \mathbb{R}^s \to \mathbb{R}$ that interpolates the given data, i.e., such that

$$\mathscr{P}_N u(\mathbf{x}_i) = u(\mathbf{x}_i), \quad i = 1, \ldots, N. \tag{2}$$

In the RBF literature (see, e.g., [8, 28]) one assumes that this interpolant is of the form

$$\mathscr{P}_N u(\mathbf{x}) = \sum_{j=1}^{N} c_j \varphi\big(\|\mathbf{x} - \mathbf{x}_j\|\big), \tag{3}$$

where the basic function φ is assumed to be RBF and the coefficients $\mathbf{C} = [c_1, ..., c_N]^T$ are found by enforcing the interpolation constraints (2). This implies that

$$\mathbf{AC} = \mathbf{U}, \tag{4}$$

where $\mathbf{A}_{ij} = \varphi(\|\mathbf{x}_i - \mathbf{x}_j\|)$ and $\mathbf{U} = [u(\mathbf{x}_1), \ldots, u(\mathbf{x}_N)]^T$. If the matrix $\mathbf{A}$ is such that $\mathbf{C^T A C}$ is strictly positive for all possible choices of $X = \{\mathbf{x}_1, \ldots, \mathbf{x}_N\}$ and $\mathbf{C} = [c_1, ..., c_N]^T \in \mathbb{R}^N - \{0\}$ the solution of the interpolation problem is guaranteed.

The following results establish invertibility of the matrix A for different radial basis functions:

Definition 2. [28] A function ϕ is called completely monotone on $(0, \infty)$ if it satisfies $\phi \in C^{\infty}(0, \infty)$, and

$$(-1)^l \phi^{(-l)}(r) \geq 0,$$

for all $l \in \mathbb{N}_0$ and all $r > 0$. The function ϕ is called completely monotone on $[0, \infty)$ if it is in addition in $C[0, \infty)$.

Theorem 1. *[27] If $\phi(r) = \varphi(\sqrt{r})$ is completely monotone but not constant on $[0, \infty)$, then for any set of N distinct points $\{\mathbf{x}_1, \ldots, \mathbf{x}_N\}$, the $N \times N$ matrix $\mathbf{A}$ with entries $\varphi(\|\mathbf{x}_i - \mathbf{x}_j\|)$ is positive definite (and therefore non-singular).*

Theorem 2. *[24] Let $\phi(r) = \varphi(\sqrt{r}) \in C^0[0, \infty)$, $\phi(r) > 0$ for $r > 0$, $\phi^{'}(r)$ completely monotone but not constant on $(0, \infty)$, then for any set of N distinct points $\{\mathbf{x}_1, \ldots, \mathbf{x}_N\}$, the $N \times N$ matrix $\mathbf{A}$ with entries $\varphi(\|\mathbf{x}_i - \mathbf{x}_j\|)$ is positive definite.*

It is easy to prove that the radial basis functions IMQ, IQ and GA satisfy the sufficient conditions of Theorem 1, whereas the MQ and linear RBFs satisfy the sufficient conditions of Theorem 2, and hence for these types of RBFs the system (4) is uniquely solvable for any set of distinct data points. Although the matrix $\mathbf{A}$ is non-singular in the above cases, usually it is very ill-conditioned. Therefore, a small perturbation in initial data may produce large amount of perturbation in the solution.

As given in Table 1, the types of RBF are mainly divided into two categories, infinitely smooth and piecewise smooth RBFs [2, 22]. The infinitely smooth RBFs contain a free parameter c, called the shape parameter, which affects both the accuracy of a solution and the conditioning of the collocation matrix. In Figure 2, a data set is interpolated with the Gaussian function, with different shape parameters. A smaller value of c causes the function to become flatter, while increasing c leads to a more peaks RBF. The optimal value of the shape parameter that can produce relatively accurate results is to be found numerically. But the optimal choice of the shape parameters is an open problem which is still under intensive investigation. Several proposals for the choice of an adequate shape parameter can be found in the papers of Hardy [16], Franke [10] and Fasshauer [9]. All these proposals are somehow related with the number of points in the grid and the distance between those points.

Definition 3. Hardy's shape parameter

$$c = 0.815d \quad where \quad d = \frac{1}{N}\sum_{i=1}^{N} d_i,$$

where d_i is the distance from i^{th} center to the nearest neighbor and N is the total number of centers.

Definition 4. Franke's shape parameter

$$c = \frac{1.25D}{\sqrt{N}},$$

where D is the diameter of smallest circle encompassing all the center locations and N is the total number of centers.

Definition 5. Fasshauer's shape parameter

$$c = \frac{2}{\sqrt{N}},$$

where N is the total number of centers.

3 Solution of linear integral equations

In this paper, we solve the three-dimensional linear Fredholm integral equation given in the form

$$u(x,y,z) - \lambda \int_e^f \int_c^d \int_a^b K(x,y,z,r,s,t)u(r,s,t)drdsdt = h(x,y,z), (x,y,z) \in D, \quad (5)$$

where h and K are known functions, $u(x,y,z)$ is the unknown function to be determined, λ is a constant and D is an cubic domain.

Consider equation (5) with the following assumptions:

(i) $h \neq 0$ is continuous in $C(D)$,

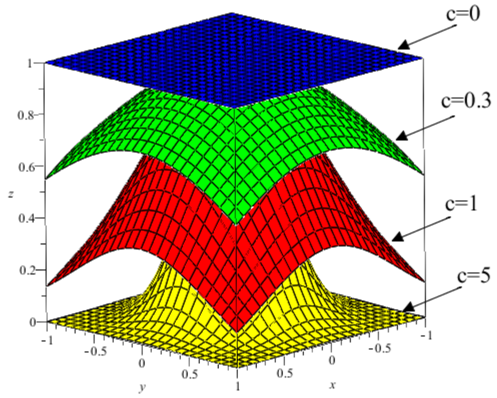

Figure 2: The Gaussian function, with different shape parameters, c.

(ii) K is continuous in $C(D \times D)$,

(iii) kernel $K(x,y,z,r,s,t)$ is real, continuous and bounded in the domain D, i.e.

$$L = \sup_{(x,y,z)\in D} \left\{ \int_e^f \int_c^d \int_a^b \left|K(x,y,z,r,s,t)\right| drdsdt \right\} < \infty.$$

Theorem 3. *Existence and uniqueness of solution to equation (5) follow by assumptions* $(i) - (iii)$ *and the condition*

$$|\lambda| L < 1.$$

Proof. It can be proved using Banach's fixed point theorem in a similar method as done in [4], Chapter 5 (for one-dimensional linear Fredholm integral equations).

3.1 The proposed method

To apply the method, we need a RBF ϕ and N nodal scattered points to initiate the RBF method. These nodes can be selected arbitrary on the whole of the domain D, such as $X = \{(x_1, y_1, z_1), ..., (x_N, y_N, z_N)\}$. Therefore, to solve equation (5), we estimate the unknown function $u(x,y,z)$ by the RBF interpolation method as

$$u(x,y,z) \approx \sum_{k=1}^{N} \bar{c}_k \phi_k(x,y,z) = \bar{C}^T.\Psi(x,y,z), \qquad (x,y,z) \in D \subset \mathbb{R}^3, \quad (6)$$

where

$$\bar{C}^T = [\bar{c}_1, \ldots, \bar{c}_N],$$
$$\Psi^T(x,y,z) = [\phi_1(x,y,z), \ldots, \phi_N(x,y,z)],$$
$$\phi_k(x,y,z) = \varphi\Big(\sqrt{(x-x_k)^2 + (y-y_k)^2 + (z-z_k)^2}\Big), \qquad k = 1, \ldots, N.$$

We replace the expansion (6) with $u(x,y,z)$ and install the collocation points $(x_i, y_i, z_i), i = 1, 2, \ldots, N$ in equation (5). Thus we obtain

$$\bar{C}^T.\left\{\Psi(x_i,y_i,z_i) - \lambda \int_e^f \int_c^d \int_a^b K(x_i,y_i,z_i,r,s,t)\Psi(r,s,t)drdsdt\right\} = h(x_i,y_i,z_i). \quad (7)$$

The integrals in (7) must usually be evaluated numerically. we convert the intervals $[a,b], [c,d]$ and $[e,f]$ to the interval $[-1,1]$ by using a simple linear transformations of the form

$$\begin{cases} r = \dfrac{b-a}{2}\xi + \dfrac{b+a}{2} = g(\xi) \Longrightarrow dr = \dfrac{b-a}{2}d\xi, \\ s = \dfrac{d-c}{2}\eta + \dfrac{d+c}{2} = h(\eta) \Longrightarrow ds = \dfrac{d-c}{2}d\eta, \\ t = \dfrac{f-e}{2}\tau + \dfrac{f+e}{2} = m(\tau) \Longrightarrow dt = \dfrac{f-e}{2}d\tau, \end{cases}$$

and so equation (7) takes the following form:

$$\bar{C}^T.\left\{\Psi(x_i,y_i,z_i) - \mu \int_{-1}^1 \int_{-1}^1 \int_{-1}^1 K(x_i,y_i,z_i,g(\xi),h(\eta),m(\tau))\Psi(g(\xi),h(\eta),m(\tau))d\xi d\eta d\tau\right\}$$
$$= h(x_i,y_i,z_i), \quad (8)$$

where

$$\mu = \frac{\lambda(b-a)(d-c)(f-e)}{8}.$$

Using an m_N -point Gauss - Legendre quadrature formula with the points r_p, s_q, t_k in the interval $[-1,1]$ and weights w_p, w_q, w_k for numerical integration in equation (8), we can approximate the integral

$$\int_{-1}^1 \int_{-1}^1 \int_{-1}^1 K(x,y,z,g(\xi),h(\eta),m(\tau))\Psi(g(\xi),h(\eta),m(\tau))d\xi d\eta d\tau, \qquad (9)$$

with

$$\sum_{p=1}^{m_N}\sum_{q=1}^{m_N}\sum_{k=1}^{m_N} w_p w_q w_k K(x,y,z,g(\xi_p),h(\eta_q),m(\tau_k))\Psi(g(\xi_p),h(\eta_q),m(\tau_k)). \tag{10}$$

Utilizing this numerical integration rule in equation (8), we obtain the following linear system of algebraic equations

$$\hat{C}^T.\Big\{\Psi(x_i,y_i,z_i)-\mu\sum_{p=1}^{m_N}\sum_{q=1}^{m_N}\sum_{k=1}^{m_N} w_p w_q w_k K(x_i,y_i,z_i,g(\xi_p),h(\eta_q),m(\tau_k))\Psi(g(\xi_p),h(\eta_q),m(\tau_k))\Big\} = h(x_i,y_i,z_i), \tag{11}$$

where $i = 1, 2, \ldots, N$. This is a linear system of equations that can be solved by iterative methods to obtain the unknown vector $\hat{C}^T$.

4 Error analysis

This section includes the error estimate and the rate of convergence of the presented method. To understand the numerical behavior of the interpolant or approximant it is essential to have bounds on the approximation error and on the condition number of the interpolation matrix. These bounds are usually expressed employing two different geometric measures. For the approximation error, it is crucial to know how well the data sites X fill the region . This can be measured by the fill distance

$$h_{X,D} := \sup_{x\in D}\min_{1\leq j\leq N}\|\mathbf{x}-\mathbf{x}_j\|_2,$$

which gives the radius of the largest data-site free ball in D. The condition number, however, will obviously only depend on the data sites X and not on the region D. Moreover, if two data sites tend to coalesce then the corresponding interpolation matrix has two rows which are almost identical. Hence, it is reasonable to measure the condition number in terms of the separation distance

$$q_X := \frac{1}{2}\min_{i\neq j}\|\mathbf{x}_i-\mathbf{x}_j\|.$$

A set X of data sites is said to be quasi-uniform with respect to a constant $c_{qu} > 0$ if

$$q_X \leqslant h_{X,D} \leqslant c_{qu} q_X.$$

Definition 6. [28] The definition of the native space is

$$\aleph_{\phi}(D)=\left\{f\in L_2(\mathbb{R}^s)\cap C(\mathbb{R}^s): \frac{\hat{f}}{\sqrt{\hat{\phi}}}\in L_2(\mathbb{R}^s)\right\},$$

where $\hat{\phi}$ is a Fourier transform of ϕ.

Theorem 4. *[2] Let ϕ is positive definite RBF with infinitely smoothness. Suppose that $D\subset\mathbb{R}^s$ be open and bounded, satisfying an interior cone condition. Denote the interpolant of a function $u\in\aleph_{\phi}(D)$ based on this RBF and the distinct set $X=\{x_1,\dots,x_N\}$ by $\mathscr{P}_N u$. Then for every $l\in\mathbb{N}$ there exist constants $h_0(l), C_l$ such that*

$$\|u-\mathscr{P}_N u\|_{L^{\infty}(D)}\le C_l h^l_{X,D}\|u\|_{\aleph_{\phi}(D)}, \tag{12}$$

for all $x\in D$, provided $h_{X,D}\leqslant h_0(l)$.

Remark 1. As a conclusion from Theorem 4, for Gaussians $\phi(\mathbf{x})=e^{(-c\|\mathbf{x}\|^2)}, c>0$, we get for some positive constant l that

$$\|u-\mathscr{P}_N u\|_{L^{\infty}(D)}\le e^{\left(\frac{-l|\log h_{X,D}|}{h_{X,D}}\right)}\|u\|_{\aleph_{\phi}(D)}, \tag{13}$$

provided that $h_{X,D}$ is sufficiently small and $u\in\aleph_{\phi}(D)$.

The corresponding result for (inverse) multiquadrics $\phi(\mathbf{x})=(\|\mathbf{x}\|+c^2)^{\alpha}, c>0, \alpha<0$, or $\alpha>0$ and $\alpha\neq\mathbb{N}$, is

$$\|u-\mathscr{P}_N u\|_{L^{\infty}(D)}\le e^{\left(\frac{-l}{h_{X,D}}\right)}\|u\|_{\aleph_{\phi}(D)}, \tag{14}$$

For thin plate splines $\phi(\mathbf{x})=(-1)^{k+1}\|\mathbf{x}\|^{2k}\log\|\mathbf{x}\|_2$, $k\in\mathbb{N}$, we get

$$\|u-\mathscr{P}_N u\|_{L^{\infty}(D)}\le C h^k_{X,D}\|u\|_{\aleph_{\phi}(D)}. \tag{15}$$

Let $\mathscr{K}$ be the Urysohn integral operator:

$$(\mathscr{K}u)(x,y,z)=\lambda\int_e^f\int_c^d\int_a^b K(x,y,z,r,s,t)u(r,s,t)drdsdt, \tag{16}$$

we can rewrite the integral equation (5) in operator form as

$$u-\mathscr{K}u=h. \tag{17}$$

Define the approximating operator $\mathscr{K}_N, N\ge 1$, on $C(D)$ by

$$\mathscr{K}_N u(x,y,z)=\mu\sum_{p=1}^{m_N}\sum_{q=1}^{m_N}\sum_{k=1}^{m_N} w_p w_q w_k K(x,y,z,g(\xi_p),h(\eta_q),m(\tau_k))\hat{C}^T\Psi(g(\xi_p),h(\eta_q),m(\tau_k)). \tag{18}$$

The abstract form of equation (8) is

$$u_N - \mathscr{P}_N \mathscr{K} u_N = \mathscr{P}_N h,$$

for N sufficiently large and the above equation can be rewritten as

$$(I - \mathscr{P}_N \mathscr{K}) u_N = \mathscr{P}_N h. \tag{19}$$

Remark 2. Note that, $\mathscr{P}_N : C(D) \longrightarrow V_N$ is the collocation projection operator on the collocation points $X = \{(x_1, y_1, z_1), ..., (x_N, y_N, z_N)\} \subset D$, where the subspace $V_N := span\{\phi_1, \ldots \phi_N\} \subset C(D)$ has finite dimension. Suppose $\hat{u} \in V_N$, we simply have $\mathscr{P}_N \hat{u} = \hat{u}$.

The abstract form of equation (11) is

$$(I - \mathscr{P}_N \mathscr{K}_N) \hat{u}_N = \mathscr{P}_N h, \tag{20}$$

which shows that the scheme is a discrete collocation method [3].
Consequently an iterated discrete collocation solution can be obtained. For this purpose we set

$$\bar{u}_N = h + \mathscr{P}_N \mathscr{K}_N (\hat{u}_N), \tag{21}$$

and by applying the operator $\mathscr{P}_N$ on both sides of (21), and using the relation (20) we simply have

$$\mathscr{P}_N \bar{u}_N = \hat{u}_N. \tag{22}$$

Thus we conclude

$$(I - \mathscr{P}_N \mathscr{K}_N) \bar{u}_N = h. \tag{23}$$

Theorem 5. *[3] Assume the family $\{\mathscr{K}_N\}$ of (8) is collectively compact and pointwise convergent on $C(D)$. Let $\{\mathscr{P}_N\}$ be a family of interpolatory projection operators on $C(D)$ to $C(D)$, and assume*

$$\mathscr{P}_N u \longrightarrow u \quad as \quad N \longrightarrow \infty, \tag{24}$$

for all $u \in C(D)$. Finally, assume the integral equation (17) is uniquely solvable for all $h \in C(D)$ and u_* be a unique solution of this equation. Then for all sufficiently large N, say $N \geqslant M$, $(I - \mathscr{K}_N \mathscr{P}_N)^{-1}$ exists and is uniformly bounded. Also, for the solution $\bar{u}_N$

$$\|\bar{u}_N - u_*\|_{L^\infty(D)} \leq \|(I - \mathscr{K}_N \mathscr{P}_N)^{-1}\| \|\mathscr{K} u_* - \mathscr{K}_N \mathscr{P}_N u_*\|_{L^\infty(D)}. \tag{25}$$

Remark 3. From (24) and the principle of uniform boundedness for the radial basis functions,

$$c_p = \sup \|\mathscr{P}_N\| < \infty. \tag{26}$$

Similarly, from the pointwise convergence of $\{\mathscr{K}_N\}$,

$$c_k = \sup \|\mathscr{K}_N\| < \infty. \tag{27}$$

Theorem 6. *Having in mind the assumptions of (5). Suppose that $u_* \in \aleph_\phi(D)$ is the unique exact solution of equation (5) and the proposed method has been installed on the quasi-uniform set $X = \{(x_i, y_i, z_i)\}_{i=1}^N$. Then there exists $M > 0$ such that for every $N > M$, the method has a unique solution $\hat{u}_N$*

$$\|\hat{u}_N - u_*\|_{L^\infty(D)} \longrightarrow 0 \quad as \quad N \longrightarrow \infty. \tag{28}$$

In addition, for the iterative solution $\bar{u}_N$ for equation (23) we have

$$\|\bar{u}_N - u_*\|_{L^\infty(D)} \leq c_I\{\|\mathscr{K}u_* - \mathscr{K}_N u_*\|_{L^\infty(D)} + c_k(1 + c_p)C_l h^l_{X,D}\|u_*\|_{\aleph_\phi(D)}\},$$

provided that $u_* \in \aleph_\phi(D)$, and for the discrete collocation solution $\hat{u}_N$ of equation (20) we have

$$\|\hat{u}_N - u_*\|_{L^\infty(D)} \leq c_p c_I\|\mathscr{K}u_* - \mathscr{K}_N u_*\|_{L^\infty(D)} + (1 + c_p)(1 + c_p c_I c_k)C_l h^l_{X,D}\|u_*\|_{\aleph_\phi(D)},$$

where $c_I < \infty$ is a bound for $(I - \mathscr{K}_N \mathscr{P}_N)^{-1}$.

Proof. From Theorem 5, the iterated method has a solution $\bar{u}_N$ and

$$\begin{aligned}
\|\bar{u}_N - u_*\|_{L^\infty(D)} &\leq \|(I - \mathscr{K}_N\mathscr{P}_N)^{-1}\|\|\mathscr{K}u_* - \mathscr{K}_N\mathscr{P}_N u_*\|_{L^\infty(D)} \\
&\leq c_I\|\mathscr{K}u_* - \mathscr{K}_N\mathscr{P}_N u_*\|_{L^\infty(D)} \\
&\leq c_I\{\|\mathscr{K}u_* - \mathscr{K}_N u_*\|_{L^\infty(D)} + \|\mathscr{K}_N(u_* - \mathscr{P}_N u_*)\|_{L^\infty(D)}\} \\
&\leq c_I\{\|\mathscr{K}u_* - \mathscr{K}_N u_*\|_{L^\infty(D)} + c_k\|(u_* - \mathscr{P}_N u_*)\|_{L^\infty(D)}\} \\
&\leq c_I\{\|\mathscr{K}u_* - \mathscr{K}_N u_*\|_{L^\infty(D)} + c_k(\|u_* - \hat{u}_*\|_{L^\infty(D)} + \|\mathscr{P}_N u_* - \mathscr{P}_N\hat{u}_*\|_{L^\infty(D)})\} \\
&\leq c_I\{\|\mathscr{K}u_* - \mathscr{K}_N u_*\|_{L^\infty(D)} + c_k(1 + c_p)\|(u_* - \hat{u}_*)\|_{L^\infty(D)}\} \\
&\leq c_I\{\|\mathscr{K}u_* - \mathscr{K}_N u_*\|_{L^\infty(D)} + c_k(1 + c_p)C_l h^l_{X,D}\|u_*\|_{\aleph_\phi(D)}\}
\end{aligned}$$

The last inequality is implied by (15). Moreover, let $\hat{u}_N = p_N\bar{u}_N$, and consider the decomposition

$$u_* - \hat{u}_N = u_* - \mathscr{P}_N\bar{u}_N = (u_* - \mathscr{P}_N u_*) + \mathscr{P}_N(u_* - \bar{u}_N), \tag{29}$$

which yields

$$\begin{aligned}
\|\hat{u}_N - u_*\|_{L^\infty(D)} &\le \|u_* - \mathscr{P}_N u_*\|_{L^\infty(D)} + c_p\|\bar{u}_N - u_*\|_{L^\infty(D)} \\
&\le (1+c_p)C_l h^l_{X,D}|u_*|_{\aleph_\phi(D)} + c_p(c_I\{\|\mathscr{K}u_* - \mathscr{K}_N u_*\|_{L^\infty(D)} \\
&\quad + c_k(1+c_p)C_l h^l_{X,D}|u_*|_{\aleph_\phi(D)}\}) \\
&\le \underbrace{c_p c_I\|\mathscr{K}u_* - \mathscr{K}_N u_*\|_{L^\infty(D)}}_{N\longrightarrow\infty \implies \mathscr{K}_N\longrightarrow\mathscr{K}} \\
&\quad + \underbrace{(1+c_p)(1+c_p c_I c_k)C_l h^l_{X,D}\|u_*\|_{\aleph_\phi(D)}}_{N\longrightarrow\infty \implies h_{X,D}\longrightarrow 0}
\end{aligned}$$

Finally, we obtain

$$\|\hat{u}_N - u_*\|_{L^\infty(D)} \longrightarrow 0 \quad as \quad N \longrightarrow \infty.$$

Corollary 1. *Theorem 6 shows that, both the quadrature and the RBF approximation error bounds affect the final estimation. If for a sufficiently smooth kernel $K(x,t,y,s)$ a high order quadrature is employed then the total error is dominated by the error of the RBF approximation.*

5 Numerical examples

In this section, we present some numerical examples where D is a bounded domain in $\mathbb{R}^3$. In addition to the Hardy, Franke and Fasshauer shape parameters, the minimum error obtained by trial and error is presented. We have used the ten-point Gauss-Legendre quadrature rule for numerical integration. All of the computations have been done using the Maple 14 with just 80 digits precision. we calculate the RMS error in 2197 points that are distributed uniformly in the computational domain. The RMS error of the numerical result is described using

$$RMS = \sqrt{\frac{1}{2197}\sum_{i=1}^{2197} \mid u(x_i,y_i,z_i) - \hat{u}(x_i,y_i,z_i) \mid^2}$$

where $u(x,y,z)$ is the exact solution, $\hat{u}(x,y,z)$ is the approximate solution.

Example 1. Consider the three-dimensional linear Fredholm integral equation

$$u(x,y,z) - \frac{1}{2}\int_{-1}^{1}\int_{-1}^{1}\int_{-1}^{1} \frac{xyz}{1+x+y+z}u(r,s,t)drdsdt = f(x,y,z),$$

where

$$f(x,y,z) = \sin^2(x)\sin^2(y)\sin^2(z) + \big(\cos(1)\sin(1) - 1\big)^3 \frac{xyz}{2 + 2x + 2y + 2z}.$$

The exact solution for this equation is $u(x,y,z) = \sin^2(x)\sin^2(y)\sin^2(z)$.

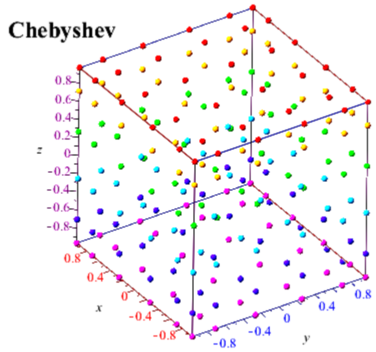

Figure 3: Node distribution with 216 nodes for Example 1.

The results obtained by the Chebyshev distribution of points for different numbers of N in terms of RMS is given in Tables 2, 3 and 4. The distribution of nodes are depicted for N = 216 in Figure 3. As we expected, from Theorem 6, the results converge to the exact values along with the increase of the nodes. In computations, for GA RBFs, to obtain the better result, we can use the small(big) parameter c but the condition number of the final system is grown fast instead. As can be seen, the convergence rate of the method is arbitrarily high when GAs and IQs are used and is approximately $O(h^k_{X,D})$ when TPSs and CSs are used. Therefore the numerical results confirm the theoretical error estimates.

Example 2. Consider the three-dimensional linear Fredholm integral equation

$$u(x,y,z) - \frac{1}{2}\int_0^2\int_0^1\int_{-1}^1 \sin(xyz)u(r,s,t)drdsdt = f(x,y,z),$$

where

$$f(x,y,z) = x^2y^2z^2 - \frac{8}{27}\sin(xyz),$$

with exact solution $u(x,y,z) = x^2y^2z^2$. The results obtained by the Regular distribution of points for different numbers of N in terms of RMS is given in Tables 5, 6 and 7. The distribution of nodes are depicted for N = 294 in Figure 4. It should be noted that for a fixed sufficiently large m_N, by increasing N, the error of the method is of $O(h^l_{X,D})$ (i.e., arbitrarily high for the use of MQs and IMQs and approximately $O(h^k_{X,D})$ for the use of

Table 2: Results provided by Chebyshev distribution for Example 1.

N	$h_{X,D}$	*shape parameter*	c	GA
27	0.7339	*Hardy*	0.70	7.36×10^{-2}
		Franke	0.72	8.13×10^{-2}
		Fasshauer	0.38	2.52×10^{-4}
		a^*	0.38	2.52×10^{-4}
64	0.6334	*Hardy*	0.44	7.88×10^{-4}
		Franke	0.50	1.59×10^{-3}
		Fasshauer	0.25	4.83×10^{-3}
		a^*	0.43	7.75×10^{-4}
125	0.4991	*Hardy*	0.30	2.11×10^{-4}
		Franke	0.37	2.51×10^{-4}
		Fasshauer	0.18	7.50×10^{-5}
		a^*	0.20	4.24×10^{-6}
216	0.4189	*Hardy*	0.22	5.13×10^{-5}
		Franke	0.28	2.02×10^{-4}
		Fasshauer	0.14	2.35×10^{-4}
		a^*	0.20	2.20×10^{-6}

a^* indicates the shape parameter which minimum error is observed.

Table 3: Results provided by Chebyshev distribution for Example 1.

N	$h_{X,D}$	CS		TPS	
		$k=1$	$k=2$	$k=1$	$k=2$
27	0.7339	9.14×10^{-2}	3.92×10^{-2}	1.56×10^{-1}	2.21×10^{-1}
64	0.6334	3.36×10^{-2}	1.71×10^{-2}	5.88×10^{-2}	4.82×10^{-2}
125	0.4991	2.29×10^{-2}	5.76×10^{-3}	1.17×10^{-2}	4.54×10^{-3}
216	0.4189	1.71×10^{-2}	3.34×10^{-3}	6.05×10^{-3}	2.64×10^{-3}

Table 4: Results provided by Chebyshev distribution for Example 1.

N	$h_{X,D}$	*shape parameter*	c	IQ
27	0.7339	*Hardy*	0.70	2.24×10^{-2}
		Franke	0.72	2.29×10^{-2}
		Fasshauer	0.38	3.52×10^{-2}
		a^*	1.25	1.57×10^{-3}
64	0.6334	*Hardy*	0.44	7.44×10^{-3}
		Franke	0.50	6.27×10^{-3}
		Fasshauer	0.25	9.30×10^{-3}
		a^*	0.93	8.91×10^{-4}
125	0.4991	*Hardy*	0.30	6.60×10^{-3}
		Franke	0.37	4.82×10^{-3}
		Fasshauer	0.18	8.22×10^{-3}
		a^*	1.61	1.43×10^{-4}
216	0.4189	*Hardy*	0.22	4.34×10^{-3}
		Franke	0.28	2.35×10^{-3}
		Fasshauer	0.14	6.23×10^{-3}
		a^*	0.92	7.84×10^{-5}

a^* indicates the shape parameter which minimum error is observed.

TPSs and CSs) because the RBF interpolation error overcomes the error of integration method and so increasing N has no significant effect on the error. Based on the obtained fill distance, the results confirm Theorem 6.

Example 3. Consider the three-dimensional linear Fredholm integral equation

$$u(x,y,z) - \frac{1}{2}\int_0^1\int_0^1\int_0^1 xyzu(r,s,t)drdsdt = f(x,y,z),$$

where

$$f(x,y,z) = xyz\exp(-x^2-y^2-z^2) - \frac{1}{16}\left(1-\frac{1}{\exp(1)}\right)^3 xyz,$$

with exact solution $u(x,y,z) = xyz\exp(-x^2-y^2-z^2)$. The results obtained by the Halton distribution of points for different numbers of N in terms of RMS is given in Tables 8, 9 and 10. A set of 216 Halton points in the unit cubic in $\mathbb{R}^3$ has been shown in Figure 5. For sufficiently large m_N, increasing

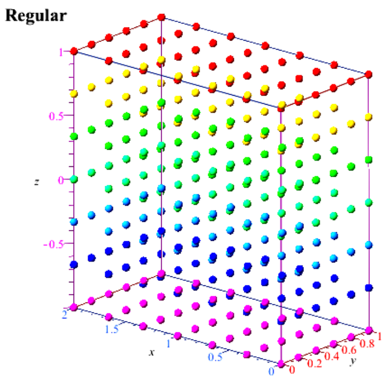

Figure 4: Node distribution with 294 nodes for Example 2.

Table 5: Results provided by Regular distribution for Example 2.

N	$h_{X,D}$	*shape parameter*	c	MQ
48	0.5246	*Hardy*	0.41	1.01×10^{-2}
		Franke	0.54	9.82×10^{-3}
		Fasshauer	0.29	1.12×10^{-2}
		a^*	1.82	7.21×10^{-3}
100	0.3842	*Hardy*	0.27	5.16×10^{-3}
		Franke	0.37	4.81×10^{-3}
		Fasshauer	0.20	5.26×10^{-3}
		a^*	4.23	9.39×10^{-4}
180	0.3039	*Hardy*	0.20	3.26×10^{-3}
		Franke	0.28	3.09×10^{-3}
		Fasshauer	0.15	3.30×10^{-3}
		a^*	5.54	2.20×10^{-4}
294	0.2517	*Hardy*	0.16	2.16×10^{-3}
		Franke	0.22	2.04×10^{-3}
		Fasshauer	0.12	2.19×10^{-3}
		a^*	5.52	3.88×10^{-5}

a^* indicates the shape parameter which minimum error is observed.

the number of integration nodes m_N has no significant effect on the error and the proposed method will be of $O(h^l_{X,D})$, by increasing N. The numerical

Table 6: Results provided by Regular distribution for Example 2.

N	$h_{X,D}$	*shape parameter*	c	IMQ
48	0.5246	*Hardy*	0.41	1.35×10^{-2}
		Franke	0.54	1.39×10^{-2}
		Fasshauer	0.29	1.20×10^{-2}
		a^*	2.79	4.72×10^{-3}
100	0.3842	*Hardy*	0.27	7.23×10^{-3}
		Franke	0.37	7.73×10^{-3}
		Fasshauer	0.20	6.32×10^{-3}
		a^*	4.71	6.68×10^{-4}
180	0.3039	*Hardy*	0.20	4.51×10^{-3}
		Franke	0.28	5.08×10^{-3}
		Fasshauer	0.15	4.11×10^{-3}
		a^*	8.40	8.02×10^{-5}
294	0.2517	*Hardy*	0.16	3.07×10^{-3}
		Franke	0.22	3.51×10^{-3}
		Fasshauer	0.12	3.13×10^{-3}
		a^*	5.52	3.88×10^{-5}

a^* indicates the shape parameter which minimum error is observed.

Table 7: Results provided by Regular distribution for Example 2.

N	$h_{X,D}$	CS		TPS	
		$k=1$	$k=2$	$k=1$	$k=2$
48	0.5246	9.92×10^{-2}	8.70×10^{-2}	1.05×10^{-1}	1.00×10^{-1}
100	0.3842	4.87×10^{-2}	3.76×10^{-2}	4.63×10^{-2}	3.15×10^{-2}
180	0.3039	3.18×10^{-2}	2.06×10^{-2}	2.71×10^{-2}	1.53×10^{-2}
294	0.2517	2.22×10^{-2}	1.16×10^{-2}	1.69×10^{-2}	7.76×10^{-3}

results confirm the theoretical error estimates. In addition, the numerical results shows that the accuracy of RBFs with shape parameter is better than RBFs without shape parameter.

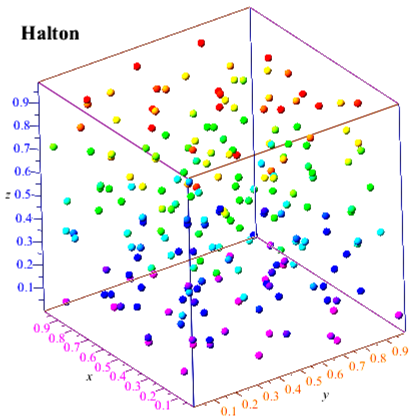

Figure 5: Node distribution with 216 nodes for Example 3.

6 Conclusion

In this paper, a collocation method based on RBFs for numerical solution of three-dimensional linear Fredholm integral equations of the second kind on the cubic domains is presented. The proposed method is a meshless method, which requires no domain elements for the interpolation or approximation. The Gauss-Legendre quadrature formula is employed for numerical integration. Error analysis was provided for suffficiently smooth kernel and source functions. The method is very convenient for solving higher dimensional integral equations because the RBF is defined as the function of distance. The proposed method can be easily expanded into non-cube domains. It means the process of solving is no more complicated in spite of increasing the dimension of problem. This is significant advantage of the method in comparision with other strategy for solving Integral Equations in three dimension.

Acknowledgements

Authors are grateful to there anonymous referees and editor for their constructive comments.

Table 8: Results provided by Halton distribution for Example 3.

N	$h_{X,D}$	*shape parameter*	c	GA
27	0.4912	*Hardy*	0.22	4.16×10^{-3}
		Franke	0.29	3.88×10^{-3}
		Fasshauer	0.38	3.56×10^{-3}
		a^*	1.57	1.81×10^{-3}
64	0.3456	*Hardy*	0.14	9.10×10^{-4}
		Franke	0.20	7.84×10^{-4}
		Fasshauer	0.25	6.89×10^{-4}
		a^*	0.88	8.57×10^{-5}
125	0.2820	*Hardy*	0.12	1.76×10^{-4}
		Franke	0.17	1.51×10^{-4}
		Fasshauer	0.18	1.46×10^{-4}
		a^*	0.84	7.45×10^{-6}
216	0.2780	*Hardy*	0.09	2.14×10^{-5}
		Franke	0.13	1.70×10^{-5}
		Fasshauer	0.14	1.61×10^{-5}
		a^*	0.90	9.10×10^{-8}

a^* indicates the shape parameter which minimum error is observed.

Table 9: Results provided by Halton distribution for Example 3.

N	$h_{X,D}$	CS		TPS	
		$k=1$	$k=2$	$k=1$	$k=2$
27	0.4912	5.34×10^{-2}	1.09×10^{-2}	2.12×10^{-2}	4.07×10^{-2}
64	0.3456	3.61×10^{-3}	3.22×10^{-3}	1.47×10^{-2}	5.90×10^{-3}
125	0.2820	2.28×10^{-3}	1.60×10^{-3}	9.15×10^{-3}	3.43×10^{-3}
216	0.2780	1.74×10^{-3}	4.88×10^{-4}	2.04×10^{-3}	1.35×10^{-3}

Table 10: Results provided by Halton distribution for Example 3.

N	$h_{X,D}$	*shape parameter*	c	MQ
27	0.4912	*Hardy*	0.22	3.91×10^{-3}
		Franke	0.29	3.77×10^{-3}
		Fasshauer	0.38	3.65×10^{-3}
		a^*	1.60	2.95×10^{-3}
64	0.3456	*Hardy*	0.14	2.38×10^{-3}
		Franke	0.20	2.14×10^{-3}
		Fasshauer	0.25	1.99×10^{-3}
		a^*	1.80	2.06×10^{-4}
125	0.2820	*Hardy*	0.12	1.64×10^{-3}
		Franke	0.17	1.46×10^{-3}
		Fasshauer	0.18	1.43×10^{-3}
		a^*	2.60	1.74×10^{-5}
216	0.2780	*Hardy*	0.09	1.20×10^{-3}
		Franke	0.13	1.02×10^{-3}
		Fasshauer	0.14	9.73×10^{-4}
		a^*	2.10	1.46×10^{-6}

a^* indicates the shape parameter which minimum error is observed.

References

1. Alipanah, A. and Esmaeili, S. *Numerical solution of the two-dimensional Fredholm integral equations using Gaussian radial basis function*, J. Comput. Appl. Math. 235 (2011), 5342-5347.

2. Assari, P., Adibi, H. and Dehghan, M. *A numerical method for solving linear integral equations of the second kind on the non-rectangular domains based on the meshless method*, Applied Mathematical Modelling, 37 (2013), 9269-9294.

3. Atkinson, K.E. *The Numerical Solution of Integral Equations of the Second Kind*, vol. 4, Cambridge University Press, Cambridge, UK, 1997.

4. Atkinson, K.E. and Han, W. *Theoretical Numerical Analysis: a Functional Analysis Framework*, Springer-Verlag New York, INC, 2001.

5. Brunner, H. *Collocation Methods for Volterra Integral and Related Functional Equations*, Cambridge University Press, 2004.

6. Dehghan, M. and Mirzaei, D. *Meshless Local Petrov-Galerkin (MLPG) method for the unsteady magnetohydrodynamic (MHD) flow through pipe with arbitrary wall conductivity*, App. Numer. Math. 59 (2009), 1043-1058.

7. Dehghan, M. and Salehi, R. *The numerical solution of the non-linear integro-differential equations based on the meshless method*, J. Comput. Appl. Math. 236 (2012), 2367-2377 .

8. Fasshauer, G. E. *Meshfree approximation methods with MATLAB*, Interdisciplinary Mathematical Sciences, vol. 6. World Scientific Publishing Company, Singapore, 2007.

9. Fasshauer, G.E. *Newton iteration with multiquadrics for the solution of nonlinear PDEs*, Computers and Mathematics with Applications, 43 (2002), 423-438.

10. Franke, R. *Scattered data interpolation: Tests of some methods*, Mathematics of Computation, 38 (1982), 181-200.

11. Golbabai, A., Mammadov, M. and Seifollahi, S. *Solving a system of nonlinear integral equations by an RBF network*, Comput. Math. Appl. 57 (2009), 1651-1658.

12. Golbabai, A. and Seifollahi, S. *Numerical solution of the second kind integral equations using radial basis function networks*, Appl. Math. Comput. 174 (2006), 877-883.

13. Golbabai, A. and Seifollahi, S. *Radial basis function networks in the numerical solution of linear integro-differential equations*, Appl. Math. Comput. 188 (2007), 427-432.

14. Guoqiang, H., Hayami, K., Sugihara,K. and Jiong, W. *Extrapolation method of iterated collocation solution for two-dimensional nonlinear Volterra integral equations*, Appl. Math. Comput. 112 (2000), 49-61.

15. Guoqiang, H. and Jiong, W. *Extrapolation of nystrom solution for two dimensional nonlinear Fredholm integral equations*, J. Comput. Appl. Math. 134 (2001), 259-268.

16. Hardy, R. L. *Multiquadric equations of topography and other irregular surfaces*, J. Geophys. Res. 176 (1971), 1905-1915.

17. Hon, Y.C., Cheung, K.F., Mao, X.Z. and Kansa, E.J. *Multiquadric solution for shallow water equations*, ASCE J. Hydraul. Eng. 125 (5) (1999), 524-533.

18. Hon, Y.C. and Mao, X.Z. *An efficient numerical scheme for Burgers equation*, Appl. Math. Comput. 95 (1) (1998), 37-50.

19. Hon, Y.C. and Mao, X.Z. *A radial basis function method for solving options pricing model*, Financ. Eng. 8 (1) (1999), 31-49.

20. Kansa, E.J. *Multiquadrics - A scattered data approximation scheme with applications to computational fluid dynamics-I*, Comput. Math. Appl. 19 (1990), 127-145.

21. Kansa, E.J. *Multiquadrics - A scattered data approximation scheme with applications to computational fluid dynamics-II*, Comput. Math. Appl. 19 (1990), 147-161.

22. Larsson, E. and Fornberg, B. *A numerical study of some radial basis function based solution methods for elliptic PDEs*, Comput. Math. Appl. 46 (2003), 891-902.

23. Marcozzi, M., Choi, S. and Chen, C.S. *On the use of boundary conditions for variational formulations arising in financial mathematics*, Appl. Math. Comput. 124 (2001), 197-214.

24. Micchelli, C.A. *Interpolation of scattered data: distance matrices and conditionally positive denite functions*, Constr. Approx., 2 (1986), 11-22.

25. Parand, K. and Rad, J.A. *Numerical solution of nonlinear Volterra-Fredholm-Hammerstein integral equations via collocation method based on radial basis functions*, Appl. Math. Comput. 218 (2012), 5292-5309.

26. Salehi, R. and Dehghan, M. *A moving least square reproducing polynomial meshless method*, Appl. Numer. Math. 69 (2013), 34-58.

27. Schoenberg, I. J. *Metric spaces and completely monotone functions*, Ann. Math., 39 (1938), 811-841.

28. Wendland, H. *Scattered data approximation*, Cambridge Monographs on Applied and Computational Mathematics, vol. 17. Cambridge University Press, Cambridge 2005.

29. Xie, W. J. and Lin, F. R. *A fast numerical solution method for two dimensional Fredholm integral equations of the second kind*, Applied Numerical Mathematics, 59 (2009), 1709-1719.

30. Zerroukat, M., Power, H. and Chen, C.S. *A numerical method for heat transfer problem using collocation and radial basis functions*, Internat. J. Numer. Methods Engrg. 42 (1992), 1263-1278.

Iranian Journal of Numerical Analysis and Optimization
Vol. 7, No. 2, (2017), pp 39–55
DOI:10.22067/ijnao.v7i2.46395

Payment scheduling under project crashing based on project progress

M. Mortazavi Nejad, H.R. Tareghian and Z. Sari*

Abstract

In this paper, we address a new problem in the context of project payment scheduling when project activities are allowed to be crashed with the purpose of maximizing the contractors *net present value* (NPV). We assume that the contractor is paid at some pre-specified points of time according to the volume of work performed. Upon completion of activities, the cost of their execution is paid. Two different approaches are used to determine the volume of work performed at so called review points. In the first approach, only completed activities are considered. In the second approach, any portions of the activities that are executed are considered. To increase the volume of work performed at the review points, the contractor may decide to crash some activities and as such may possibly increase his NPV. As activity crashing costs the contractor money, a compromise needs to be made. Two mathematical models are developed to study each approach and hence help the contractor to make the best decision. These models offer a means of investigating whether it is advisable to crash some activities and are therefore of practical importance. It is shown that the contractor may increase his NPV, even when he pays for the activity crashing costs. The performance of the mathematical models is illustrated using a numerical example.

Keywords: Payment scheduling; Progress payment; Project crashing; Contractor's net present value.

---

*Corresponding author
Received 29 April 2015; revised 8 November 2016; accepted 3 Desember 2016
M. Mortazavi Nejad
Department of Applied Mathematics, Faculty of Mathematical Sciences, Ferdowsi University of Mashhad, Mashhad, Iran. e-mail: mamortazavi2012@gmail.com

H.R. Tareghian
Department of Applied Mathematics, Faculty of Mathematical Sciences, Ferdowsi University of Mashhad, Mashhad, Iran. e-mail: taregian@ferdowsi.um.ac.ir

Z. Sari
Department of Applied Mathematics, Faculty of Mathematical Sciences, Ferdowsi University of Mashhad, Mashhad, Iran. e-mail: zeynabsari89@gmail.com

1 Introduction and Background

The *Critical path method* (CPM) is essentially a time-oriented technique based on network structure which is mainly used to schedule project activities under resource availability or scarce resources. Time cost trade-off problem (TCTP) in which the compression of the project schedule is sought in order to achieve an improved outcome in terms of project duration, cost, and projected revenues is one of the earliest applications of the CPM in which cost factors are considered. The objective of the TCTP is to compress the project to the optimum duration which minimizes the total project costs. Other project cost monitoring are mainly focused on reporting the total amount of project costs and no consideration is given to the time value of money [13]. Considering that large scale projects usually have long life cycles, *net present value* (NPV) is suggested as a criterion for the financial control of projects. Russell introduced the concept of cash flow in a project [15]. He assumed that the project is represented in *activity-on-arrow* (AOA) format and that the payments, i.e. outward cash flows and the receipts, i.e. inward cash flows occur at some or all of the project network's nodes. Considering the inward and outward cash flows the problem is to schedule the network's events in a manner that the present value of cash flows is maximized. In order to maximize the NPV of the projects cash flows, Russell developed a mathematical model with a nonlinear objective function and a set of linear constraints [15].The model's objective function was then linearized by the Taylor's series expansion around a feasible solution. The dual of the linearized model which possess the characteristics of the minimum cost network flow can be rapidly solved in small networks and can be efficiently solved in larger networks. The final solution is then obtained iteratively. In addition, Russell came to some interesting conclusions: *the critical path may not be very cost significant but that there exists a cost-critical tree of activities to each of which a marginal cost of lengthening the duration can be ascribed*.

In 1972, Grinold considered a deadline for the project and transformed the non-linear model of Russell into an equivalent linear model. The linear model that has the structure of a weighted distribution problem was then solved using an efficient procedure [7]. In 1982, Talbot developed a mixed integer programming model for the project cash flow problem under the limitation of resources [18]. In 1990, Elmaghraby et al. developed a procedure to solve the cash flow problem with fixed amounts of inward and outward flows [6]. They showed that it is beneficial to advance the events that correspond to positive flows and delay the events that relate to negative flows as much as possible (see e.g. the review papers [11] and [19]).

In the majority of the articles, the flows are assumed to be of constant and known values. The contractor knows the costs of performing the project activities and therefore can negotiate the amount and time of the client's payments in order to maximize his returns. As payments are usually done according to the volume of the work performed (*progress payment*), scheduling of activities find significant importance. The problem of determining the amount as well as the timing of payments to maximize NPV is called the *payment scheduling problem* (PSP). It was first studied from the contractor's view point by Dayanand et al. [2]. Kazaz et al. considered the problem for projects with unlimited resources and developed a mixed integer programming model to maximize NPV. They showed that Bender's decomposition can reduce the running time of the model significantly [13]. Sepil et al. studied the performance of a number of heuristics to solve the PSP under resource limitation [16].

In continuation of their previous research, Dayanand et al. developed a 0-1 programming model together with a number of heuristics. Dayanand et al. altered Russell, Grinold and Talbot's models by adding some new constraints and claimed that their models can be used for both the contractor's and client's view points subject to some modifications [3]. Ulusoy et al. considered the PSP from the simultaneous view points of the contractor and the client. They developed a two loop genetic algorithm to study the problem. The outer loop represents the client and the inner loop represents the contractor. In the outer loop and under the assumptions of fixed schedules as well as the timing of payments, the client changes the amount of payments. Fixing the amount of payment, the inner loop is executed such that by rescheduling the activities, the contractor's NPV is maximized. The two loops negotiate their solutions until they come to a "fair" solution that is accepted by both parties [20]. Four types of payment scheduling models: *lump sum payment at the terminal event*-LSP, *payments at event occurrences*-PEO, *the equal time intervals*-ETI and *progress payment*-PP were distinguished by Ulusoy et al. They used the two loops genetic algorithm developed in [20] to study the PSP under resource limitations and in respect of each of the payment scheduling models [21]. Dayanand et al. developed a two stage search heuristic to solve PSP. They utilized a simulated annealing model in the first stage to find a set of payments. To improve the solution, they tuned the solution in the second stage by rescheduling activities [4]. Dayanand et al. modeled the PSP from the client's view point and developed a number of mixed integer programming models to study the problem [5]. Vanhoucke et al. considered the PSP under unlimited resources and developed a branch and bound procedure to study and analyze it [22].

Szmereskovsky developed a branch-and-bound procedure for a novel PSP model where the client selects the payment schedule and the contractor protects his interests by selecting the activity schedule. However, the contractor rejects the payment schedule if his NPV does not exceed a given threshold [17]. The multi-mode resource constrained project scheduling problem with discounted cash flow under the four payment scheduling models proposed by Ulusoy et al., was studied by Mika et al. who considered only positive cash flows and employed a simulated annealing as well as a genetic algorithm to solve the problem [14].

Discrete time cost trade-off problem (DTCTP) involves the selection of a set of execution modes in order to achieve a certain objective. Although DTCTP has been combined with the maximum NPV project scheduling problem (see e.g. [23]), its influence on project payment scheduling has not been studied extensively [9]. The resulting problem is called the *multi-mode project payment scheduling problem* (MPSP) where the objective is to assign activity modes and progress payments so as to maximize the NPV under the constraint of project deadline. He et al. analyzed the effect of the bonus-penalty structure on payment scheduling and found that this structure can enhance the flexibility of payment scheduling greatly [8]. In 2009, He et al. developed two heuristics, i.e. simulated annealing and tabu search to study the MPSP and compared their performance on a data set constructed randomly [9].

Kavlak et al. investigated client-contractor bargaining in project scheduling with limited resources using *activity-on-node* (AON) networks. They considered two different payment models. In the first model, contractor receives payments at predetermined regular time intervals. In the second model, he receives only one payment at activity completions. They developed a simulated annealing and a genetic algorithm as solution procedures. The client and the contractors desire to seek a compromise are reflected in an objective function [12]. He et al. defined a new problem called the multi-mode capital-constrained project payment scheduling problem (MCCPSP) as the combination of the capital-constrained project scheduling problem and the MPSP. They studied the MCCPSP where the objective is to assign activity modes and payments concurrently so as to maximize the NPV of the contractor under the constraint of capital availability [10].

In this paper, we consider the PSP with unlimited resources, and address the question of activity compression from the contractor's view point. Our assumptions are as follows: (i) a deadline is specified for the project; (ii) the negative cash flows occur at the completion of activities; (iii) the payments are done at review points; (iv) the amount of each payment is based on the volume of work completed; (v) any extra costs for compression of activities are paid by the contractor. Two approaches are considered for the determination of the volume of finished work: (i) only finished activities are considered; (ii) any part of work completed by the review point is accounted for. Considering that by increasing the volume of work at each review point, the contractor can increase the amount of payments due to him and as such increase his NPV, an interesting question arises about the suitability of compressing some activities so that more activities can be performed within the current review points. From now on, we call this problem *crash max* NPV^{PP}

problem and develop some mathematical models to study it.

The rest of the paper is organized as follows. In Section 2, we present two models for the problem to account for the two approaches proposed to determine the volume of finished work. In Section 3, we tailor the models of Section 2 for the problem. In Section 4, we discuss the results and determine the most significant parameters. Some conclusions are drawn in Section 5.

2 *max* NPV^{PP} Problem

To study *max* NPV^{PP} Problem, we assume that the project with activities is represented in AON format. Finish to start precedence with zero lag governs the relations between activities. The following notations are used in our analysis:

d_i	:	Duration of activity i $(1 \leq i \leq n)$
c_i	:	Cost of performing activity i $(1 \leq i \leq n)$
s_i	:	Starting time for activity i $(1 \leq i \leq n)$
f_i	:	Completion time for activity i $(1 \leq i \leq n)$
Ef_i	:	Earliest finish time for activity i $(1 \leq i \leq n)$
Lf_i	:	Latest finish time for activity i $(1 \leq i \leq n)$
α	:	Discount rate
D	:	Project deadline
c_t	:	Discount factor for time t, $c_t = e^{-\alpha t}, t = 0, 1, ..., D$
T	:	A constant period of time , $mT \geq D, (m-1)T < D$
P_t	:	Payment amount at review point t, $t = T, 2T, ..., mT$
ω_{it}	:	Percentage of activity i completed in the interval $(t-T, t]$, $t = T, 2T, ..., mT$
W_{it}	:	Percentage of activity i completed in the interval $(0, t]$, $t = T, 2T, ..., mT$

The negative and positive cash flows with respect to activity i is c_i and $(1+\gamma_i)$ c_i respectively. Let $\{T, 2T, ..., mT\}$ denotes the set of review points (if $mT > D$ then $mT = D$). The amount of payment is based on two different approaches. We use example of Fig.1 to illustrate the differences between the two approaches. There are three activities in Fig.1 whose durations, costs and marginal profits are 20, 600 and 20 respectively. we assume that it is required to determine the amount of payments at $T = 30$ and $2T = 60$. We have:

Approach 1 -In Approach 1 we only consider the cost of those activities that are finished in the time interval $(t-T, t]$. With reference to Fig.1, $P_T = 0$, because no activity is completed in the interval $(0, T]$. However, in the interval $(T, 2T]$ all the three activities are completed, therefore

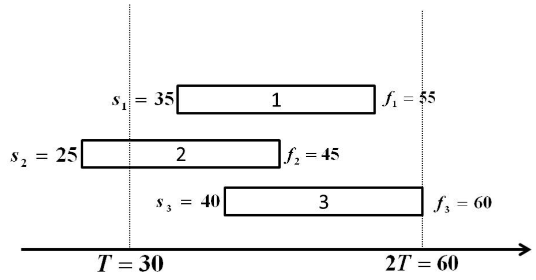

Figure 1: Schedule of three activities.

$P_{2T} = (1 + \gamma_1)\ c_1 + (1 + \gamma_2)\ c_2 + (1 + \gamma_3)\ c_3 = 2160.$

Approach 2 -In this approach the cost of performing any section of the activities in the time interval $(t-T, t]$ is considered. Up to the point T, only 25% of activity 2 is completed. So $\omega_{2,T} = 5/20$ and $P_T = (1 + \gamma_2)\ \omega_{2,T}\ c_2 = 180$. In the interval $(T, 2T]$ we have: $\omega_{1,2T} = \omega_{3,2T} = 1$ and $\omega_{2,2T} = 15/20$. Therefore, $P_{2T} = (1+\gamma_1)\ \omega_{1,2T}\ c_1 + (1+\gamma_2)\ \omega_{2,2T}\ c_2 + (1+\gamma_3)\ \omega_{3,2T}\ c_3 = 1980$. As it can be seen, the total amount of payments in the two review points is 2160. In fact, the total amount of payments can be obtained from $\sum_{i=1}^{n}(1 + \gamma_i)\ c_i$. However, the discounted amount of payments at rate α at time t is given by $P_t e^{-\alpha t}$. In the next section we present two models for the $max\ NPV^{PP}$ according to the given approaches. Model $max\ NPV^{PP}$ with respect to Approach 1 is called $max\ NPV_1^{PP}$ and with respect to Approach 2 is called $max\ NPV_2^{PP}$.

2.1 Models

We develop our models based on the aforementioned assumptions. Note that the contractor's estimate of the amount due to him is based on the marginal profit, the costs of performing the activities and the approach adopted for determining the volume of the work performed. In order to illustrate the features of the proposed models we use the example project given in Appendix A.

2.1.1 Model $max\ NPV_1^{PP}$

For each activity i and time t, variable δ_{it} indicates whether activity i has occurred before time period t, namely $\delta_{it} = 1$ if $f_i \leq t$ and 0 otherwise. Thus, $\delta_{iD} = 1$ for $i = 1, 2, ..., n$.

$$Max \sum_{t=T,2T,...,mT} P_t \; e^{-\alpha t} - \sum_{i=1}^{n} c_i \; e^{-\alpha f_i} \tag{1}$$

s.to.

$$f_1 = 0 \tag{2}$$

$$f_j - d_j \geq f_i \qquad (i,j) \in A \tag{3}$$

$$f_i \leq t + (1 - \delta_{it})D \qquad i = 1,2,...,n; t = 0,1,...,D \tag{4}$$

$$f_i \geq t - \delta_{it}D \qquad i = 1,2,...,n; t = 0,1,...,D \tag{5}$$

$$\sum_{s=T}^{t} P_t \leq \sum_{i=1}^{n} (1+\gamma_i)\delta_{it} \; c_i \qquad t = T, 2T, ..., mT \tag{6}$$

$$f_i \geq 0 \qquad i = 1,2,...,n \tag{7}$$

$$P_t \geq 0 \qquad t = T, 2T, ..., mT \tag{8}$$

$$\delta_{it} \in \{0,1\} \qquad i = 1,2,...,n; t = 0,1,...,D \tag{9}$$

The objective function in (1) maximizes the NPV. Constraint (2) enforces the project to start at time 0. The set of constraints in (3) ensure the precedence relations between the activities while constraints (4) and (5) display the relations between f_i , δ_{it} and t with respect to activity i and determine the values of δ_{it}. Constraint (6) ensures that the payment at each review point t is not more than the volume of work performed. Model $max\ NPV_1^{PP}$ as described by (1) to (9) is a mixed integer program with a nonlinear objective function and a set of linear constraints. The objective can be linearized as follows. Let $x_{it} = 1$ denotes the completion of activity i at time t, and $x_{it} = 0$ denotes otherwise. The completion time for an activity can be expressed as $f_i = \sum_{t=Ef_i}^{Lf_i} t \; x_{it}$. Similarly, the variable δ_{it} can be expressed as $\delta_{it} = \sum_{s=0}^{t} x_{is}$.
Since $x_{if_i} = 1$ and $x_{it} = 0$ for $t \neq f_i$ then $\sum_{t=Ef_i}^{Lf_i} c_t x_{it} = c_{f_i}$. Now the second part of (1) becomes

$$\sum_{i=1}^{n} c_i \; e^{-\alpha f_i} = \sum_{i=1}^{n} c_i \; c_{f_i} = \sum_{i=1}^{n} c_i \sum_{t=Ef_i}^{Lf_i} c_t x_{it}$$

which if substituted in model $max\ NPV_1^{PP}$, produces a linear programming model (10-16) that we call *linear max* NPV_1^{PP}.

$$Max \sum_{t=T,2T,...,mT} P_t\ c_t - \sum_{i=1}^{n} c_i \sum_{t=Ef_i}^{Lf_i} c_t\ x_{it} \tag{10}$$

$s.to.$

$$x_{1,0} = 0 \tag{11}$$

$$\sum_{t=Ef_i}^{Lf_i} x_{it} = 1 \qquad i = 1, 2, ..., n \tag{12}$$

$$\sum_{t=Ef_j}^{Lf_j} (t - d_j)x_{jt} \geq \sum_{t=Ef_i}^{Lf_i} tx_{it}, \qquad (i, j) \in A \tag{13}$$

$$\sum_{s=T}^{t} P_t \leq \sum_{i=1}^{n}(1 + \gamma_i)c_i \sum_{s=0}^{t} x_{is} \qquad t = T, 2T, ..., mT \tag{14}$$

$$P_t \geq 0 \qquad t = T, 2T, ..., mT \tag{15}$$

$$x_{it} \in \{0, 1\} \qquad i = 1, 2, ..., n;\ t = 0, 1, ..., D \tag{16}$$

Constraint (12) ensures that there is only one finish time for each activity as no activity preemption is allowed. Set of constraints in (13) ensure the precedence relations between the activities. Using model (10-16), the example project is solved by GAMS and BONMIN as the solver [1]. The optimal schedule with the NPV of 2611.977 is shown in Fig.2. As it can be seen activities have been scheduled so that the maximum amount is paid at review points, and also they are scheduled as late as possible to delay the accruement of costs. For instance, in the time interval (0,30], activity 2 and after that, activities 3, 4, 5 and 6 have been scheduled as late as possible. In addition, if activity 2 was to finish on day 8, the NPV would have decreased to 2523.324. This is because the increase in payments due to activities 7 and 8 being finished on day 30 does not compensate the costs of performing the activities that now had to be paid earlier.

2.1.2 Model $max\ NPV_2^{PP}$

In this model any parts of the activities that are completed are considered for the analysis of payments. To calculate W_{it}, the fraction of activity i completed at review point t, three situations might occur (see Fig.3) which should be considered. The amount of W_{it} is calculated as follows:

$$W_{it} = \delta_{it} + (1 - \delta_{it})\ max\{0, \frac{t - (f_i - d_i)}{d_i}\} \tag{17}$$

$$0 \leq W_{it} \leq 1 \qquad i = 1, 2, ..., n;\ t = T, 2T, ..., mT \tag{18}$$

Using W_{it}, we rewrite the constraint about the payments as follows:

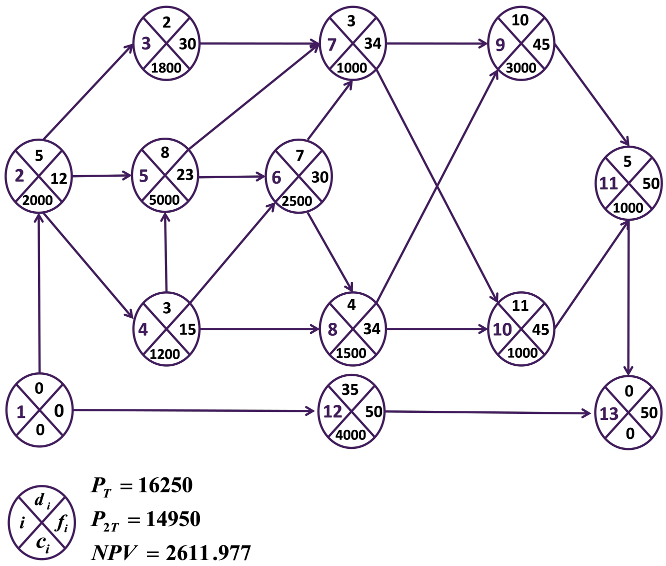

Figure 2: The *linear max* NPV_1^{PP} model - the optimal payment schedule.

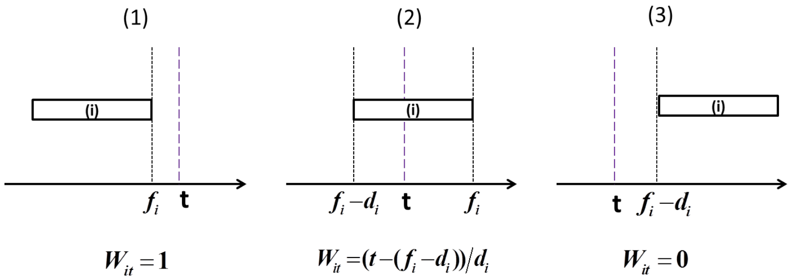

Figure 3: Portions of work completed in the interval $(0, t]$.

$$\sum_{s=T}^{t} P_s \leq \sum_{i=1}^{n} (1+\gamma_i)\ W_{it} c_i \qquad t = T, 2T, ..., mT \tag{19}$$

By adding (17) and (18) to model *max* NPV_1^{PP} and replacing constraint (6) with (19) we obtain model *max* NPV_2^{PP}. This is also a mixed integer nonlinear programming model. Using model *max* NPV_2^{PP} the example project was solved by GAMS with DICOPT as the solver. The acceptable schedule with the NPV of 2980.275 is the same as Fig.2. However the NPV has increased. This is because at review point 30 part of activity 12 which is partially completed has also been accounted for.

3 *crash max* NPV^{PP} Problem

In most projects, it is possible to compress the duration of all or some of the activities by allocating extra resources. Obviously, allocation of extra resources costs more. In spite of the fact that the contractor pays this extra cost, his motivation for crashing activities in the *crash max* NPV^{PP} problem as described previously is the possible benefit that can be gained by the earlier payment of increased volume of work performed. The activity i's duration after compression, d'_i, can be varied between its normal duration, d_i, and its crashed duration, d''_i, i.e. $d''_i \leq d'_i \leq d_i$. The cost of activity i, if performed at crashed duration is c''_i. Therefore the resource utilization rate of activity i is $c'_i = (c''_i - c_i)/(d_i - d''_i)$. The discounted cash flow for activity i is therefore $(c_i + c'_i(d_i - d'_i))\ e^{-\alpha f_i}$. Recall that costs are accrued at the completion of activities and payments are done at review points. In the next section we present our models.

3.1 *crash max* NPV^{PP} Model based on Approach 1

The following model is based on the *linear max* NPV_1^{PP} developed in the previous section.

$$Max \sum_{t=T,2T,...,mT} P_t\ c_t - \sum_{i=1}^{n}(c_i + c'_i(d_i - d'_i)) \sum_{t=0}^{D} c_t\ x_{it} \tag{20}$$

$s.to.$

$$x_{1,0} = 0 \tag{21}$$

$$\sum_{t=0}^{D} x_{it} = 1 \qquad i = 1, 2, ..., n \tag{22}$$

$$\sum_{t=0}^{D}(t - d'_j)x_{jt} \geq \sum_{t=0}^{D} t\ x_{it} \qquad (i,j) \in A \tag{23}$$

$$\sum_{s=T}^{t} P_s \leq \sum_{i=1}^{n}(1+\gamma_i)c_i \sum_{s=0}^{t} x_{is} \qquad t = T, 2T, ..., mT \tag{24}$$

$$d'_i \leq d_i \qquad i = 1, 2, ..., n \tag{25}$$

$$d'_i \geq d''_i \qquad i = 1, 2, ..., n \tag{26}$$

$$P_t \geq 0 \qquad t = T, 2T, ..., mT \tag{27}$$

$$x_{it} \in \{0, 1\} \qquad i = 1, 2, ..., n;\ t = 0, 1, ..., D \tag{28}$$

Constraints (25) and (26) ensure that activity's compressed duration is within its corresponding bounds. We now linearize the objective function in (20).

To that end, we replace $d'_i x_{it}$ with the new variable, F_{it}. This is a standard subsititution requring additional constraints to link x_{it}, d'_i and F_{it}. The values of F_{it} are determined by the following additional constraints.

$$F_{it} - x_{it}\ d_i \leq 0 \qquad i = 1, 2, ..., n;\ t = 0, 1, ..., D \tag{29}$$

$$F_{it} - d'_i \leq 0 \qquad i = 1, 2, ..., n;\ t = 0, 1, ..., D \tag{30}$$

$$F_{it} \geq d'_i - (1 - x_{it})d_i \qquad i = 1, 2, ..., n;\ t = 0, 1, ..., D \tag{31}$$

$$F_{it} \geq 0 \qquad i = 1, 2, ..., n;\ t = 0, 1, ..., D \tag{32}$$

Now the second part of (20) becomes

$$\sum_{i=1}^{n}\sum_{t=0}^{D}((c_i + c'_i d_i)x_{it} - c'_i F_{it})c_t \tag{33}$$

The resulting model is a mixed integer linear program which we call *linear crash max* NPV_1^{PP}. The optimum solution for the example problem using the above model is shown in Fig.4. Note that the project NPV has increased to 3036.982 when compared with the case where no crashing of activities was allowed. This shows that even when the contractor pays for the extra cost of activity crashing, it can increase his NPV. As can be seen, activities 5, 6, 7, and 8 have been compressed resulting in a larger volume of work being performed up to review point of 30. Activity 11 which has been crashed by 2 days has caused activities 9 and 10 to end 2 days later and as a result their corresponding costs accrued in later time.

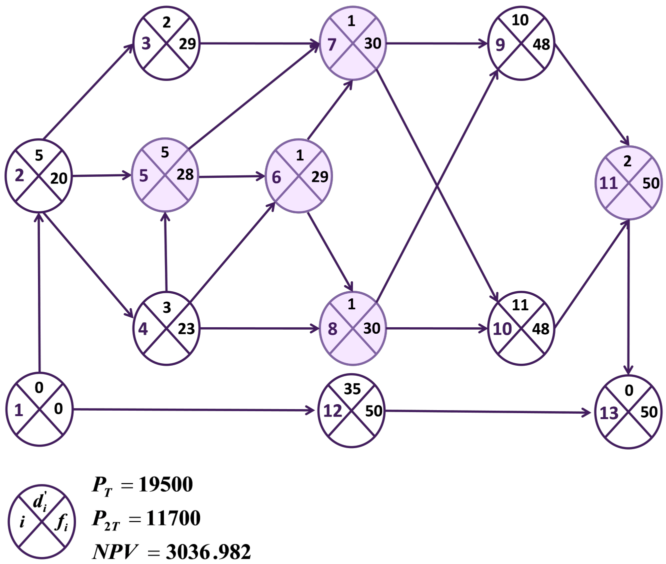

Figure 4: The *linear crash max* NPV_1^{PP} model - the optimal payment schedule.

3.2 *crash max* NPV^{PP} Model based on Approach 2

The following model is based on the *max* NPV_2^{PP}.

$$Max \sum_{t=T,2T,...,mT} P_t \; e^{-\alpha t} - \sum_{i=1}^{n}(c_i + c'_i(d_i - d'_i)) \; e^{-\alpha f_i} \tag{34}$$

$s.to.$

$$f_1 = 0 \tag{35}$$

$$f_j - d'_j \geq f_i \qquad (i,j) \in A \tag{36}$$

$$f_i \leq t + (1-\delta_{it})D \qquad i = 1,2,...,n; t = 0,1,...,D \tag{37}$$

$$f_i \geq t - \delta_{it}D \qquad i = 1,2,...,n; t = 0,1,...,D \tag{38}$$

$$W_{it} = \delta_{it} + (1-\delta_{it}) \; max\{0, \frac{t-(f_i - d'_i)}{d'_i}\} \qquad i = 1,2,...,n; \; t = T,2T,...,mT \tag{39}$$

$$\sum_{s=T}^{t} P_s \leq \sum_{i=1}^{n}(1+\gamma_i)W_{it} \; c_i \qquad t = T,2T,...,mT \tag{40}$$

$$d'_i \leq d_i \qquad i = 1,2,...,n \tag{41}$$

$$d'_i \geq d''_i \qquad i = 1,2,...,n \tag{42}$$

$$0 \leq W_{it} \leq 1 \qquad i = 1,2,...,n; \; t = T,2T,...,mT \tag{43}$$

$$f_i \geq 0 \qquad i = 1,2,...,n \tag{44}$$

$$P_t \geq 0 \qquad t = T,2T,...,mT \tag{45}$$

$$\delta_{it} \in \{0,1\} \qquad i = 1,2,...,n; \; t = 0,1,...,D \tag{46}$$

The resulting model is a mixed integer non-linear program which we call *crash max* NPV_2^{PP}. An acceptable solution for the example problem using above model is the same as Fig.4. However the project's NPV has increased to 3405.28. This is because at a review point 30 part of activity 12 which is partially completed has also been accounted for.

4 Discussion of Results

The results obtained by our proposed four models with respect to the project example are given in Table 1. In this example, payments are done at the end of the review points 30 and 50. Since the time and the total amount of payments are known, increasing the amount of payments in review points nearer to the beginning of the project will increase the contractors profit. Therefore, in the example project the compression of activities is used to increase the amount of payments at review point 30. As expected, the amount of payment at review point 30 when some activities are crashed has increased from 16250 to 19500 under Approach 1 and from 18478.57 to 21728.57 under Approach 2. The schedule obtained by the $max\ NPV^{PP}$ model and the

Table 1: Models and results.

Model	Amount of Payments	NPV
$linear\ max\ NPV_1^{PP}$	$P_T = 16250$	2611.944
	$P_{2T} = 14950$	
$linear\ crash\ max\ NPV_1^{PP}$	$P_T = 19500$	3036.982
	$P_{2T} = 11700$	
$max\ NPV_2^{PP}$	$P_T = 18478.57$	2980.275
	$P_{2T} = 12721.43$	
$crash\ max\ NPV_2^{PP}$	$P_T = 21728.57$	3405.280
	$P_{2T} = 9471.43$	

$crash\ max\ NPV^{PP}$ model is shown in Fig.5. Observe that in both generated schedules, the activities are scheduled as near to the review points as possible. This is done so that the costs are incurred as near as possible to the locations where payments are due. In addition, the payment of costs has also been delayed as much as possible. For instance, in $crash\ max\ NPV^{PP}$ model, activities 9 and 10 can start at time instance of 30. Note that, this does not affect volume of the work performed up to this point of time. Should these activities start at time instance 30, the payment of their costs that is now advanced will affect the NPV adversely. Therefore, the model has not scheduled them to start at time 30. The activities in $crash\ max\ NPV^{PP}$ model are compressed such that: (i) the volume of work performed up to the time instant 30 is increased as much as possible; and (ii) activities in the interval (30, 50] are scheduled as near as possible to the review point 50. Although compression of activity 11 has no effect on the volume of work performed, but it allows activities 9 and 10 to be completed 2 days later and as such delay the payment of their costs by the same amount. This will improve the NPV. Note that, the cost of compressing activity 11 is compensated by the profit yielded by delaying the payments of activities 9 and 10 costs. It is obvious that the crashing costs, the marginal profit and the discount rate are significant parameters that affect the decision regarding the compression of project activities to increase the contractor's NPV. For example, high compression costs and low marginal profit may convince the contractor not to proceed with activity crashing. In fact, the contractor pays for the cost of crashing some of the activities by the profit yielded from increasing the volume of work up to each review point and also by delaying some other activities. Therefore, if crashing of activities does not yield any profit for the contractor, he has no motivation to proceed with activity crashing. In the example project, if we consider the profit margin as 15% and the crashing

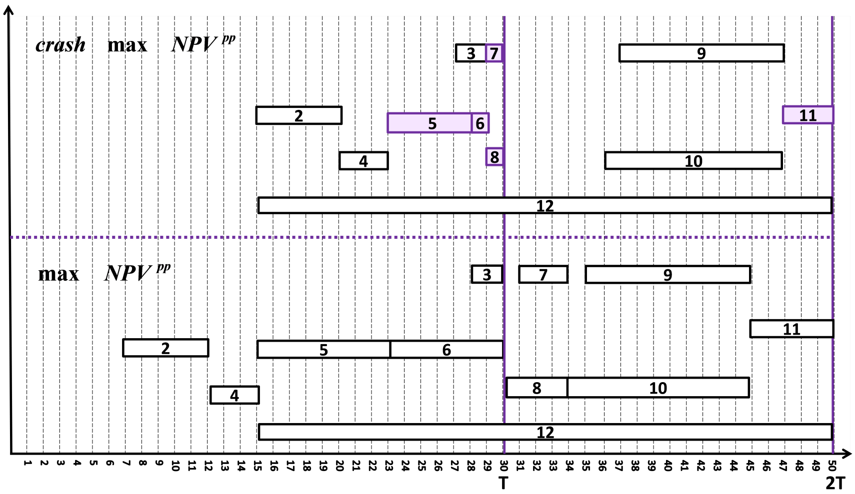

Figure 5: Comparison of normal and compressed schedules.

costs of activities as 0, 2700, 1800, 1200, 5800, 4000, 1400, 2400, 4500, 1500, 1800, 5900 and 0, no activity will be crashed.

5 Conclusions

In this paper, we addressed the problem of project payment scheduling when a project deadline is specified and activities are allowed to be compressed with the purpose of maximizing the contractor's *net present value* (NPV). The cost of activity compression is paid by the contractor. We assumed that the payments are made to the contractor based on the volume of work performed, at some pre-specified points of time. We also assumed that the costs of activities are incurred at the completion of activities. We developed four mathematical models based on two different approaches to account for the volume of work performed. In the first approach, only those activities that by the review time have been completed were considered as the volume of work performed. In the second approach, we considered any section of activities that were completed by the review time. Through a small illustrative example, it was shown that the contractor may in fact increase his profit by crashing activities.

Appendix A

A project with 11 activities is considered. All the relevant information is given in Table 2. The earliest time that the project can be delivered is 42, whereas the deadline is 50. Marginal profit with respect to each activity is 30%, the discount rate is 1.5% and the review period is considered to be 30. Therefore, review points are at $T = 30$, $2T = 50$.

Table 2: The example project.

Activity	Predecessor(s)	Normal Duration	Crashed Duration	Normal Cost	Crashed Cost
1	–	0	0	0	0
2	1	5	1	2000	2700
3	2	2	2	1800	1800
4	2	3	3	1200	1200
5	2, 4	8	5	5000	5150
6	4, 5	7	2	2500	3000
7	3, 5	3	1	1000	1100
8	4, 6	4	1	1500	1600
9	7	10	1	3000	4000
10	7,8	11	5	1000	1500
11	9,10	5	2	1000	1150
12	1	35	20	4000	5500
13	11,12	0	0	0	0

References

1. Brooke, A., Kendrick K. and Meeraus, A. *GAMS: A Users Guide, The Scientific Press: CA*. 1988.

2. Dayanand, N. and Padman, R. *Payments in projects: a contractor's model.* Technical Report, The Heinz School, Carnegie Mellon University, Pittsburgh, 1993.

3. Dayanand, N. and Padman, R. *On modeling payments in project networks.* Journal of the Operational Research Society, 48 (1997), 906-918.

4. Dayanand, N. and Padman, R. *A two stage search heuristic for scheduling payments in projects.* Annals of Operations Research, 102 (2001), 197-220.

5. Dayanand, N. and Padman, R. *Project contracts and payment schedules: the clients problem.* Management Science, 47(12) (2001), 1654-1667.

6. Elmaghraby, S.E. and Herroelen, W.S. *The scheduling of activities to maximize the net present value of projects*. European Journal of Operational Research, 49 (1990), 35-49.

7. Grinold, R.C. *The payment scheduling problem*. Naval Research Logistics Quarterly, 19(1) (1972), 123-136.

8. He, Z. and Xu, Y. *Multi-mode project payment scheduling problems with bonus-penalty structure*. European Journal of Operational Research, 189(3) (2008), 1191-1207.

9. He, Z., Wang, N., Jia, T. and Xu, Y. *Simulated annealing and tabu search for multi-mode project payment scheduling*. European Journal of Operational Research, 198(3) (2009), 688-696.

10. He, Z., Liu, R. and Jia, T. *Metaheuristics for multi-mode capital-constrained project payment scheduling*. European Journal of Operational Research, 223 (2012), 605-613.

11. Herroelen, W.S., VAN Dommelen P. and Demeulemeester, E.L. *Project network models with discounted cash flows a guided tour through recent developments*. European Journal of Operational Research, 100 (1997), 97-121.

12. Kavlak, N., Ulusoy, G., Serifoglu, F.S. and Birbil, S.I. *Client-contractor bargaining on net present value in project scheduling with limited resources*. Naval Research Logistics, 56(2) (2009), 93-112.

13. Kazaz, B. and Sepil, C.B. *Project scheduling with discounted cash flows and progress payments*. Journal of the Operational Research Society, 47 (1996), 1262-1272.

14. Mika, M., Waligora, G. and Weglarz, J. *Simulated annealing and tabu search for multi-mode resourceconstrained project scheduling with positive discounted cash flows and different payment models*. European Journal of Operational Research, 164 (2005), 639-668.

15. Russell, A.H. *Cash Flows in networks*. Management Science, 16(5) (1970), 357-373.

16. Sepil, C. and Ortac, N. *Performance of the heuristic procedures for constrained projects with progress payments*. Journal of the Operational Research Society, 48 (1997), 1123-1130.

17. Szmereskovsky, J.G. *The impact of contractor behaviour on the client's payment scheduling problem*. Management Science, 51(4) (2005), 629-640.

18. Talbot, F.B. *Resource-constrained project scheduling with time-resource trade offs: the nonpreemptive case*. Management Science, 28(10) (1982), 1197-1210.

19. Tantisuvanichkul, V. and Kidd, M. *Maximizing net present value a review through literature.* 2^{nd} International Conference on Construction and Project Management, Singapore, 2011.

20. Ulusoy, G. and Cebelli, S. *An equitable approach to the payment scheduling problem in project management.* European Journal of Operational Research, 127 (2000), 262-278.

21. Ulusoy G., Sivrikaya-Serifoglu, F. and Sahin, S. *Four payment models for the multi-mode resource constrained project scheduling problem with discounted cash flows.* Annals of Operations Research, 102 (2001), 237-261.

22. Vanhoucke, M., Demeulemeester, E. and Herroelen, W. *Progress payments in project scheduling problems.* European Journal of Operational Research, 148 (2003), 604-620.

23. Vanhoucke, M. and Debels, D. *The discrete time cost trade-off problem under various assumptions exact and heuristic procedures.* Journal of Scheduling, 10 (2007), 311-326.

Iranian Journal of Numerical Analysis and Optimization
Vol. 7, No. 2, (2017), pp 57–64
DOI:10.22067/ijnao.v7i2.57912

Augmented Lagrangian method for finding minimum norm solution to the absolute value equation

S. Ketabchi* and H. Moosaei

Abstract

In this paper, we give an algorithm to compute the minimum 1-norm solution to the absolute value equation (AVE). The augmented Lagrangian method is investigated for solving this problem. This approach leads to an unconstrained minimization problem with once differentiable convex objective function. We propose a quasi-Newton method for solving unconstrained optimization problem. Computational results show that convergence to high accuracy often occurs in just a few iterations.

Keywords: Absolute value equation; Minimum norm solution; Generalized Newton method; Augmented Lagrangian method.

1 Introduction

As shown in [1, 2, 9–11], many mathematical programming problems can be reduced to LCP which is equivalent to absolute value equation as follows [7, 8, 12]:

$$Ax - |x| = b, \tag{1}$$

where $A \in R^{n\times n}$ and $b \in R^n$ are given, and $|x|$ denotes the component-wise absolute value of vector $x \in R^n$.

---

*Corresponding author
Received 2 August 2016; revised 28 December 2016; accepted 22 February 2017
S. Ketabchi
Department of Applied Mathematics, Faculty of Mathematical Sciences, University of Guilan, P.O. Box 1914, Rasht, Iran. e-mail: sketabchi@guilan.ac.ir

H. Moosaei
Department of Mathematics, Faculty of Science, University of Bojnord, Bojnord, Iran. e-mail: hmoosaei@gmail.com, moosaei@ub.ac.ir

The absolute value equation (1) seems to be a useful tool in optimization since it subsumes the linear complementarity problem and thus also linear programming and convex quadratic programming.

In general, AVE may have a finite number of solutions (at most 2^n) or infinitely many solutions, if it has solutions [7]. In such cases, the selection of a particular solution may be important and a natural choice is the solution with the minimum norm [4, 5, 9].
In this paper, we consider AVE in the case where it has multiple (e.g., exponentially many) solutions; we try to compute its minimum $1-norm$ solution.

In [5], for finding minimum $2-norm$ solution of AVE, need a solution of AVE and special assumptions on A. But, in this paper to find minimum $1-norm$ solution of AVE, not only do not need a solution of AVE but also do not need any special assumptions on A.

Consider the following problem :

$$\begin{aligned} & \min_{x\in R^n} \|x\|_1 \\ \textit{subject to} \qquad & Ax - |x| = b. \end{aligned} \tag{2}$$

Motivated by the study of minimum $1-norm$ solution of the AVE formulated as a linear programming problem. To solve this linear programming problem, we suggest augmented Lagrangian method.

This paper is organized as follows. Minimum norm solution of AVE is described in Section 2. The augmented Lagrangian method is discussed in Section 3. In Section 4 compute minimum norm solution for some randomly generated AVE to demonstrate the effectiveness of our method. Concluding remarks are given in Section 5.

We now describe our notations. Let $a = [a_i]$ be a vector in R^n. By a_+ we mean a vector in R^n whose ith entry is 0 if $a_i < 0$ and equals a_i if $a_i \geq 0$. By A^T we mean the transpose of matrix A, and $\nabla f(x_0)$ is the gradient of f at x_0. For two vectors x and y in the $n-$dimensional real space, $x^T y$ will denote the scalar product. For $x \in R^n$, $\|x\|$ and $\|x\|_1$ denote 2−norm and 1−norm respectively and $|x|$ will denote the vector in R^n of absolute values of components of x.

2 Minimum Norm Solution of AVE

In this section we first mention the cases in which the AVE has multiple solutions. Then, we examine the problem (1) to obtain its minimum norm solution.

Proposition 1. *(Existence of 2^n solutions). If $b < 0$ and $\|A\|_\infty < \gamma/2$ where $\gamma = c/d$, $c = min_i|b_i|$, $d = max_i|b_i|$, then the AVE has exactly 2^n distinct solutions, each of which has no zero components and a different sign pattern.*

Proof. See [7]. □

Consider the absolute value equation (1) for which $A = -\frac{1}{4}eye(n)$ and $b = -2ones(n,1)$, it is obvious that, it has exactly 2^n distinct solutions. Now, consider for example of an AVE that has infinite number of solutions. Consider the absolute value equation (1) for which $A = eye(n)$ and $b = zeros(n,1)$. Obviously, in this case, every x for which $x \geq 0$ is a solution of AVE. Let's again consider the problem (2). This problem can be rewritten in the equivalent form:

$$\min_{p,q\in\mathbb{R}^n} \|p-q\|_1, \quad s.t. \quad Ap - Aq - Ip - Iq = b, \qquad p,q \geq 0, \tag{3}$$

where $p = \frac{|x|+x}{2}$ and $q = \frac{|x|-x}{2}$.

Now (3) is equivalent to linear programming problem as follows:

$$\min_{X\in\mathbb{R}^n} c^T X, \quad s.t. \quad BX = b, \quad X \geq 0, \tag{4}$$

where $X = [p \quad q]^T$, $c = [e \quad e]^T$ and $B = [A - I \quad -A - I]$.

To solve the problem (4), we use augmented Lagrangian method, which is described in the next section.

3 Augmented Lagrangian Method

Now, we briefly discuss applications of augmented Lagrangian method to the linear programming subproblem (4).

In the augmented Lagrangian method, an unconstrained maximization problem is solved which gives the projection of a point on the solution set of the subproblem

$$\min_{x\in X_*} \frac{1}{2} \parallel x - \bar{x} \parallel^2, \tag{5}$$
$$X_* = \{x \in R^n : Ax = b, c^T x = f_*, \quad x \geq 0_n\}.$$

The Lagrange function for the problem (5) is

$$L(x,u,\alpha,\bar{x}) = \frac{1}{2} \parallel \bar{x} - x \parallel^2 - u^T(Ax - b) + \alpha\ (c^T x - f_*),$$

where $u \in R^m$, $\alpha \in R^1$ are Lagrange multipliers and $\bar{x}$ is considered as a fixed parameter. The dual problem of (5) is

$$\max_{u\in R^m}\max_{\alpha\in R^1}\min_{x\in R^n_+} L(x,u,\alpha,\bar{x}). \tag{6}$$

The optimality conditions of the inner minimization of the problem (6) is

$$\nabla L_x(x,u,\alpha,\bar{x}) = x-\bar{x}-A^Tu+\alpha c \geq 0, \tag{7}$$

$$x^\top(x-\bar{x}-A^Tu+\alpha c)=0, \qquad x\geq 0. \tag{8}$$

It follows from (7) and (8) that the solution of this minimization problem is given in the following form:

$$x=(\bar{x}+A^Tu-\alpha c)_+, \tag{9}$$

we replace x by $(\bar{x}+A^Tu-\alpha c)_+$ into $L(x,u,\alpha,\bar{x})$ and obtain the dual function

$$\Phi(u,\alpha,\bar{x}) = b^Tu-\frac{1}{2}\parallel(\bar{x}+A^Tu-\alpha c)_+\parallel^2 -\alpha f_* + \frac{1}{2}\parallel \bar{x}\parallel^2 .$$

Hence the problem (5) is reduce to its dual problem

$$\max_{u\in R^m}\max_{\alpha\in R^1}\Phi(u,\alpha,\bar{x}). \tag{10}$$

This problem is an optimization problem without any constrain and its objective function contains an unknown value f_*. By [3] there exists a positive number $\alpha_*>0$ such that, for each $\alpha>\alpha_*$, the projection x of the arbitrary vector $\bar{x}\in R^n$ onto X_* can be obtained as following:

$$x=(\bar{x}+\alpha(A^Tu(\alpha)-c))_+, \tag{11}$$

where $u(\alpha)$ is the solution of the problem (10), such that $\alpha\in R^1$, $\alpha>\alpha_*$ is fixed.

We note that, the function $\Phi(u,\alpha,\bar{x})$ is the augmented Lagrangian function for dual problem of (5) (see [3]),

$$f_*=\max_{u\in U} b^Tu, \quad U=\{u\in R^m : A^Tu\leq c\}. \tag{D}$$

The function $\Phi(u,\alpha,\bar{x})$ is piecewise quadratic, convex and just has the first derivative, but it is not twice differentiable. Suppose that s and t are arbitrary points in R^m. Then for $\nabla\Phi_u(u,\alpha,\bar{x})$ we have

$$\|\nabla\Phi_u(s,\alpha,\bar{x})-\nabla\Phi_u(t,\alpha,\bar{x})\|\leq\|A\|\|A^T\|\|s-t\|, \tag{D}$$

this means that $\nabla\Phi$ is globally Lipschitz continues with constant $K=\|A\|\|A^T\|$. Thus for this function generalized Hessian exists and is defined the $m\times m$ symmetric positive semidefinite matrix [6, 9].

Now we introduce the following iterative process :

$$u^{k+1} = arg \min_{u \in R^n} \{-b^T u + \frac{1}{2\alpha} \parallel (x^k + \alpha(A^T u - c))_+ \parallel^2, \tag{12}$$

$$x^{k+1} = (x^k + \alpha(A^T u^{k+1} - c))_+, \tag{13}$$

where u^0 and x^0 are arbitrary starting point.

Theorem 2. *Let the solution set X_* of the problem (5) be nonempty. Then, for all $\alpha > 0$ and an arbitrary initial x^0, the iterative process (12), (13) converges to $x_* \in X_*$ in finite number of step k and the primal minimum norm solution $\widehat{x}_*$ was obtained after the first iteration from above process, i.e. $k = 1$. Furthermore, $u_* = u^{k+1}$ is an exact solution of the dual problem (D).*

The proof of the finite global convergence is given in [6]

Considering the advantage of the differentiability of the objective function of problems (12) and (D) allow us to use a quadratically convergent quasi-Newton algorithm with an Armijo stepsize [6] that makes the algorithm globally convergent.

We will now present a quasi-Newton-Armijo algorithm for solving the problem (12).

Algorithm 1 Newton method with the Armijo rule
Choose any $u_0 \in R^m$ and $tol > 0$
i=0;
while $\|\nabla f(u_i)_\infty\| \geq tol$
Choose $\alpha_i = max\{s, s\delta, s\delta^2, ...\}$ *such that*
$f(u_i) - f(u_i + \alpha_i d_i) \geq -\alpha_i \mu \nabla f(u_i)^T d_i$,
where $d_i = -\nabla^2 f(u_i)^{-1} \nabla f(u_i)$, $s > 0$ *be a constant,* $\delta \in (0,1)$ *and* $\mu \in (0,1)$.
$u_{i+1} = u_i + \alpha_i d_i$
$i = i + 1$;
end

In this algorithm, the Hessian may be singular, thus we used a modified Newton direction as follows :

$$-(\nabla^2 f(u_i) + \delta I_m)^{-1} \nabla f(u_i),$$

where δ is a small positive number ($\delta = 10^{-4}$), and I_m is the identity matrix of order m.

4 Numerical Experiments

In this section, we present some numerical results using the previous process on various randomly generated system (see Table 1) to illustrate the performance of the proposed algorithm. The algorithm has been tested using MATLAB *7.9.0* on a *Core 2 Duo 2.53 GHz* with main memory *4 GB*.
System generator creates a random matrix A for a given n, with singular value greater than or equal to 1. Then, we choose a random vector x from a uniform distribution on [0, 100]. Finally, we computed $b = Ax - |x|$. These systems are generated using the following MATLAB code:
`%Sgen: Generate random system` $A * x - |x| = b$ `with infinitely many solutions;`
$n = input('Enter n :');$
$A = spdiags(sign((rand(n,1) - 2 * rand(n,1))) + 2, 0, n, n);$ `% generates matrices in the MATLAB sparse storage organization.`
$x = 10 * ((rand(n,1) - rand(n,1)));$
$b = A * x - abs(x);$

Computational results for the test problems taken from our algorithm are given in Table 1.

The first column indicates the size of matrix A and the second column headed f indicates $\|A\widetilde{x^*} - |\widetilde{x^*}| - b\|$, the third column indicates minimum 1-norm solution and the forth column indicates 1-norm solution and the final column indicates CPU time.

Table 1: Minimum norm solution of $Ax - |x| = b$.

n	f	$\|\widetilde{x^*}\|_1$	$\|x^*\|_1$	time(sec)
10	0	0	2.3057e+003	0.13
100	1.4211e-014	3.7329e+003	1.3824e+004	0.49
200	1.1369e-013	1.2783e+004	3.4507e+004	0.73
300	5.6843e-014	1.5145e+004	5.7900e+004	1.45
400	5.6843e-014	1.2150e+004	6.6566e+004	1.88
500	1.1369e-013	1.8853e+004	8.6618e+004	2.78
600	1.1369e-013	2.2635e+004	9.4418e+004	4.32
700	1.1369e-013	2.5670e+004	1.1879e+005	5.66
800	1.1369e-013	3.6042e+004	1.3374e+005	6.89
900	1.1369e-013	3.7086e+004	1.5515e+005	11.02
1000	1.1369e-013	4.4200e+004	1.6893e+005	11.38
2000	1.1369e-013	7.5278e+004	3.3016e+005	74.18
3000	1.1369e-013	1.2762e+005	4.8708e+005	205.81
4000	1.1369e-013	1.7599e+005	6.7238e+005	493.59
5000	1.1369e-013	2.1200e+005	8.2995e+005	875.87

5 Conclusion

In this paper, the augmented Lagrangian algorithm was proposed and used for solving the minimum 1-norm solution to the absolute value equation. With this idea, we obtain the problem with fewer variables and smaller in size than the nonlinear problem (3). To obtain the solution to the reduced problem, we have proposed an extension of Newton's method with the step size chosen by the Armijo rule. As the numerical results show, this algorithm has appropriate speed in most of the problems and, specifically this can be observed in problems with a large sparse matrix A.

Acknowledgements

The authors are grateful to the anonymous referees and editor for their constructive comments.

References

1. Cottle, R.W. and Dantzig, G. *Complementary pivot theory of mathematical programming*, Linear Algebra Appl, 1 (1968), 103-125.

2. Cottle, R.W, Pang, J.S. and Stone, R.E. *The linear complementarity problem*, Academic Press, New York, 1992.

3. Evtushenko, Yu.G., Golikov, A.I. and Mollaverdi, N. *Augmented lagrangian method for large-scale linear programming problems*, Optimization Methods and Software, 20 (2005), 515-524.

4. Kanzow, C., Qi, H. and Qi, L. *On the minimum norm solution of linear programs*, J. Optim. Theory Appl, 116 (2003), 333-345.

5. Ketabchi, S. and Moosaei, H. *Minimum norm solution to the absolute value equation in the convex case*, J. Optim. Theory Appl, 154 (2012), 1080-1087.

6. Mangasarian, O.L. *A Newton method for linear programming*, J. Optim. Theory Appl, 121 (2004), 1-18.

7. Mangasarian, O.L. and Meyer, R.R. *Absolute value equations*, Linear Algebra Appl, 419 (2006), 359-367.

8. Moosaei, H., Ketabchi, S., Noor, M., Iqbal, J. and Hooshyarbakhsh, V. *Some techniques for solving absolute value equations*, Applied Mathematics and Computation, 268 (2015), 696-705.

9. Pardalos, P.M., Ketabchi, S. and Moosaei, H. *Minimum norm solution to the positive semidefinite linear complementarity problem*, Optimization, 63(3) (2014), 359-369.

10. Pardalos, P.M. and Rosen, J.B. *Global optimization approach to the linear complementarity problem*, SIAM Journal on Scientific and Statistical Computing, 9 (1988), 341-353.

11. Pardalos, P.M. and Ye, Y. *Class of linear complementarity problems solvable in polynomial time*, Linear Algebra and its Applications, 152 (1991), 3-17.

12. Prokopyev, O. *On equivalent reformulations for absolute value equations*, Computational Optimization and Applications, 44 (3) (2009), 363-372.

Iranian Journal of Numerical Analysis and Optimization
Vol. 7, No. 2, (2017), pp 65–85
DOI:10.22067/ijnao.v7i2.60552

The state of the art in Dynamic Relaxation methods for structural mechanics

Part 1: Formulations

M. Rezaiee-pajand*, J. Alamatian, and H. Rezaee

Abstract

In the last sixty years, the dynamic relaxation (DR) methods have evolved significantly. These explicit and iterative procedures are frequently used to solve the linear or nonlinear response of governing equations resulted from structural analyses. In the first part of this study, the common DR formulations are reviewed. Mathematical bases and also physical concepts of these solvers are explained briefly. All the DR parameters, i.e. fictitious mass, fictitious damping, fictitious time step and initial guess are described, as well. Furthermore, solutions of structural problems along with kinetic and viscous damping formulations are discussed. Analyses of the existing studies and suggestions for future research trends are presented. In the second part, the applications of dynamic relaxation method in engineering practices are reviewed.

Keywords: Dynamic Relaxation method; Formulation; Solver; Review; Iterative technique; State of the art.

---

*Corresponding author
Received 25 November 2016; revised 12 May 2017; accepted 23 April 2017
M. Rezaiee-pajand
Department of Civil Engineering, Factualy of Engineering, Ferdowsi Unversity of Mashhad, Mashhad, Iran. e-mail: rezaiee@um.ac.ir

J. Alamatian
Civil Engineering Department, Mashhad Branch, Islamic Azad Unversity, Mashhad, Iran. e-mail: alamatian@mshadiau.ac.ir

H. Rezaee
Department of Civil Engineering, Factualy of Engineering, Ferdowsi Unversity of Mashhad, Mashhad, Iran. e-mail: hasina1383@yahoo.com

Symbols

A_1^{n+1},A_2^{n+1}, A_3^{n+1},α,β	formulation parameters
c	fictitious damping factor
$[C]^n$	artificial damping matrix in nth iteration
$\{D\}$	vector of displacement
$\left\{\dot{D}\right\}^n$	artificial velocity vector in nth iteration
$\left\{\ddot{D}\right\}^n$	artificial acceleration vector in nth iteration
$\{f\}$	vector of internal forces
$\{f_I\}$	fictitious inertia force vector
$\{f_D\}$	fictitious damping force vector
$\left\{\dot{f}\right\}$	vector of internal force increment
$[I]$	unit matrix
L	Laplace operator
$[M]^n$	artificial mass matrix in nth iteration
MFT	modified fictitious time step
OFT	optimum fictitious time step
$\{P\}$	vector of external loads
$\{P\}_{EQ}^{k+1}$	equivalent load vector at $k+1^{th}$ step of numerical dynamic integration
q	number of degrees of freedom
$\{R\}$	vector of un-balance force
$\Re$	rectangular region
$[S]$	stiffness matrix
$[S]_{EQ}^{k+1}$	equivalent stiffness matrix at $k+1^{th}$ step of numerical dynamic integration
U_k	kinetic energy of fictitious dynamic system
UEF	un-balance energy function
UFF	un-balance force function
ρ	fictitious mass factor
τ	fictitious time step
ω_{min}	the lowest natural frequency of artificial dynamic system
Superscripts k	increment's number of dynamic analysis
n	iteration number of DR method
Subscripts i	each degree of freedom of structure

1 Introduction

Final stage of any structural analysis leads to the solution of a simultaneous system of equations. In other words, the responses of structures can be computed by solving the following equations, concluding from finite element or finite difference schemes:

$$[S]\{D\} = \{f\} = \{P\} \tag{1}$$

where $[S]$ is structural stiffness matrix, $\{D\}$, $\{f\}$ and $\{P\}$ are displacement, internal force and external load vectors, respectively. In nonlinear analyses, such as geometrical, material or contact nonlinearity, internal force vector is a nonlinear function of displacement, i.e. the elements of the stiffness matrix are not constant. The analytical and iterative procedures can be used for solving Eq. (1). In the solution of linear systems, the direct or analytical methods, such as Gaussian elimination technique, Cholesky factorization and other similar procedures, are generally more effective and economic than the iterative strategies. However, these approaches cannot be utilized for nonlinear cases individually, so that they should be combined with other corrective processes to present the exact answer. It is worth emphasizing that such corrective procedures belong to the iterative methods in which nonlinear step is divided and traced by several linear domains. This approach causes some numerical errors and reduces the efficiency of the analysis. As a result, the most suitable and effective ways of solving Eq. (1), especially in the nonlinear analysis, are iterative procedures.

The first major numerical effort to utilize the finite difference method in conjunction with a relaxation scheme was performed by Allen and Southwell [5]. These researchers solved the elastic-plastic problems of a continuum. In iterative schemes, an estimation of the answer is corrected by repeating some cycles. These techniques can be classified as implicit or explicit schemes, as acknowledged by Felippa [14] and Frankel [15]. Explicit techniques use residual force to get an answer, so that all calculations are performed by vector operations. Simplicity and high efficiency in the nonlinear analysis are the main specifications of the explicit techniques. On the other hand, implicit procedures are formulated based on residual force derivatives (stiffness matrix). Because of using matrix operations, calculations of implicit strategies are complex and time consuming. For example, snap-through or snap-back points, in which stiffness matrix is zero or undefined, cause some difficulties. However, the convergence rate of implicit methods is greater than the explicit schemes.

More than six decades have been passed since the dawn of the Dynamic Relaxation (DR) methods. A lot of efforts and considerable investigations have been directed toward the formulations and applications of these powerful approaches up to now. Unfortunately, a comprehensive survey related to these solution techniques has not been published so far. The purpose of this study is to report the state of the art on different aspects of the DR schemes. This literature review will be beneficial to researchers who are interested in the field of Dynamic Relaxation method. It will provide them with an insight on how this technique was developed, how it has progressed over the years and how it has been implemented in solving different problems. In the first part of this study, the common DR formulations are reviewed. Mathematical bases and also physical concepts of the Dynamic Relaxation are presented. These foundations are discussed to clarify the main specifications of the solvers. All the DR parameters, such as fictitious mass, fictitious damping, fictitious time step and initial guess are described. The required relationships to solve the structural problems are given. Both kinetic and viscous damping formulations are discussed. Finally, numerical steps require to take advantage of the presented formulas will be explained. In the second part, the applications of DR methods in engineering practices are reviewed.

2 Mathematical Basis

Since the development of high-speed computers, the various iterative procedures such as, the Southwell relaxation method has been successfully applied for solving partial differential equations. As it was reported by Frankel, solving the Laplace equations in a rectangular region is one of the first applications of these techniques which use finite difference approximations [15];

$$L\phi_{(x,y)} = 0, \quad x, y \in \Re, \tag{2}$$

In this relationship, $\Re$ is a rectangular region. The values of $\phi_{(x,y)}$are calculated from the iterative process so that Eq. (2) is satisfied. To simplify the operations, the finite difference is used to expand Eq. (2) in the region $\Re$. This procedure is started by a first initial guess and other successive approximations are calculated based on steps of the algorithm. One of the most elementary ways of the relaxation schemes is the Richardson method. In this technique, the correction process has the following formula [15]:

$$\phi^{n+1}_{(x,y)} = \phi^{n}_{(x,y)} + \alpha L\phi^{n}_{(x,y)}, \quad x, y \in \Re, \tag{3}$$

where α is a coefficient, which verifies the convergence criteria. It can be proven that the Richardson technique is formally equivalent to the solution of the subsequent partial differential equation, with respect to the fictitious time variable:

$$\frac{\partial \phi}{\partial t} = L\phi_{(x,y)}, \quad x, y \in \Re, \tag{4}$$

In the last relation, t is a fictitious time. The values of $\phi_{(x,y)}$ are calculated in each fictitious time. If the solution being carried to a sufficiently great t, so that the rate of change with respect to τ is negligible $\left(\frac{\partial \phi}{\partial \tau} = 0\right)$, the answer is obtained. Some other strategies, such as the Liebmann scheme, have a similar basis. These approaches are categorized as the first-order Richardson techniques. It should be added that the second- order Richardson methods have also been formulated to solve differential equations. Using these procedures for solving Laplace's equations (Eq. 2), is formally equivalent to the solution of the following second order partial differential equation, which contains the derivatives with respect to the fictitious time [15];

$$\frac{\partial^2 \phi}{\partial \tau^2} + \beta \frac{\partial \phi}{\partial \tau} = L\phi_{(x,y)}, \quad x, y \in \Re, \tag{5}$$

In the former relationship, β controls the stability and convergence rate. The values of $\phi_{(x,y)}$are calculated in each time. The answer is obtained when the first and second derivatives of $\phi_{(x,y)}$, with respect to t, come near to zero $\left(\frac{\partial^2 \phi}{\partial \tau^2} = 0,\ \frac{\partial \phi}{\partial \tau} = 0\right)$.

From mathematical point of view, the DR method is based on the second-order Richardson rule. The first use of *Dynamic Relaxation* topic in scientific literatures has been performed by Otter or Day [12, 18]. In this process, simulations system of equations (Eq. 1) is transferred to the second-order differential system of equations. This differential system of equations, in terms of the fictitious time, has the following form:

$$\frac{\partial^2 \left([S]\{D\} - \{P\}\right)}{\partial \tau^2} + \beta \frac{\partial \left([S]\{D\} - \{P\}\right)}{\partial \tau} = [S]\{D\} - \{P\} \tag{6}$$

Once again, it is clear that the answer is obtained when the first and second derivatives with respect to the fictitious time become zero.

3 Physical Concepts

The DR method can be simply demonstrated by the physical rules. From this viewpoint, the structural dynamics theories are utilized to clarify the validity of DR basis. It is well-known that the dynamic response of each structure has two discrete portions; i. e. transient response and steady-state response. If the structure has damping effect, the transient response will be zero after passing some periods of time. By damping the transient response, the steady-state response remains. When the structure is excited by a dynamic load, which is variable with respect to the time, the steady-state response is a function of time. If the external load is constant during analysis time, such as the static behavior of structure, the steady-state response is equal to the answer of static analysis. The viscous DR method is based on a similar idea. In other words, the DR procedure, which is known as Viscous Dynamic Relaxation, presents the steady-state response of a fictitious dynamic system which is excited by static loads. Based on this discussion, the steady-state response of such a system is equal to the static response. To start DR process, the static system (Eq. 1) is transferred to the dynamic space by adding fictitious inertia and damping forces, as follows:

$$\{f_I\} + \{f_D\} + [S]\{D\} = \{P\} \tag{7}$$

Here, $\{f_I\}$ and $\{f_D\}$ are vectors of fictitious inertia and damping forces, respectively. These quantities are defined by the subsequent relationships:

$$\{f_I\} = [M]\left\{\ddot{D}\right\} \tag{8}$$

$$\{f_D\} = [C]\left\{\dot{D}\right\} \tag{9}$$

where $[M]$ and $[C]$ are diagonal fictitious mass and fictitious damping matrices, respectively. In the last equations, the dots denote the derivatives with respect to the fictitious time.

On the other hand, there is the Kinetic DR method which has been proposed on a different and interesting physical idea. Based on this concept, the total energy of each structure, which combines from the potential and kinetic energies, is constant. In the static equilibrium state, the potential energy is minimized, and hence the kinetic energy should be maximum. The kinetic Dynamic Relaxation method utilizes this idea and traces some successive peak in the kinetic energy of structure, which finally leads to the static equilibrium. The fundamental relationships of kinetic DR approach are very similar to the viscous version. The main difference is that kinetic DR iterations trace the un-damped vibrations of the dynamic system. The related fictitious dynamic equation has the following form:

$$\{f_I\} + [S]\{D\} = \{P\} \tag{10}$$

In the last relationship, inertia force vector is defined by Eq. (8). As discussed earlier, there are two general types of damping, which can be utilized in DR process: *Kinetic damping* and *Viscous damping*. The DR formulation depends on the type of damping model. In other words, the different fundamental DR relations can be obtained based on two types of damping model. Each of these methods has a different specification with many interesting performances. In the following sections, the fundamental DR formulations for kinetic damping and viscous damping are reviewed. All of these approaches utilize the explicit iterative relationships.

3.1 Viscous Damping Formulation

Several common DR algorithms, such as Papadrakakis [19], Underwood [33], are based on the viscous damping process. This kind of modeling is closer to the real dynamic system than the kinetic damping one. To establish the related equation, damping force is defined by utilizing the viscous damping theory, as it was shown in Eq. (9). By this definition, DR procedure leads to a common dynamic problem, which can be solved by numerical integrations.

To take advantage of the vector operations' simplicity, explicit integrations are utilized to derive DR iterative relationships [16]. The main required assumption to fulfill this goal is the diagonal property of the fictitious mass and damping matrices, which are used in Eqs. (8) and (9). As a result, Eq. (7) can be simplified as follows [34]:

$$m_{ii}\ddot{D}_i^n + c_{ii}\dot{D}_i^n + f_i^n = p_i, \quad i = 1, 2, \cdots, q \tag{11}$$

It is assumed that the structure has q degrees of freedom and m_{ii} and c_{ii} are i^{th} diagonal elements of the fictitious mass and damping matrices, respectively. To perform numerical integration, the most common approach utilizes the standard central finite difference expressions. For this purpose, Brew and Brotton developed DR formulations so that a vector form was achieved [8]. This approach is the most common formulation for iterative DR procedure. In fact, the derivatives of displacement, with respect to the fictitious time, are determined by the succeeding relationships [7,8]:

$$\{D\}^{n+1} = \{D\}^n + \tau^{n+1}\left\{\dot{D}\right\}^{n+\frac{1}{2}} \tag{12}$$

$$\left\{\ddot{D}\right\}^n = \frac{\left\{\dot{D}\right\}^{n+\frac{1}{2}} - \left\{\dot{D}\right\}^{n-\frac{1}{2}}}{\tau^n} \tag{13}$$

where τ^n is the fictitious time step in n^{th} increment of numerical time integration. Furthermore, the velocity of n^{th} time step is estimated, as follows:

$$\left\{\dot{D}\right\}^n = \frac{\left\{\dot{D}\right\}^{n+\frac{1}{2}} + \left\{\dot{D}\right\}^{n-\frac{1}{2}}}{2} \tag{14}$$

Substituting Eqs. (14) and (13) into (11) prepares the velocity of the next time step [33]:

$$\dot{D}_i^{n+\frac{1}{2}} = \frac{2m_{ii} - \tau^n c_{ii}}{2m_{ii} + \tau^n c_{ii}}\dot{D}_i^{n-\frac{1}{2}} + \frac{2\tau^n}{2m_{ii} + \tau^n c_{ii}} r_i^n, \quad i = 1, 2, \cdots, q \tag{15}$$

In the last relation, r_i^n is the residual force of the i^{th} degree of freedom, i.e., $\{R\}^n$ in the n^{th} iteration:

$$\{R\}^n = [M]\left\{\ddot{D}\right\}^n + [C]\left\{\dot{D}\right\}^n = \{P\} - \{f\}^n \tag{16}$$

In the following lines, the next estimation of the displacement can be calculated from Eq. (12). The viscous DR procedure is performed by iterating Eqs. (15) and (12), successively, until convergence criterions are satisfied. At this stage, the residual force or kinetic energy is vanished. In addition to this common formulation, Rezaiee-Pajand and Taghavian-Hakkak proposed a new iterative formula for displacement by use of Taylor's series [23], as follows:

$$\{D\}^{n+1} = \{D\}^n + \tau^n \left\{\dot{D}\right\}^n + \frac{(\tau^n)^2}{2}\left\{\ddot{D}\right\}^n \tag{17}$$

Acceleration vector is found from Eq. (16) and replaced in Eq. (17). Then, the following iterative relation is obtained:

$$\{D\}^{n+1} = \{D\}^n + \left(\tau^n - \frac{c(\tau^n)^2}{2}\right)\left\{\dot{D}\right\}^n + \frac{(\tau^n)^2}{2}[M]^{-1}\{R\}^n \tag{18}$$

In each step, the velocity vector is calculated from next equation:

$$\left\{\dot{D}\right\}^n = \frac{\{D\}^n - \{D\}^{n-1}}{\tau^n} \tag{19}$$

It should be noted that the DR iterations are usually unstable because of using numerical time integrations to solve the differential equations of motion. To overcome this drawback, the fictitious parameters, such as time step and diagonal mass and damping matrices, are determined so that the stability conditions are satisfied. It should be added that the slow convergence rate of the viscous DR method has always been a critical issue.

The most common way to study the stability and convergence rate of a viscous DR algorithm is an error analysis between two successive iterations. One of the first classified error analyses was performed by Papadrakakis [19]. He utilized the following assumptions:

$$[M] = \rho[D] \tag{20}$$

$$[C] = c[D] \tag{21}$$

In the former relations, $[D]$, ρ and c, are the main diagonal terms of stiffness matrix, fictitious mass and damping factors, respectively. The optimum values of mass and damping factors are formulated based on maximum and minimum eigen-value of the fictitious dynamic system. The estimation of these eigen-values is mostly calculated from Gerschgrin's circle theory. On the other hand, one of the famous error analyses for viscous DR iterations was performed by Underwood [33]. He assumed a linear reduction for displacement error between two successive iterations. This analysis leads to following inequality for fictitious mass:

$$m_{ii} \geq \frac{(\tau^n)^2}{4}\sum_{j=1}^{q}|s_{ij}|\,, \quad i = 1, 2, \cdots, q \tag{22}$$

In another study, Rezaiee-Pajand and Alamatian revised the error analysis of the viscous DR method. Two discrete regions were considered for eigen-value in Gerschgörin's theory by these researchers. The related formulation led to a simple and effective way of calculating the fictitious mass, as follows [21]:

$$m_{ii} = \frac{(\tau^n)^2}{4} \max\left[2s_{ii}, \sum_{j=1}^{q} |s_{ij}|\right], \quad i = 1, 2, \cdots, q \tag{23}$$

Fictitious damping is another parameter in viscous DR iterations. This factor has a great effect on convergence rate of DR procedure. The reason for this subject can be found in physical basis of the DR method, which tries to obtain the steady-state answer of a fictitious dynamic system. Based on the structural dynamics theories, the critical damping causes rapid convergence rate to the steady-state response. This concept is commonly used to calculate the fictitious damping. By utilizing the critical damping theory, Zhang et al. presented an estimation of the critical damping for viscous DR iterations, as follows [37]:

$$c_{ii} = 2m_{ii}\omega_{min}, \quad i = 1, 2, ..., q \tag{24}$$

In the last relationship, ω_{min} is the lowest natural frequency of a structure in the free vibration case. This factor can be calculated from the following Rayleigh's principle [37]:

$$\omega_{min}^2 \approx \frac{(\{D\}^n)^T \{f\}^n}{(\{D\}^n)^T [M]^n \{D\}^n} \tag{25}$$

In the former equation, Rayleigh's principle was applied to the whole structure. Another way of finding the lowest natural frequency was proposed, in which this can separately be calculated for each node [36]. This approach leads to succeeding result:

$$(\omega_{min}^i)^2 \approx \frac{\left(\{D^i\}^n\right)^T \{f^i\}^n}{\left(\{D^i\}^n\right)^T [M^i]^n \{D^i\}^n}, \quad i = 1, 2, ..., q \tag{26}$$

where ω_{min}^i, $\{D^i\}^n$, $\{f^i\}^n$ and $[M^i]^n$ are the lowest frequency, displacement, internal force vector and fictitious mass matrix of the i^{th} node, respectively. The parameter h indicates the total number of nodes of the structure. It should be added that Rezaiee-Pajand and Alamatian proposed a modified relationship for fictitious damping, as follows [21]:

$$c_{ii} = m_{ii}\sqrt{4\omega_{min}^2 - \omega_{min}^4}, \quad i = 1, 2, \cdots, q \tag{27}$$

It is evident, when the lowest natural frequency approaches zero, Eq. (27) reduces to Eq. (24). All the previous methods lack accuracy, because they exploit the Rayleigh principle to estimate the lowest natural frequency and eventually to find the fictitious damping. To overcome this drawback, the structural dynamics schemes can be utilized so that the lowest natural frequency of the fictitious dynamic system is calculated with suitable accuracy. The Stodela iterative process is a technique which has been successfully applied in DR iterations to calculate ω_{min} [24]. In addition, Rezaiee-Pajand

and Sarafrazi combined the power iteration method with DR algorithm and obtained a more accurate value for the lowest eigen-value. They utilized one step of power iterative scheme for matrix $[M^{-1}S - aI]$ in each step of DR procedure [27]. Here, factor a stand for the upper bound of the highest eigen-value, which can be set to 4.

3.2 Kinetic damping formulation

It is not required to calculate the viscous damping terms in the kinetic formulation. This technique needs only the time step and the fictitious nodal masses. In fact, the number of necessary DR parameters is reduced. In this way, time interval may be fixed [31]. As a result, the kinetic damping provides an alternative approach for DR method. Cundall proposed this procedure for application to unstable rock mechanism [11]. The high stability and rapid convergence rate for structures with large displacement are the main specification of the kinetic damping formulation. In such analyses, the un-damped motion of a structure is traced until a local peak in total kinetic energy is detected. After that, all current velocities are reset to zero and DR process is restarted with current geometry and repeated through further peaks. This procedure is generally decreasing until the energies of all modes of vibration are dissipated, and the static equilibrium is reached. The method of kinetic damping is found to be very stable and rapidly convergent when dealing with large displacements [31]. The stability of this approach depends on the time-mass relation [27]. One of the important applications of kinetic damping DR algorithm is parallel processing in the finite element analysis [13, 32]. The parallel DR scheme is undertaken in two stages. First, the overall mesh is divided into a different number of sub domains corresponding to the number of available processors. Then, DR strategy, usually based on kinetic damping algorithm, is used over the sub domains and converged results from each sub domain are received and compiled to obtain the overall results for the domain. In the case of the viscous damping factor in Eq. (15) is equal to zero ($c_{ii} = 0$), the next fundamental iterative relationships of the kinetic DR strategy could be obtained [13]:

$$\dot{D}_i^{n+\frac{1}{2}} = \dot{D}_i^{n-\frac{1}{2}} + \frac{\tau^n}{m_{ii}} r_i^n, \quad i = 1, 2, \cdots, q \tag{28}$$

$$D_i^{n+1} = D_i^n + \tau^{n+1} \dot{D}_i^{n+\frac{1}{2}}, \quad i = 1, 2, \cdots, q \tag{29}$$

By exploiting Eqs. (28) and (29) successively, the total kinetic energy of un-damped structure is traced during iterations. The position of structure with maximum kinetic energy could represent the static equilibrium, because in this condition, potential energy will be minimized. The kinetic DR algorithm uses the aforementioned idea to approach the static equilibrium position. In each iteration, the total kinetic energy, U_k, is calculated by the following relationship:

$$U_k = \sum_{i=1}^{q} m_{ii} \left(\dot{D}_i^{n+\frac{1}{2}} \right)^2 \tag{30}$$

It is worth emphasizing to mention that the DR iterations run sequentially, until an energy peak is detected. At this stage, all current velocities are reset to zero. This process should be continued through further peaks until the convergence criterions are satisfied. To establish this algorithm, it is assumed that peak of kinetic energy could occur between times τ^n and τ^{n+1}, i.e. a fall in the total kinetic energy would be taking placed at time τ^{n+1}. As described by Topping and Ivanyi [31], the displacement, which peak of the kinetic energy belongs to it, is calculated from the following equation [13]:

$$^*D_i^n = D_i^{n+1} - \frac{3}{2}\tau^{n+1}\dot{D}_i^{n+\frac{1}{2}} + \frac{(\tau^n)^2}{2m_{ii}} r_i^n, \quad i = 1, 2, \cdots, q \tag{31}$$

here $^*D_i^n, i = 1, 2, \cdots, q$ is the displacement in which the kinetic energy is maximized. The analysis can be restarted by $^*D_i^n, i = 1, 2, \cdots, q$ as the initial displacement. For fully convergence, velocities of the first time-step should be calculated at the mid point, as follows:

$$\dot{D}_i^{n+\frac{1}{2}} = \frac{\tau^n}{2m_{ii}} r_i^n, \quad i = 1, 2, \cdots, q \tag{32}$$

In the last relationship, r_i^n is calculated from displacement's components, presented by Eq. (31). Having this parameter, DR iterations can be restarted from Eqs. (28) and (29). The mentioned process will be iterated for some successive peaks of the kinetic energy until the convergence criteria are satisfied. It should be noted that the diagonal elements of the mass matrix, which control the stability of kinetic DR algorithm, are determined from the subsequent formula [13]:

$$m_{ii} \geq \frac{(\tau^n)^2}{2} \sum_{j=1}^{q} |s_{ij}|, \quad i = 1, 2, \cdots, q \tag{33}$$

In the latest study, a new formulation was proposed for the fictitious mass of the kinetic DR method. The transformed Gerschgörin theory was also utilized in the mentioned research [3].

4 Other fictitious parameters

As it was discussed earlier, there are four groups of unknown parameters in DR iterations; i. e. fictitious mass, fictitious damping, pseudo time step and initial guess of displacement. The most common approach to estimate fictitious mass and damping matrices is based on error analysis and stability verification of DR iterations. The general form of such procedure was presented in section 3. Before starting DR iterations, fictitious time step and initial guess of displacement should be determined. The researchers have presented various methods to determine these quantities. In the following lines, these approaches are reviewed, separately.

4.1 Fictitious time step

One of the important parameters in the DR techniques is the fictitious time step. This factor is utilized in the numerical integration of the fictitious system. The subsequent sections explain several ways of calculating this vital factor:

4.1.1 Constant time step

In the most common DR algorithms, the fictitious time step is kept constant and equal to one. This assumption leads to the next simple relationship:

$$\tau^n = 1.0 \tag{34}$$

4.1.2 Minimum residual force

Minimization of the out-of-balance force helps to improve DR convergence rate. In this scheme, the out-of-balance force function is defined as follows [1, 4, 17, 20]:

$$\mathrm{UFF} = \sum_{i=1}^{\mathrm{q}} \left(r_i^{n+1}\right)^2 \tag{35}$$

where, UFF is the un-balance force function in the $n+1^{th}$ iteration of DR method. By minimizing this function, the next modified fictitious time step (MFT) is calculated:

$$\frac{\partial\ \mathrm{UFF}}{\partial \tau^{n+1}} = 0 \Rightarrow \tau_{\mathrm{MFT}} = \frac{\sum_{i=1}^{\mathrm{q}} r_i^n \dot{f}_i^{n+\frac{1}{2}}}{\sum_{i=1}^{\mathrm{q}} \left(\dot{f}_i^{n+\frac{1}{2}}\right)^2} \tag{36}$$

In this equation, $\dot{f}_i^{n+\frac{1}{2}}$ is the rate of internal force of the i^{th} degree of freedom. It is possible to find this parameter by using the chain rule (differentiation), as follows [1, 4, 17, 20]:

$$\dot{f}_i^{n+\frac{1}{2}} \approx \sum_{j=1}^{q} s_{ij}^n \dot{D}_j^{n+\frac{1}{2}}, \quad i = 1, 2, \cdots, q \tag{37}$$

By using the second derivative test, it can be proven mathematically that the last time step minimizes the out-of-balance force function, in each iteration of the DR algorithm. As a result, the convergence rate will increase, and the analysis time will decrease.

4.1.3 Minimum residual energy

In the steady-state response of an artificial dynamic system, the kinetic energy is zero. Therefore, convergence to the steady-state response could be increased by minimizing the energy function. This function can be defined in the following form [2, 25]:

$$\mathrm{UEF} = \sum_{i=1}^{\mathrm{q}} \left(\delta D_i^{n+1} r_i^{n+1}\right)^2 \tag{38}$$

In the last equation, UEF is the un-balance energy function in the $n+1^{th}$ iteration of the DR process. If the out-of-balance force is minimized, the succeeding optimum fictitious time step (OFT) can be obtained [2, 25]:

$$\tau_{\mathrm{OFT}}^{n+1} = \frac{-A_2^{n+1} \pm \sqrt{(A_2^{n+1})^2 - 4A_1^{n+1}A_3^{n+1}}}{2A_1^{n+1}} \tag{39}$$

where, A_1^{n+1}, A_2^{n+1} and A_3^{n+1} are constant factors and defined as below:

$$A_1^{n+1} = 2\sum_{i=1}^{q} \left(v_i^{n+\frac{1}{2}} \dot{f}_i^{n+\frac{1}{2}}\right)^2 \tag{40}$$

$$A_2^{n+1} = -3\sum_{i=1}^{\mathrm{q}} \left[\left(v_i^{n+\frac{1}{2}}\right)^2 r_i^n \dot{f}_i^{n+\frac{1}{2}}\right] \tag{41}$$

$$A_3^{n+1} = \sum_{i=1}^{\mathrm{q}} \left(v_i^{n+\frac{1}{2}} r_i^n\right)^2 \tag{42}$$

It is clear that minimization of the out-of-balance energy function will be a conditional procedure. If Eq. (39) could not result in a real value for the fictitious time step, the presented approach is useless.

4.1.4 Zero damping method

In a published article, Rezaiee-Pajand and Sarafrazi set the damping factor to zero and obtained below equation for the fictitious time step [28, 30]:

$$\tau^{n+1} = \frac{1}{(1+\omega_{\min})^2}\tau^n \tag{43}$$

4.1.5 Error analysis in kinetic damping method

The error between two consecutive steps in kinetic DR technique was calculated by Rezaiee-Pajand and Rezaee. It resulted in formulating a new time step for this method. [24]:

$$\tau^{n+1} = \frac{(\frac{2}{\tau^n} + \tau^n\,\omega_{\min}^2) - \sqrt{(\frac{2}{\tau^n} + \tau^n\,\omega_{\min}^2)^2 - 4\,(\frac{2}{\tau^n} + \tau^n\,\omega_{\min}^2)^2}}{2(\frac{1}{\tau^n} - \tau^n\,\omega_{\min}^2)^2} \tag{44}$$

4.2 Initial guess of displacement

The DR calculations are started by an initial guess of displacement. In the iteration process, this quantity is corrected successively. The more suitable guess of displacement leads to a more rapid convergence rate of the solver. The following sections explain some approaches to estimate initial displacement in the first iteration.

4.2.1 Constant vector

The simplest approach to start DR process is using a constant vector for the initial guess of displacement. In this case, the unit or null vectors are the most common selection for the initial displacement. It should be added that the convergence rate of such techniques may not be suitable.

4.2.2 Alwar's approach

An exponential function was proposed by Alwar et al. to determine the steady-state response [6]. For each degree of freedom of structure, the aforementioned function is assumed for damped oscillation. The suggested function has the following form:

$$D_i = \alpha_i e^{-\beta_i \tau} \tag{45}$$

here α_i and β_i are unknown coefficients, which are determined by solving two equations obtained from two successive maximum in the oscillation curve. In this method, it is necessary to calculate two first successive maximum domains of the oscillation curve of each degree of freedom.

4.2.3 Zhang's method

In this strategy, the un-damped vibrations of structure are traced until first minimum and maximum displacements of each degree of freedom are obtained. After that, the initial displacement can be calculated by the next formula [37]:

$$D_i^0 = \frac{D_i^{\max} + D_i^{\min}}{2} \tag{46}$$

where $D_i^{\max}$and $D_i^{\min}$ are the first maximum and minimum displacements of i^{th} degree of freedom in the un-damped vibration.

4.2.4 Modified Zhang's method

This scheme is a modified version of Zhang's approach and is based on the concept of constant total energy of structure. In this way, the un-damped vibrations are started with initial displacement and by obtaining first minimum or maximum. Then, the initial guess is corrected by the following relationship [36]:

$$D_i^0 = \frac{D_i^0 + D_i^{\min}}{2} \quad \text{or} \quad D_i^0 = \frac{D_i^0 + D_i^{\max}}{2} \tag{47}$$

In each cycle, the initial guess is corrected so that by iterating Eq. (46), a suitable initial guess is obtained. It should be added that there are some other papers, which deal with DR stability and its convergence rate [9,10,35].

5 DR algorithms

Dynamic Relaxation, which is an iterative method, can be performed by some simple steps. As discussed in the previous sections, the basic foundation of these steps is given by mathematical formulations. For better clarification, the main algorithms of DR process are presented in this part. These algorithms can be classified based on two DR formulations; i.e. Viscous and Kinetic damping theories. It should be noted that there are several similarities between these two main procedures. In the following, the viscous and kinetic DR algorithms will be briefly explained.

5.1 Viscous DR steps

The viscous DR method requires the following steps:

(a) Assume initial values for artificial velocity (null vector), displacement (available methods presented in section 4.2 or null vector or convergence displacement on the previous increment), fictitious time step ($\tau = 1$) and convergence criterion for out of balance force and kinetic energy ($e_R = 1.0E-6$ and $e_K = 1.0E-12$).

(b) Construct the tangent stiffness matrix and internal force vector.

(c) Apply boundary conditions.

(d) Calculate out of balance (residual) force vector (Eq. 16).

(e) If $\sqrt{\sum_{i=1}^{q}(r_i^n)^2} \leq e_R$, go to (m), otherwise, continue.

(f) Construct the artificial diagonal mass matrix (section 3.1).

(g) Form artificial damping matrix (section 3.1).

(h) Update artificial velocity vector using Eq. (15).

(i) If $\sum_{i=1}^{q}\left(\dot{D}_i^{n+\frac{1}{2}}\right)^2 \leq e_K$, go to (m), otherwise, continue.

(j) Calculate fictitious time step (section 4.1)

(k) Update displacement vector using Eq. (12).

(l) Set $n = n + 1$ and go to (b).

(m) Print results of the current increment.

(n) If increments are not complete, go to (a), otherwise, stop.

5.2 Kinetic DR steps

The subsequent steps are needed to obtain the solution by the kinetic DR method:

(a) Assume values for initial fictitious velocity (null vector), initial displacement (available methods presented in section 4.2 or null vector or convergence displacement on the previous increment), fictitious time step (1), initial kinetic energy ($KE^0 = 0$) and a convergence criterion for the out-of-balance force and the kinetic energy ($e_R = 1.0E-6$ and $e_K = 1.0E-12$),

(b) Construct the tangent stiffness matrix and internal force vector,

(c) Calculate the out-of-balance force vector using Eq. (16),

(d) If $\sqrt{\sum_{i=1}^{q}(r_i^n)^2} \leq e_R$, go to (q), otherwise continue,

(e) Construct the fictitious diagonal mass matrix using (section 3.2),

(f) Update the fictitious velocity vector using Eq. (28),

(g) If $\sum_{i=1}^{q}\left(\dot{d}_i^{n+\frac{1}{2}}\right)^2 \leq e_K$, go to (q), otherwise, continue,

(h) Calculate the kinetic energy from Eq. (30),

(i) If $KE^{n+1} \leq KE^n$, go to (m), otherwise, continue,

(j) $\tau^{n+1} = \tau^n$

(k) Update the displacement vector using Eq. (29),

(l) Go to (b),

(m) Calculate the initial displacements of the restarted analysis (section 3.2),

(n) Construct the tangent stiffness matrix and the internal force vector,

(o) Calculate the initial velocities of the restarted analysis (section 3.2),

(p) Go to (g)

(q) Print results of the current increment,

(r) If increments are not complete, go to (a), otherwise, stop.

As it was demonstrated in the related steps, the kinetic and viscous DR algorithms have many similarities. However, they use different relationships for mass and damping matrices. Based on this fact, Rezaiee-Pajand and et al. selected twelve well-known DR procedures in order to analyze the geometric nonlinear behavior of several frames and trusses. They graded these methods in terms of the number of iterations and the analysis time. In this way, the five most efficient algorithms were introduced by these investigators [29]. Moreover, Rezaiee-Pajand and Estiri compared these different approaches in the geometric nonlinear analysis of 3D frames and found the three most efficient algorithms [22].

6 Conclusion

In this paper, a comprehensive review of the Dynamic Relaxation (DR) methods was presented. At the first stage, the most common DR schemes, which include the kinetic and viscous damping formulations, were briefly explained. To utilize these techniques, several parameters are required. All the related factors were also described. Simplicity, full explicit vector operations and no sensitivity to nonlinear behaviors are the main specifications of the DR procedure. Moreover, solution methodologies for the structural problems were presented. The strategies reported in this paper could be used to evaluate the responses of different structures. It is worth emphasizing that DR techniques have the great ability to be implemented in all branches of structural analyses. They are very simple and also eliminate the round-off errors.

As it was mentioned by the researchers, the interest in obtaining more accurate and efficient results, using a variety of DR strategies remains strong, even in the presence of some simplifying assumptions. By analyzing the outcomes of presented studies, it can be seen that several investigations on the different aspects of these solvers are needed. For instance, no attempt has been made for considering a broad comparison study, so far. Consequently, no recommendations are made as to the most appropriate technique selection for a particular problem. The principal concepts of the various DR formulations can be summarized in two main categories, i.e. the numerical stability and the convergence rate. In other words, researchers try to guarantee the DR stability, especially in the case of intense non-linearity. From the future research point of view, the DR formulation could be enhanced by modification of its parameters. On the other hand, improving the convergence rate of DR iterations may be one of the interesting topics for further studies. The second part of the article will concentrate on the DR applications.

References

1. Alamatian, J. *Structural analysis using dynamic relaxation method*, MS Dissertation, Department of Civil Engineering, Ferdowsi University, Mashhad, Iran, (2002).

2. Alamatian, J. *Numerical integration for structural analysis*, PhD Thesis, Department of Civil Engineering, Ferdowsi University, Mashhad, Iran, (2007).

3. Alamatian, J. *A new formulation for fictitious mass of the Dynamic Relaxation method with kinetic damping*, Computers and Structures 90-91 (2012), 42-54.

4. Alamatian, J. and Kadkhodayan, M. *Optimum time step for Dynamic Relaxation method*, Amirkabir Journal of Science & Technology 17(65-C) (2006), 43-52.

5. Allen, D.N.G. and Southwell, R.V. *Dynamic Relaxation*, Phil. Trans. 42 (1950), 379-414.

6. Alwar, R.S., Rao, N.R. and Rao, M.S. *An altenative procedure in Dynamic Relaxation.* Computers and Structures 5(2) (1975), 271-274.

7. Barnes, M.R. *Form finding and analysis of tension structures by Dynamic Relaxation*, International Journal of Space Structures 14(2) (1999), 89-104.

8. Brew, J.S. and Brotton, M. *Non-linear structural analysis by Dynamic Relaxation method*, International Journal of Numerical Methods Engineering 3(4) (1971), 463-483.

9. Bunce, J.W. *A note on estimation of critical damping in Dynamic Relaxation*, International Journal of Numerical Methods Engineering 4(1972), 301-304.

10. Cassell, A.C. and Hobbs, R.E. *Numerical stability of Dynamic Relaxation analysis of non-linear structures*, International Journal of Numerical Methods Engineering 10 (1976), 1407-1410.

11. Cundall, P.A. *Explicit finite-difference methods in geomechanics*, Proceeding 2nd International Conference on Numerical Methods in Geomechanics. Blacksburg, Virginia, USA, 1 (1976), 132–150.

12. Day, A.S. *An introduction to Dynamic Relaxation*, The Engineer 219 (1965), 218-221.

13. Ivanyi, P. and Topping, B.H.V. *Parallel Dynamic Relaxation formfinding*, In: Papadrakakis M, Topping BHV, editors. *Innovative Computational Methods in Structural Mechanics.* Edinburgh: Saxe-Coburg Publications, 1999.

14. Felippa, C.A. *Nonlinear finite element methods*, ASEN 5017, Course Material, (1999), http://kaswww.colorado.edu /courses.d /NFEMD/.

15. Frankel, S.P. *Convergence rates of iterative treatments of partial differential equations*, Mathl Tabl Natn Res Coun 4 (1950), 65-75.

16. Gosling, P.D. and Lewis, W.J. *Optimal structural membranes - II. Formfinding of prestressed membranes using a curved quadrilateral finite element for surface definition*, Computers and Structures 61(5) (1996), 885-895.

17. Kadkhodayan, M., Alamatian, J. and Turvey, G.J. *A new fictitious time for the Dynamic Relaxation (DXDR) method*, International Journal of Numerical Methods Engineering 74 (2008), 996-1018.

18. Otter, J.R.H., Cassell, A.C. and Hobbs, R.E. *Poisson. Dynamic Relaxation*, Institute of Civil Engineersrs, ICE proceedings Journal, USA, 35(4) (1966), 633-656.

19. Papadrakakis, M.A. *Method for automatic evaluation of the Dynamic Relaxation parameters*, Computational Methods in Applied Mechanics and Engineering 25 (1981), 35-48.

20. Rezaiee-Pajand, M. and Alamatian, J. *Superior time step for geometrical nonlinear analysis by Dynamic Relaxation method*, Modarres Technical and Engineering 19 (2005), 61-74.

21. Rezaiee-Pajand, M. and Alamatian, J. *The Dynamic Relaxation method using new formulation for fictitious mass and damping*, Journal of Structural Engineering and Mechanics 34(1) (2010), 109-133.

22. Rezaiee-Pajand, M. and Estiri, H. *Comparative analysis of three-dimensional frames by dynamic relaxation methods*, *Mechanics of Advanced Materials and Structures* (2017).

23. Rezaiee-Pajand, M. and Hakkak, M.T. *Nonlinear analysis of truss structures using Dynamic Relaxation*, International Journal of Engineering, Transactions B: Applications 19(1) (2006), 11-22.

24. Rezaiee-Pajand, M., Kadkhodayan, M., Alamatian, J. and Zhang, L.C. *A new method of fictitious viscous damping determination for the Dynamic Relaxation method*, Computers and Structures 89 (2011), 783–794.

25. Rezaiee-Pajand, M., Kadkhodayan, M. and Alamatian, J. *Timestep Selection for Dynamic Relaxation Method*, Mechanics Based Design of Structures and Machines 40 (2012), 42–72.

26. Rezaiee-Pajand, M. and Rezaee, H. *Fictitious time step for the kinetic dynamic relaxation method*, Mechanics of Advanced Materials and Structures 21 (2014), 631–644.

27. Rezaiee-Pajand, M. and Sarafrazi, S.R. *Nonlinear structural analysis using dynamic relaxation method with improved convergence rate*, International Journal of Computational Methods 7 (2010), 1-28.

28. Rezaiee-Pajand, M. and Sarafrazi, S.R. *Nonlinear dynamic structural analysis using dynamic relaxation with zero damping*, Computers and Structures 89 (2011), 1274-1285.

29. Rezaiee-Pajand, M., Sarafrazi, S.R. and Rezaiee, H. *Efficiency of dynamic relaxation methods in nonlinear analysis of truss and frame structures*, Computers and Structures 112-113 (2012), 295-310.

30. Sarafrazi, S.R. *Numerical integration for structural dynamic analysis*, PhD Thesis, Department of Civil Engineering, Ferdowsi University, Mashhad, Iran, (2010).

31. Topping, B.H.V.and Ivanyi, P. *Computer aided design of cable-membrane structures*, Saxe-Coburg Publications on Computational Engineering, Chapter 3, 39–82, 2007.

32. Topping, B.H.V. and Khan, A.I. *Parallel schemes for dynamic relaxation, engineering computations*, International Journal of Computer Aided Engineering Software 11 (1994), 513–548.

33. Underwood, P. *Dynamic Relaxation*, In: Belytschko T, Hughes TJR, Editors. Computational Methods for transient analysis. Computational Methods in Mechanics, 1 (1983), Elsevier Science, 245-256.

34. Wakefield, D.S. *Engineering analysis of tension structures: Theory and practice*, Engineering Structures 21(8) (1999), 680-690.

35. Wood, W.L. *Note on Dynamic Relaxation*, International Journal of Numerical Methods Engineering 3 (1971), 145-147.

36. Zhang, L.C., Kadkhodayan, M. and Mai, Y.W. *Development of the maDR method*, Computers and Structures 52 (1994), 1-8.

37. Zhang, L.C. and Yu, T.X. *Modified adaptive Dynamic Relaxation method and its application to elastic-plastic bending and wrinkling of circular plates*, Computers and Structures 34 (1989), 609-614.

Iranian Journal of Numerical Analysis and Optimization
Vol. 7, No. 2, (2017), pp 87–114
DOI:10.22067/ijnao.v7i2.67470

The state of the art in Dynamic Relaxation methods for structural mechanics

Part 2: Applications

M. Rezaiee-pajand*, J. Alamatian, and H. Rezaee

Abstract

The most significant advances over the sixty years relative to the Dynamic Relaxation applications in structural engineering are summarized. Emphasized are given towards plates, form finding, cable structures, dynamic analysis, and other applications. The role of DR solver in the linear and non-linear analyses is discussed. This investigation is undertaken to explain the application of the solution technique to the static, dynamic and stability problems. The influence of the methods on the use of isotropic and composite materials, such as orthotropic and laminated ones, is briefly covered. Critical analyses and suggestions regarding future research and applications will be presented.

Keywords: Dynamic Relaxation method; Application; Survey; Solver; Review; Iterative technique; State of the art.

1 Introduction

The first part of the paper entitled "The state of art in Dynamic Relaxation methods" devoted entirely to the DR formulations and its fictitious param-

---

*Corresponding author
Received 25 November 2016; revised 12 May 2017; accepted 23 April 2017
M. Rezaiee-pajand
Department of Civil Engineering, Factualy of Engineering, Ferdowsi Unversity of Mashhad, Mashhad, Iran. e-mail: rezaiee@um.ac.ir

J. Alamatian
Civil Engineering Department, Mashhad Branch, Islamic Azad Unversity, Mashhad, Iran. e-mail: alamatian@mshadiau.ac.ir

H. Rezaee
Department of Civil Engineering, Factualy of Engineering, Ferdowsi Unversity of Mashhad, Mashhad, Iran.

eters. For this purpose, the main two categories of the DR methods was reviewed; i.e., the viscous damping and the kinetic damping formulations. In spite of several similarities in formulation and iterative relationships, the viscous and kinetic approaches have the different physical basis. Furthermore, the proposed formulations for fictitious parameters are different. However, the parameters such as fictitious time step and initial displacement have unique form in both methods.
It is worth emphasizing that these solvers have been exploited in a vast area of the structural analyses. In other words, most of the DR research topics conducted so far have been related to their applications. There is only a little fraction of the papers which deal with DR formulations and their efficiencies, such as accuracy, stability and convergence rate. Therefore, the important issues of the DR applications require special consideration. Based on this fact, the applications of the DR schemes in the different structural analysis are reviewed. It should be noted that these strategies have been used for the different kind of analyses, such as static, dynamic, stability, form-finding and, etc. Verities of investigators have found the solution of diverse structures, like: truss, frame, shell, plate and, etc. The reasons for these wide ranges of applications can be found in some interesting DR specifications, which create unique potentials in engineering problems. The main specifications of DR algorithms will be listed in the following lines:

(a) Full vector operations

(b) Calculations are based on internal force rather than the secant stiffness matrix

(c) Simple numerical algorithm

(d) Iterative process

(e) Not sensitive to critical points in structural behavior

(f) Full automatic procedure (personal judgments have no effect on the solution efficiency)

The aforementioned advantages cause numerous usages in different structural engineering problems. The existing restrictions have not affected the vast applications of these solvers. So far, the analysts have found that there are verities of interesting and attractive applications of the DR methods. In the following sections, some of them are briefly reviewed.

2 Plates

Rushton applied Dynamic Relaxation to non-linear systems by analyzing variable thickness plates with geometrical non-linear behavior [101]. He also used this technique for solving the large deflection equations resulted from analyzing the post-buckling of variable thickness plates [103]. In another paper, this researcher analyzed the small and large deflection of simply supported plates with corners free to lift [104]. Moreover, DR method was utilized to analyze the post-buckling of variable thickness flat rectangular plates with mixed boundary conditions by Rushton [105]. This investigator used the DR method to study the large deflection of plates with small initial curvature [106]. By utilizing of the DR technique, Rushton found large deflection of rectangular plates with unsupported edges [107]. In another research, he also examined the buckling of laterally loaded plates having initial curvature [108].

In 1972, Alami analyzed the elastic large deflection behavior of plates under transverse loading by a method based on Dynamic Relaxation [1]. The DR approach was applied to non-linear analysis of clamped orthotropic skew plates having a constant thickness subjected to a uniformly-distributed transverse load by Alwar and Ramachandra [5]. Turvey and Wittrick utilized the DR method to solving flexural and stability problems of elastic geometrically behavior of laminated plates [158]. In another study, this solver was used to analyze the large deflection of skew sandwich plates with clamped edges by Alwar and Ramachandra [6].

Tuma and Galletly described the use of Dynamic Relaxation for analyzing large-deflection of circular and rectangular plates with various boundary conditions [128]. This technique was also employed for the analysis of non-linear behavior of clamped isotropic skew plates of constant thickness subjected to a uniformly distributed transverse load by Alwar and Rao [7]. Moreover, Murthy et al. adopted the DR scheme for analyzing the non-linear bending of circular plates of the linear elastic material and variable profiles subjected to a uniformly distributed lateral loading [78]. Dowling and Bawa used Dynamic Relaxation to solve the finite difference form of orthotropic small deflection plate equations. They took advantage from an analytical method of producing influence surfaces for stiffened steel bridge decks [33]. Utilizing this iterative approach, Turvey found the large deflections of square plates, obeying the Foeppl and Von Karman theories [129]. In another study, Chaplin used the DR approach to analyze the large elastic deformations of clamped skewed plates [21].

Turvey calculated the large deflection of circular plates with variable thickness utilizing two different DR methods. In the first technique, fictitious densities were chosen arbitrarily and in the second one, they were calculated using Gerschgorin bounds. By comparing the results, it was demonstrated that the latter improves the convergence characteristics. This researcher also implemented the second procedure for solving variable thickness annular plates subjected to a uniform lateral load [130]. In the other application, Frieze et al. took advantage of the DR algorithm to analyze the large deflection of elasto-plastic plates. They extended the strategy to include both geometrical and material non-linear effects in plates. Particularly, these investigators discussed the iteration parameters which control convergence [37]. Frieze and Dowling proposed a process based on Dynamic Relaxation for the exact interactive buckling analysis of plates forming box sections subjected to a generalized loading [38]. Using the DR approach, Turvey analyzed the axisymmetric large deflection behavior of circular plates with linear thickness tapers and affine imperfections [131]. He also applied the mentioned strategy to the analysis of the axisymmetric, elasto-plastic large deflection response of laterally loaded circular plates [132]. Moreover, Turvey utilized the method of Dynamic Relaxation for solving the set of non-incremental equations describing the axisymmetric, elasto-plastic, large deflection response of laterally loaded, thickness-tapered, circular plates [133].

There have been a lot of more studies related to the plate problems. Sherbourne and Murthy applied the DR method to analyze bending of circular plates with variable profile [120]. Webb and Dowling utilized Dynamic Relaxation to solve the governing equations from the material and geometric non-linear analysis of eccentrically stiffened plates, subjected to the combined or separate actions of lateral and in-plane loading [161]. By using this solver, Turvey analyzed the axisymmetric elastic large deflection behavior of glass-steel and glass-aluminum circular plates [137]. He also employed this kind of algorithm for analyzing axisymmetric small deflection equations for shear deformation of circular plates [138]. It should be added that Turvey and Lim applied several refinements to the DR method in order to improve computational efficiency. Then, they solved the equations coming from the analysis of axisymmetric full-range response of transverse pressure loaded, clamped and simply supported, circular plates [147]. Turvey and Der Avanessian used the DR method for a numerical solution of the governing equations for the axisymmetric elastic large deflection analysis of ring-stiffened plates [140]. In another research, Lim and Turvey adopted the DR approach to solve the plate equations for examining the elastic integrity degradation of uniform flat simply supported, and clamped circular plates subjected to uniform transverse pressure [148]. They also utilized this way in solution of the incremental equations governing the axisymmetric elasto-plastic large deflection response of circular steel plates with initial deflections [71].

Numerical solutions of the equations governing the elastic post-buckling response of flat and imperfect polar orthotropic circular and annular plates was carried out using a finite-difference version of the DR algorithm by Turvey and Drinali [145]. By utilizing weighting factors for mass and damping, Al-Shawi and Mardirosian used Dynamic Relaxation in the finite element analysis of plate bending [118]. Method of Dynamic Relaxation was successfully exploited to large deflection analysis of circular plates by Turvey and Der Avanessian [141]. Turvey and Lim utilized the DR procedure in numerical solution of the incremental equations governing the full-range axisymmetric flexural response of thickness-tapered circular plates [149]. For ensuring the numerical stability of DR procedure, Xiao-qing and Wan-lin proposed a method for calculation of fictitious densities. Then, they applied the DR technique to the non-linear bending problems of rectangular plates laminated of bimodular composite materials [164]. Machacek employed this solution process in the analysis of thin steel isotropic, and stiffened plates loaded in compression and bending [73]. In the other study, Turvey and Osman utilized the DR method in solution of first-order orthotropic shear deformation equations for the non-linear elastic bending response of rectangular plates [150].

Using Dynamic Relaxation, Machacek analyzed large deflection elasto-plastic behavior of thin steel eccentrically stiffened plates subjected to the lateral and/or in-plane load [74]. The large-deflection elasto-plastic behavior of flat plates and attached flat-bar stiffeners, including the effects of interaction was also presented using Dynamic Relaxation by Caridis and Frieze [16]. Turvey and Der Avanessian utilized the DR method in solution of the governing system of equations for the axisymmetric elasto-plastic large deflection analysis of ring-stiffened circular plates [143]. The application of the Dynamic Relaxation to study the post-buckling path of cylindrically curved panels of laminated composite materials during loading and unloading was also described by Wan-lin and Xiao-qing [160]. Using the DR technique in conjunction with graded finite-differences for a numerical solution of the stiffened plate equations, Turvey and Der Avanessian suggested a discretely stiffened plate theory for the elasto-plastic large deflection analysis of pressure loaded ring-stiffened circular plates [144]. In the other research, the DR procedure was coupled with an interlacing central finite-difference discretization scheme by Turvey and Salehi. They utilized the aforementioned way in solving equations for elastic large deflection of uniformly loaded sector plates [153]. A finite-difference implementation of the DR process was developed to solve the non-axisymmetric elastic large deflection equations of annular sector plate by Salehi and Turvey [114]. In another study, Turvey and Osman utilized finite differences in conjunction with the DR procedure for numerical solutions of the Mindlin laminated plate equations in large deflection initial failure analysis of square angle-ply laminated plates subjected to uniform pressure loading [151].

Combining DR scheme with finite-difference discretization, Salehi et al. analyzed geometrically non-linear behavior of sector plates [111]. In the other study, Salehi and Shahidi utilized the mentioned technique for solving the governing equations for the elastic large deflection of uniformly pressure loaded sector Mindlin plates [112]. Caridis employed the DR method on an interlacing finite difference grid for solving the large-deflection elasto-plastic equations of equilibrium of flat and stiffened plates [17]. Turvey and Salehi proposed a discretely stiffened circular plate theory. They obtained the solution of the large deflection plate equations with the aid of a finite-difference implementation of the DR algorithm [154]. The large deflection axisymmetric circular plate equations were solved using a finite-difference implementation of the DR method by Turvey and Drinali [146]. In the other application, Kadkhodayan et al. utilized this solution approach to predict the bifurcation point of elastic plates subjected to in-plane and transverse external forces [56]. Turvey and Salehi described a theory for the non-axisymmetric elastic large deflection analysis of sector plates stiffened by a single eccentric rectangular cross-section radial stiffener. They used the DR procedure for solving the discrete system of equations [155]. Using a finite difference implementation of the DR scheme, Turvey and Salehi also solved the governing equations for an elasto-plastic large deflection analysis of pressure loaded sector plates. The material of structure obeyed the Ilyushin full-section yield criterion and the flow theory of plasticity [156].

Kadkhodayan investigated the implementation of interlacing, and irregular rectangular meshes used in conjunction with the DXDR method, which is a modified DR technique, to study the large deflection behavior of elastic plates [53]. Moreover, this solver together with the finite difference discretization technique were utilized in analyzing the plate structure for geometrically linear and non-linear elastic. The plate material was assumed to be thick composite sector plates by Salehi and Sobhani [113]. Salehi and Aghaei took advantage of the DR technique together with the finite difference discretization method in non-linear shear analysis of non-axisymmetric circular viscoelastic plates [110]. The elasto-plastic large deflection equations for annular sector plates were solved by the DR procedure. This study was performed by Turvey and Salehi [157]. Furthermore, the DXDR method, which is a modified DR strategy, was utilized for solving equations of large deflection of rectilinear orthotropic square and circular plates by Kadkhodayan [54]. In another investigation, combination of the DR method with the finite difference technique was used to solve the discretized equations in the analysis of the non-linear bending of annular functionally graded plate (FGM) under mechanical loading [41]. In a recent research, Rezaiee and Estiri graded sixteen well-known DR procedures based on their performance in terms of the number of iterations and the analysis time in solving several bending plate examples with geometrical nonlinear behavior [96].

3 Form-finding

One of the extensive uses of DR algorithms is in the structural form-finding. In 1988, Barnes performed the form-finding analysis and fabrication patterning of wide span cable net and pre-stressed membrane roofs by taking advantage of the DR method with kinetic damping [9]. A procedure for numerical form-finding of the stable minimal surfaces represented by soap-film models, based on the DR technique, was also suggested by Lewis and Gosling [65]. In another study, Gosling and Lewis applied the matrix-based finite element method to the vector-based DR algorithm for form-finding of minimal surface membranes [42]. Moreover, the form-finding of lightweight tension structures comprising pre-stressed cable nets and fabric membranes was performed by

Lewis WJ and Lewis TS. They utilized DR technique for solving the resulting non-linear set of equilibrium equations [66]. Adriaenssens and Barnes developed a Dynamic Relaxation based method for form-finding and load analysis of a class of tensegrity structures with continuous tubular compression booms forming curved splines. This structure could be deployed from straight by pre-stressing a cable bracing system [2].

In the other research, Zhang and Shan utilized the DR method for form-finding of the pre-stressed cable and membrane structures [166]. By Dynamic Relaxation with kinetic damping, Brew and Lewis presented a computational methodology for form-finding of tension membrane structures (TMS), or fabric structures, used as roofing forms [13]. Li and Wei used the DR method in the formulation of the form-finding under uniform pre-tensioned force and the behavior analysis under static loads [70]. Han et al. proposed a form-finding strategy for tension structures with elastic supports with the aid of DR method [43]. The aforementioned algorithm was also applied to form-finding of a grid shell in composite materials by Douthe et al. They modeled the large structural rotations by means of the DR technique [31]. It should be noted that this kind of rotations may occur by bending of pre-stressed constructions during the erection process. Furthermore, the form-finding of non-regular tensegrity structures by the aid of a scheme, which was based on the DR method with kinetic damping, and was described by Zhang et al. [167].

Using the DR process, Baudriller et al. suggested a form-finding method for generating non-regular tensegrity shapes of higher diversity and complexity [11]. Lu and Ren utilized the DR method for the form-finding of three-dimensional cable structures in simulation of the cable mesh reflector for the large radio telescope [72]. In another investigation, Wu and Deng exploited the DR method for form-finding of slack cable-bar assembly [162].

Douthe and Baverel proposed a simple way using the DR algorithm to find the form and perform a structural analysis of multi-reciprocal frame systems. This technique is also called nexorades [30]. Furthermore, Ye and Zhou modified the DR method in two aspects. The first was a simple procedure to gain the damp value directly, which is close to that of the critical damp. In the second feature is an extension of the classic DR scheme, which was suggested [165] to obtain the desired membrane shapes. In another research, Lee and Han use DR method for geodesic shape finding of membrane structure with geodesic string [62].

4 Cable structures

The DR strategy is suitable for finding the response of the flexible structures, such as cable. This solution technique was employed for the analysis of cable structures by Day and Bunce [28]. Moreover, Lewis et al. developed a

DR method for the analysis of the non-linear static response of pre-tensioned cable roofs [68]. Using the aforementioned procedure, Lewis et al. investigated cladding-network stiffening effects in pre-tensioned cable roofs [69]. In another study, Lewis and Shan obtained the solution of the governing equilibrium and compatibility equations in the analysis of cladding-network interaction in pre-tensioned cable roof structures under static loads with the aid of the DR scheme with kinetic damping [67]. The DR method was also used in the analysis of cable net systems with many loads relieving devices by Shan et al. [117]. Form-finding, analysis and fabrication patterning of wide-span cable nets and grid shells, uniform or variably pre-stressed fabric membranes and battened membrane roofs was carried out using a Dynamic Relaxation with kinetic damping based technique by Barnes [10]. Chen et al. applied DR method to static analysis of cable nets [25]. They also employed this solver for finding equilibrium state of construction procedures of cable-domes by controlling the original length simulation of the construction process [24]. In order to analyze the nonlinear behavior of cable domes, which is affected by creep over time, a modified dynamic relaxation procedure was introduced by Kmet and Mojdis [59].

5 Dynamic analysis

Utilizing DR method in the dynamic structural analysis is a new application, which has been introduced since 2008. There are only a few papers, which deal with this interesting application of the DR method, most of them were presented by Rezaiee and Alamatian [3,93]. In this approach, DR algorithm is combined with numerical time integrations. It is well known that numerical integration procedures are appropriate for dynamic analysis of structures. These schemes are commonly applied to both linear and non-linear structural behaviors. The aforementioned techniques can calculate the dynamic responses via step by step process. Numerical integration strategies are divided to the implicit and explicit scheme. In the implicit formulation, the dynamic equilibrium equation of structure at time $t^{k+1}$is converted to the below equivalent static system [3, 93]:

$$[S]_{EQ}^{k+1}\{D\}^{k+1} = \{P\}_{EQ}^{k+1} \tag{1}$$

where $[S]_{EQ}^{k+1}$, $\{D\}^{k+1}$ and $\{P\}_{EQ}^{k+1}$ are the equivalent stiffness matrix, the displacement vector and equivalent load vector at $k+1^{th}$ step of numerical integration formulation, respectively. The equivalent stiffness matrix and equivalent load vector are dependent to the implicit dynamic algorithm. Rezaiee-Pajand and Alamatian [93] used the DR method to solve Eq. (1). The proposed technique led to a considerable reduction in errors of non-linear dynamic analysis. Moreover, Sarafrazi presented a different scheme to analyze the structures. He assumed real and also fictitious time axes. In this strategy, real and fictitious times were considered simultaneously [115]. Recently, an explicit dynamic analysis was performed by the Dynamic Relaxation method [79].

6 Other applications

Because of interesting specifications of the DR method, it has a great potential ability to be used in other kinds of structural engineering problems. For instance, Hussain Khan and Lafitte employed a finite difference based strategy exploiting the DR procedure for performing design analysis of a cylindrical pre-stressed concrete pressure vessel [52]. Moreover, Rushton discussed the determination of the critical damping and optimum time increment. He utilized the DR method for stress analysis problems [102]. The DR method was also developed for time dependent stress analysis of the pre-stressed concrete pressure vessels by Cederberg and David [20]. Cassell introduced the concept of fictitious densities to the DR method. He analyzed doubly curved shells under arbitrary surface tractions and temperature loading [18]. Furthermore, Brew and Brotton formulated the DR method using the first-order dynamic equilibrium relationship and studied the stability conditions of the frame structures [12]. Shmuel and Alterman proposed a scheme for analyzing the dynamic stress distribution close to a crack which cuts through the finite thickness of a given plate. They utilized the aforementioned technique to rapidly improve the convergence of their suggested strategy [121]. The DR procedure was also applied to the analysis of bridge slabs by Cassell et al. [19].

In another application, Hansson used this solver for calculation of plane problems with general shape and non-linear material behavior [45]. Bunce and Brown utilized the DR approach in solving the equilibrium equations resulted from analyzing the finite deflection of plane frames [14]. The DR method was also exploited to computation of stresses, and displacements induced by underground excavations by Crouch and Fairhurst [27]. In addition, Hansson and Schnellenbach analyzed some special problems of local stress conditions of pre-stressed concrete reactor pressure vessels with non-linear material behavior. They performed calculations by the DR process [46]. By use of this solution strategy, Rushton and Hook analyzed the large deflections of rectangular plates and beams obeying a non-linear stress-strain law [109]. The DR approach was also used for analyzing disks with anisotropic material, complying with Ramberg-Osgood stress-strain relations with variable profiles by Sherbourne and Murthy [119]. In the other research, Hook and Rushton investigated beams and plates problems, which deflect until contact is made with internal restraints, using a modified form of the DR method [51]. Swan took advantage of the DR scheme for the dynamic stress analysis of certain linear elastic fracture problems [124]. Moreover, the DR methodology was utilized in calculations for the analysis of two-dimensional behavior of the liners in pre-stressed concrete reactor pressure vessels by Oberpichler et al. [83].

Hansson and Stoever described a process based on the DR algorithm for three-dimensional analysis of local crack development in pre-stressed concrete pressure vessels [47]. On the other hand, Bunce and Brown proposed a technique based on Dynamic Relaxation for analyzing the non-linear behavior of large deflection of thin ideally elastic rods [15]. Using the method of Dynamic Relaxation, Frieze and Dowling analyzed the elastic post-buckling interaction behavior of box sections [38]. In another investigation, Frieze applied Dynamic Relaxation to the analysis of interactive buckling in the elasto-plastic range of thin-walled rectangular sections [37]. Harding used the DR method to solve governed equations from elasto-plastic analysis of initially imperfect thin cylinders subjected to axial compression and external pressure [48]. The DR method was also utilized to solve the axisymmetric, large deflection response of a uniformly loaded, circular membrane subjected to an initial pre-stress/pre-strain by Turvey [134]. In another study, Tsotsos and Hatzigogos adopted the DR procedure for the analysis of the foundations of dams and embankments [127].

Oberpichler performed calculations for designing the liner-anchor system of concrete vessels by the DR method [81]. Moreover, Turvey combined the Dynamic Relaxation with the Tsai-Hill failure criterion and obtained a non-linear elastic solution for the large deflection of laminated strip equations [135]. In another research, Oberpichler used the DR approach for design calculations of steel-liners (in Pre-stressed Concrete Reactor Pressure Vessel (PCRV) or a Concrete Containment Vessel (PCCV)) and their anchorage with regard to non-linear behavior of liner-material and anchorage [82]. Turvey also utilized the DR method to solve the equations for anti-symmetrical laminated, cross-ply strips [136]. In the other paper, Papadrakakis developed DR scheme for the post-buckling behavior of spatial structures [84]. Numerical studies were carried out on the elastic large deflection behavior of cross-ply laminated bi-modular strips employing the DR method by Turvey [139]. In 1982, an implicit DR relationship exploring general increment control was introduced by Felippa [36]. Moreover, Estefen and Harding described a finite difference DR program for the analysis of ring-stiffened shells, including the behavior of the rings as discrete elements [34]. The DR method was also applied to the solution of the non-linear equilibrium equations governing the analysis of the post-critical ultimate load conditions of space trusses by Papadrakakis and Manolis [85].

Krings et al. performed the requisite non-linear calculations for the design of concrete tunnel linings with non-linear material behavior by the DR scheme [61]. Zienkiewicz et al. suggested an accelerated procedure for improvement of the convergence rate [172]. Using the DR technique, a method was proposed for finding the optimum layout of modularly constrained truss structures subjected to multiple load conditions by Topping [125]. Estefen and Harding also investigated the inter-ring buckling of cylindrical leg members by use of the DR scheme [35]. Analysis of a small-deflection beam was carried out with the aid of DR technique by Turvey and Der Avanessian [142]. In order to facilitate static analysis of non-linear problems, Rericha modified the DR method. He exploited continuous loading in time instead of the ordinary step function of time. Inertia and damping forces arising during the loading process were kept at a minimum using an optimum load time history [92]. In another study, Chou and Wu proposed a Dynamic Relaxation finite element method for metal forming processes [26]. Using a natural combination of Lyaponov's dynamic criterion on stability and the modified adaptive DR method, Zhang et al. obtained an approach for predicting the bifurcation points of elastic-plastic buckling of plates and shells [169].

Qiang determined fictitious time and damping by Rayleigh's principle [87]. In another investigation, Lewis used the DR process in the analysis of the non-linear static response of pre-tensioned cable net and pin-jointed frame structures [64]. The modified adaptive DR method (maDR method) was applied to study of the axisymmetric deformation mechanism of work-pieces in conical cup tests by Zhang et al. [170]. Chen et al. also developed a numerical method for modeling plane strain rolling based on DR technique [22]. Furthermore, Rao et al. investigated the use of the DR scheme in the problems with geometric and material non-linearities. It was found from numerical studies that in the case of geometric non-linearity, obtained steady-state solution compares well with the static solution. In this technique, the process of convergence to steady state can be accelerated by choosing higher mass densities and an appropriate mass proportional damping. On the other hand, when both non-linearities were existed, diverse steady-state solutions were obtained for different values of artificial damping [91]. The application of the DR method to study the post-buckling path of cylindrically curved panels of laminated composite materials during loading and unloading was also described by Wan-lin and Xiao-qing [160]. In another paper, Moncrieff and Topping introduced a new procedure for generating cutting patterns for membrane structures, by means of a two-dimensional Dynamic Relaxation analysis for each cloth [77].

Using an improved adaptive DR method, Zhang analyzed the shape effects on the tensile strength of axisymmetric rock specimens [168]. Shugar proposed the automated Dynamic Relaxation (ADR) algorithm. He determined the initial equilibrium configuration and pre-stressed state of compliant structures by this scheme [123]. Moreover, the application of DR method to model discrete crack propagation was described by Gerstle et al. [40]. Sauve and Badie combined the shell formulation with the DR technique, a three-dimensional contact algorithm and generalizations of the constitutive equations for time-dependent deformation to yield accurate simulations of creep response in nuclear reactor fuel channels [116]. In an interesting application, a variable-arc-length approach was introduced by Ramesh and Krishnamoorthy, which can trace snap-through or snap-back regions of the load-deflection path, automatically. They proposed a displacement incrementation procedure to handle multiple loadings in the post-buckling analysis of structures by Dynamic Relaxation [88]. DR approach was also used to analyze equilibrium configurations of partly wrinkled membranes by Haseganu and Steigmann [49].

New schemes for Elastic Post-Buckling (EPB) analysis and Inelastic Post-Buckling (IEPB) analysis of truss structures using the DR method were introduced by Ramesh and Krishnamoorthy. These researchers used the variable-arc-length technique for tracing the post-buckling paths for elastic, EPB and IEPB analyses [89]. In the other research, a parallel algorithm for the DR strategy was presented by Topping and Khan [126]. Moreover, Kommineni and Kant described a unified approach for linear and geometrically non-linear analyses of composite and sandwich shells by means of the DR process [60]. The DR iteration was also adopted for the geometrically non-linear analysis of plates and shells involving large deflections, small rotations and strains by Ramesh and Krishnamoorthy [90]. Kadkhodayan and Zhang combined two vital components: the DXDR algorithm and a stable consistent algorithm for the integration of the constitutive equations of plasticity. They used this strategy for analyzing general elastic-plastic problems [55]. Furthermore, the DR method was adopted for solving delayed hydride cracking (DHC) problems by Metzger and Sauvé [75].

Using the DR process, Turvey and Osman analyzed small and large deflection Mindlin plate equations for unsymmetrical laminated cross-ply strips subjected to uniform lateral pressure [152]. Oakley and Knight Jr suggested a parallel adaptive Dynamic Relaxation (ADR) algorithm for non-linear structural analysis [80]. By means of finite differences together with DR method, Atai and Steigmann developed an equilibrium theory for the coupled finite deformations of elastic curves and surfaces [8]. The DR procedure was also employed in the analysis the fracture of materials by Metzger [76]. Moreover, Wakefield presented the application of DR approach to the analysis of tensile structures [159]. Xiaoqing and Hong utilized the DR solver to investigate the influence of compression-bending coupling on non-linear behavior of cylindrically slightly curved panels of unsymmetrical laminated composite materials subjected to uniform uniaxial compression during loading and unloading [163]. Han and Lee employed DR procedure for stabilizing of unstable structures [44]. In addition, the Dynamic Relaxation was combined with neural networks to increase model accuracy of tensegrity structures by Domer et al. [29]. Shoukry et al. employed DR approach for analyzing large transportation structures as dowel jointed concrete pavements and 306-m-long, reinforced concrete bridge superstructure under the effect of temperature variations [122]. In another study, Chen et al. used the DR method and obtained a technique to find the internal force of the elements, and the nodal coordinates of the structures composed of cables in tension and struts in compression in the equilibrium state by controlling the original length [23].

Hegyi et al. employed the DR method for membrane analysis by an eight-node quadrilateral element [50]. Kan and Ye described a way based on modified Dynamic Relaxation for solving the problem of rigid displacement [57]. In another study, Douthe et al. exploited the DR method in numerical modeling of grid shell with composite materials [32]. Plotzitza et al. employed the DR technique in the numerical simulation of concrete under explosive loading [86]. Moreover, the DR method was utilized to obtain the analytical solution of free damped vibrations of a linear viscoelastic oscillator, based on the fractional derivative model involving more than one different fractional parameter and several relaxation (retardation) times by Rossikhin et al. [100]. For reducing the calculation cost of the DR technique, Kashiwa and Onoda combined this method with an iterative technique via two switching rules. In this strategy, the numerical scheme used in the analysis is selected as the situation of the analysis. An unstable region of the analysis, in which the static iterative method cannot obtain the converged solution, is performed by the robust DR method. Then, a stable region that is costly to be solved by the DR technique is performed by the efficient iterative method. The performance of the suggested process was verified through a comparison of numerical analyses for the wrinkled membrane with the new way and conventional ones [58].

Based on the fact that a static problem has an equivalent wave speed of infinity, and a dynamic problem has a wave speed of finite value, an effective loading algorithm associated with the explicit DR procedure was presented to produce meaningful numerical solutions for static problems by Zhao et al. [171]. Rezaiee-Pajand and Alamatian proposed a method for tracing static path of truss structures using DR technique [94]. Furthermore, an automatic DR method was proposed for tracing the static path of structures, which have snap-through or snap-back regions, by these researchers [95]. In a recent research by Rezaiee and Estiri, a variable load factor, obtained from minimization of the unbalanced displacement increment, was employed in DR algorithm. Consequently, their proposed process was capable of tracing the equilibrium path at snap-through and snap-back points in addition to possessing high accuracy and efficiency [96]. In another paper, they minimized the work increment by the external loads and obtained a new formulation of the load factor [96]. Utilizing the structural equilibrium path, which was obtained from the DR method, these researchers calculated the buckling limit load. They set the work increment of the external forces to zero and found a new equation to derive the load factor [96]. Moreover, the first structural buckling load was recently calculated by simple DR algorithm [4]. Lee et al. presented an explicit arc-length method based on cylindrical arc-length method using Dynamic Relaxation with kinetic damping for tracing the post-buckling equilibrium path of structures [63].

7 Conclusion

This paper was devoted to the applications of the DR methods. According to all the evidence presented throughout this study, these techniques fit quite well with the linear and also non-linear behaviors of structures. They were successfully utilized in static and dynamic problems. A variety of the structures, such as trusses, frames, plates, membranes, shells and cables, can be analyzed by the aforementioned formulations. This survey showed that the applications of DR methods in structural engineering problems are very vast. The enormous usage of these solvers in different branches of structural analysis is due to simplicity, full explicit vector operations and no sensitivity to non-linear behaviors, which are the main specifications of DR procedure. In this paper, a wide range of DR applications was analyzed, and very useful reference sources were introduced. Due to important roles of these strategies, providing a reasoned and evidence critique and also more practical ways of function are still remained to be found. Based on the broad features of presented studies, it is suitable to make some suggestions for the future research and applications of these non-linear solvers. From the relevance point of view, the DR method has a great potential of abilities to be use in different engineering problems. These applications could not be limited to the structural analysis, so that the DR algorithms may be utilized for other branches of civil engineering, such as hydraulics, numerical solution of water flows, and soil mechanics. It should be noted that there in no limitation for using DR tactic in the other engineering and applied mathematics branches.

References

1. Aalami, B. *Large deflection of elastic plates under patch loading*, ASCE Journal of the Structural Division 98 (ST11) (1972), 2567-2586.

2. Adriaenssens, S.M.L.a and Barnes, M.R. *Tensegrity spline beam and grid shell structures*, Engineering Structures 23(1) (2001), 29-36.

3. Alamatian, J. *New implicit higher order time integration for dynamic analysis*, Structural Engineering and Mechanics 48(5) (2013), 711-736.

4. Alamatian, J. and Hosseini Nejad Goshik, M. *An efficient explicit framework for determining the lowest structural buckling load using Dynamic Relaxation method*, Mechanics Based Design of Structures and Machines (2016), 1-12.

5. Alwar, R.S. and Rao, N.R. *Nonlinear analysis of orthotropic skew plates*, AIAA Journal 11(4) (1973-a), 495-498.

6. Alwar, R.S. and Rao, N.R. *Nonlinear analysis of skew sandwich plates*, proceeding of the Canadian Congress of Applied Mechanics (CANCAM), Montreal, Canada, (1973-b).

7. Alwar, R.S. and Rao, N.R. *Large elastic deformations of clamped skewed plates by dynamic relaxation*, Computers and Structures 4(2) (1974), 381-398.

8. Atai, A.A. and Steigmann, D.J. *Coupled deformations of elastic curves and surfaces*, International Journal of Solids and Structures 35(16) (1998), 1915-1952.

9. Barnes, M.R. *Form-finding and analysis of prestressed nets and membranes*, Computers and Structures 30(3) (1988), 685-695.

10. Barnes, M.R. *Form finding and analysis of tension structures by Dynamic Relaxation*, International Journal of Space Structures 14(2) (1999), 89-104.

11. Baudriller, H., Maurin, B., Cañadas, P., Montcourrier, P.H., Parmeggiani, A. and Bettache, N. *Form-finding of complex tensegrity structures: application to cell cytoskeleton modeling*, Comptes Rendus–Mecanique 334(11) (2006), 662-668.

12. Brew, J.S. and Brotton, M. *Non-linear structural analysis by Dynamic Relaxation method*, International Journal of Numerical Methods in Engineering 3(4) (1971), 463-483.

13. Brew, J.S. and Lewis, W.J. *Computational form-finding of tension membrane structures - Non-finite element approaches: Part 3. Comparison of mesh constraint methods*, International Journal of Numerical Methods in Engineering 56(5) (2003), 685-697.

14. Bunce, J.W. and Brown, E.H. *The finite deflection of plane frames*, International Journal of Mechanical Sciences 15(3) (1973), 189-198.

15. Bunce, J.W. and Brown, E.H. *Non-linear bending of thin, ideally elastic rods*, International Journal of Mechanical Sciences 18(9-10) (1976), 435-441.

16. Caridis, P.A. and Frieze, P.A. *Flexural-torsional elasto-plastic buckling in flat stiffened plating using dynamic relaxation. Part 1: Theory*, Thin-Walled Structures 6(6) (1988), 453-481.

17. Caridis, P. *Panel 2D - a program for the static and dynamic full-range analysis of unstiffened and stiffened plates*, International Conference on Computational Structures Technology – Proceedings, Napier University, Edinburgh, UK, (1994), 131-140.

18. Cassell, A.C. *Shells of revolution under arbitrary loading and the use of fictitious densities in dynamic relaxation*, Institute of Civil Engineers, ICE proceedings Journal, USA 45 (1970), 65-78.

19. Cassell, A.C., Hobbes, R.E., Bridgett, M.S. and Awotwi, P.A.K. *Dynamic Relaxation analysis of multiple span slabs*, Structural Engineering 49(12) (1971), 549-559.

20. Cederberg, H. and David, M. *Computation of creep effects in prestressed concrete pressure vessels using Dynamic Relaxation*, Nuclear Engineering and Design 9(4) (1969), 439-448.

21. Chaplin, T.K. *Large elastic deformations of clamped skewed plates by Dynamic Relaxation*, Computers and Structures 8(2) (1978), 257-258.

22. Chen, B.K., Choi, S.K. and Thomson, P.F. *Analysis of plane strain rolling by the dynamic relaxation method*, International Journal of Mechanical Sciences 31(11-12) (1989), 839-851.

23. Chen, L.M., Dong, S.L. and Yuan, X.F. *Theoretical and experimental study on the construction of cable domes*, Tumu Gongcheng Xuebao/China Civil Engineering Journal 39(11) (2006), 33-36.

24. Chen, L.M., Dong, S.L. and Yuan, X.F. *Theoretical analysis of construction procedures of cable-domes*, Gongcheng Lixue/Engineering Mechanics 25(4) (2008), 134-139.

25. Chen, S., Lin, W., Xu, G. and Huang, J. *Dynamic Relaxation method for static analysis of cable nets*, Yingyong Lixue Xuebao/Chinese Journal of Applied Mechanics 19(2) (2002), 34.

26. Chou, P.C. and Wu, L. *A Dynamic Relaxation finite-element method for metal forming processes*, International Journal of Mechanical Sciences 28(4) (1986), 231-250.

27. Crouch, S.L. and Fairhurst, C.F. *Analysis of rock mass deformations due to excavations*, ASME AMD 3(1973), 203-210.

28. Day, A.S. and Bunce, J.W. *Analysis of cable networks*, Civil Engineering Published Works Revelation 65(765) (1970), 383-386.

29. Domer, B., Fest, E., Lalit, V. and Smith, I.F.C. *Combining Dynamic Relaxation method with artificial neural networks to enhance simulation of tensegrity structures*, ASCE Journal of Structural Engineering 129(5) (2003), 672-681.

30. Douthe, C. and Baverel, O. *Design of nexorades or reciprocal frame systems with the dynamic relaxation method*, Computers and Structures 87(21-22) (2009), 1296-1307.

31. Douthe, C., Baverel, O. and Caron, J.F. *Form-finding of a grid shell in composite materials*, Journal of the International Association for Shell and Spatial Structures 47(150) (2006), 53-62.

32. Douthe, C., Baverel, O. and Caron, J.F. *Gridshell in composite materials: Towards wide span shelters*, Journal of the International Association for Shell and Spatial Structures 48(155) (2007), 175-180.

33. Dowling, P.J. and Bawa, A.S. *Influence surfaces for orthotropic steel bridge decks*, Institute of Civil Engineers, ICE proceedings Journal, USA, 59(1975), 149-168.

34. Estefen, S.F. and Harding, J.E. *Ring stiffener behavior and its interaction with cylindrical panel buckling*, Institute of Civil Engineers, ICE proceedings Journal, USA, 75(1983), 243-264.

35. Estefen, S.F. and Harding, J.E. *Effect of ring stiffeners on inter-ring cylindrical panel buckling*, *Offshore Engineering, Volume 5: Proceedings of the 5th International Symposium on Offshore Engineering. Rio De Janeiro, Brazil*; Code 10983 (1986), 460-476.

36. Felippa, C.A. *Dynamic Relaxation under general increment control*, Mathematical Programming 24 (1982), 103-133.

37. Frieze, P.A. *Elasto-plastic buckling in short thin-walled beams and columns*, Institute of Civil Engineers, ICE proceedings Journal, USA, 65 (1978) 857-874.

38. Frieze, P.A. and Dowling, P.J. *Interactive buckling analysis of box sections using dynamic relaxation*, Computers and Structures 9(5) (1978), 431-439.

39. Frieze, P.A., Hobbs, R.E. and Dowling, P.J. *Application of Dynamic Relaxation to the large deflection elasto-plastic analysis of plates*, Computers and Structures 8(2) (1978), 301-310.

40. Gerstle, W.H. and Xie, M. *FEM modeling of fictitious crack propagation in concrete*, Journal of Engineering Mechanics 118(2) (1992), 416-434.

41. Golmakani, M.E. and Kadkhodayan, M. *Nonlinear bending analysis of annular FGM plates using higher-order shear deformation plate theories*, Composite Structures 93(2) (2011), 973-982.

42. Gosling, P.D. and Lewis, W.J. *Optimal structural membranes - II. Form-finding of prestressed membranes using a curved quadrilateral finite element for surface definition*, Computers and Structures 61(5) (1996), 885-895.

43. Han, D.J., Song, X.B. and Wang, H.T. *Dynamic Relaxation for integer form-finding analysis of tension structures with elastic supporting bars*, Huanan Ligong Daxue Xuebao/Journal of South China University of Technology (Natural Science) 33(11) (2005), 66-71.

44. Han, S.E. and Lee, K.S. *A study of the stabilizing process of unstable structures by dynamic relaxation method*, Computers and Structures 81(17) (2003), 1677-1688.

45. Hansson, V. *Calculation of plane problems of random shapes and nonlinear material behavior*, Konstr Ingenieurbau Ber 14 (1973), 70-78.

46. Hansson, V. and Schnellenbach, G. *Some special problems regarding the analysis of prestressed concrete reactor pressure vessels with due consideration towards non-stationary temperature fields and nonlinear behavior of the material*, Konstr Ingenieurbau Ber 19 (1974), 30-38.

47. Hansson, V. and Stoever, R. *Three-dimensional analysis of cracked concrete in prestressed concrete pressure vessels and comparisons with experimental results*, International Conference on Structural Mechanics in Reactor Technology. 3rd Transaction; London, UK, (1975), 10-22.

48. Harding, J.E. *Elasto-plastic analysis of imperfect cylinders*, Institute of Civil Engineers, ICE proceedings Journal, USA, 65 (1978), 875-892.

49. Haseganu, E.M. and Steigmann, D.J. *Analysis of partly wrinkled membranes by the method of dynamic relaxation*, Computational Mechanics 14(6) (1994), 596-614.

50. Hegyi, D., Sajtos, I., Geiszter, G. and Hincz, K. *Eight-node quadrilateral double-curved surface element for membrane analysis*, Computers and Structures 84(31-32) (2006), 2151-2158.

51. Hook, P.M. and Rushton, K.R. *Buckling of beams and plates onto an intermediate support studied by the Dynamic Relaxation method*, Journal of Strain Analysis 10(3) (1975), 153-158.

52. Hussain Khan, M. and Lafitte, R. *Analysis of a cylindrical prestressed concrete pressure vessel with a large central penetration in the slab*, Nuclear Engineering and Design 5(2) (1967), 191-198.

53. Kadkhodayan, M. *Using interlacing and irregular meshes in plate analysis*, Iranian Journal of Science and Technology, Transaction B: Technology 26(3) (2002), 419-430.

54. Kadkhodayan, M. *An investigation to the orthotropic plates by using irregular rectilinear mesh*, Proceedings of 26th IASTED International Conference on Modelling, Identification and Control, Innsbruck, Austria, 12 -14 February (2007), 259-264.

55. Kadkhodayan, M. and Zhang, L.C. *Consistent DXDR method for elastic-plastic problems*, International Journal of Numerical Methods in Engineering 38(14) (1995), 2413-2431.

56. Kadkhodayan, M., Zhang, L.C. and Sowerby, R. *Analyses of wrinkling and buckling of elastic plates by DXDR method*, Computers and Structures 65(4) (1997), 561-574.

57. Kan, Y. and Ye, J.H. *Form finding of cable domes by modified dynamic relaxation*, Gongcheng Lixue/Engineering Mechanics 24(9) (2007), 50-55.

58. Kashiwa, M. and Onoda, J. *Wrinkling analysis using improved dynamic relaxation method*, AIAA Journal 47(7) (2009), 1601-1607.

59. Kmet, S. and Mojdis, M. *Time-dependent analysis of cable domes using a modified dynamic relaxation method and creep theory*, Computers and Structures 125 (2013), 11-22.

60. Kommineni, J.R. and Kant, T. *Pseudo-transient large deflection analysis of composite and sandwich shells with a refined theory*, Computational Methods in Applied Mechanics and Engineering 123(1-4) (1995), 1-13.

61. Krings, W. and Meiswinkel, R. *Design of concrete tunnel linings with non-linear material behavior installed during driving*, Beton-und Stahlbetonbau 79(3) (1984), 63-69.

62. Lee, K. and Han, S. *Geodesic shape finding of membrane structure with geodesic string by the dynamic relaxation method*, Structural Engineering and Mechanics 39(1) (2011), 16-23.

63. Lee, K., Han, S. and Park, T. *A simple explicit arc-length method using the dynamic relaxation method with kinetic damping*, Computers and Structures 89 (2011), 216-233.

64. Lewis, W.J. *The efficiency of numerical methods for the analysis of prestressed nets and pin-jointed frame structures*, Computers and Structures 33(3) (1989), 791-800.

65. Lewis, W.J. and Gosling, P.D. *Stable minimal surfaces in form-finding of lightweight tension structures*, International Journal of Space Structures 8(3) (1993), 149-166.

66. Lewis, W.J. and Lewis, T.S. *Application of formian and dynamic relaxation to the form-finding of minimal surfaces*, Journal of the International Association for Shell and Spatial Structures 37(122) (1996), 165-186.

67. Lewis, W.J. and Shan, J. *Numerical modelling of the non-linear static response of clad cable net structures*, Computers and Structures 35(1) (1990), 15-22.

68. Lewis, W.J., Jones, M.S., Lewis, G. and Rushton, K.R. *Cladding-network interaction in retensioned cable roofs, studied by Dynamic Relaxation*, Computers and Structures 19(5-6) (1984), 885-897.

69. Lewis, W.J., Jones, M.S. and Rushton, K.R. *Dynamic Relaxation analysis of the non-linear static response of pretensioned cable roofs*, Computers and Structures 18(6) (1984), 989-997.

70. Li, C.Y. and Wei, D.M. *Analysis of cable-membrane structures by Dynamic Relaxation method*, Huanan Ligong Daxue Xuebao/Journal of South China University of Technology (Natural Science) 32(6) (2004), 80-84.

71. Lim, G.T. and Turvey, G.J. *Axisymmetric elasto-plastic large deflection behaviour of circular steel plates with initial deflections-A parametric study*, Computers and Structures 21(6) (1985), 1187-1196.

72. Lu, Y.J. and Ren, G.X. *Simulation of the cable mesh reflector for the large radio telescope fast*, Gongcheng Lixue/Engineering Mechanics 24(10) (2007), 165-169.

73. Machacek, J. *Analysis of thin plates with eccentric stiffeners*, Stavebnicky casopis 36(3) (1988-a), 191-212.

74. Machacek, J. *Study on imperfections of stiffened plating*, Acta Technica CSAV (Ceskoslovensk Akademie Ved) 33(5) (1988-b), 582-606.

75. Metzger, D.R. and Sauvé, R.G. *A self-induced stress model for simulating hydride formation at flaws*, American Society of Mechanical Engineers, Pressure Vessels and Piping Division (Publication) 326(1996), 137-142.

76. Metzger, D.R. *Explicit finite element formulation for a general strip yield model*, American Society of Mechanical Engineers, Pressure Vessels and Piping Division (Publication) 370(1998), 189-195.

77. Moncrieff, E. and Topping, B.H.V. *Computer methods for the generation of membrane cutting patterns*, Computers and Structures 37(4) (1990), 441-450.

78. Murthy, S. and Sherbourne, N.A. *Nonlinear bending of elastic plates of variable profile*, ASCE Journal of Engineering Mechanics Division 100(2) (1974), 251-265.

79. Namadchi, A.H. and Alamatian, J. *Explicit dynamic analysis using Dynamic Relaxation method*, Computers and Structures 175 (2016), 91-99.

80. Oakley, D.R. and Knight, Jr.N.F. *Non-linear structural response using adaptive dynamic relaxation on a massively parallel-processing system*, International Journal of Numerical Methods in Engineering 39(2) (1996), 235-259.

81. Oberpichler, R. *Design calculations for anchored steel linings of concrete vessels*, Konstruktiver Ingenieurbau Berichte 33 (1980), 1-52.

82. Oberpichler, R. *Design of steel-liners and their anchorage with regard to non-linear behavior of liner-material and anchorage*, International Conference on Structural Mechanics in Reactor Technology, London, UK (1981), 11-23.

83. Oberpichler, R., Schnellenbach, G. and Weber, R. *Stress analysis of liners for prestresssed concrete reactor pressure vessels with regard to non-linear behavior of liner material and of anchor-characteristics*, International Conference on Structural Mechanics in Reactor Technology, 3rd Transaction; London, UK (1975), 50-67.

84. Papadrakakis, M. *Post-buckling analysis of spatial structures by vector iteration methods*, Computers and Structures 14(5-6) (1981), 393-402.

85. Papadrakakis, M. *Inelastic post-buckling of trusses*, Journal of Structural Engineering 109(9) (1983), 2129-2147.

86. Plotzitza, A., Rabczuk, T. and Eibl, J. *Techniques for numerical simulations of concrete slabs for demolishing by blasting*, Journal of Engineering Mechanics 133(5) (2007), 523-533.

87. Qiang, S. *An adaptive Dynamic Relaxation method for non-linear problems*, Computers and Structures 30(1988), 855-859.

88. Ramesh, G. and Krishnamoorthy, C.S. *Post-buckling analysis of structures by dynamic relaxation*, International Journal of Numerical Methods in Engineering 36(8) (1993), 1339-1364.

89. Ramesh, G. and Krishnamoorthy, C.S. *Inelastic post-buckling analysis of truss structures by dynamic relaxation method*, International Journal of Numerical Methods in Engineering 37(21) (1994), 3633-3657.

90. Ramesh, G. and Krishnamoorthy, C.S. *Geometrically non-linear analysis of plates and shallow shells by Dynamic Relaxation*, Computational Methods in Applied Mechanics and Engineering 123(1-4) (1995), 15-32.

91. Rao, A., Rama, M. and Shantaram, D. *Non-linear finite element analysis by dynamic relaxation*, International Journal of Structures 10(1) (1990), 37-53.

92. Rericha, P. *Optimum load time history for non-linear analysis using Dynamic Relaxation*, International Journal of Numerical Methods Engineering 23(12) (1986), 2313-2324.

93. Rezaiee-Pajand, M. and Alamatian, J. *Nonlinear dynamic analysis by Dynamic Relaxation method*, Journal of Structural Engineering and Mechanics 28(5) (2008), 549-570.

94. Rezaiee-Pajand, M. and Alamatian, J. *Dynamic Relaxation method for tracing static path of truss structures*, Modeling in engineering 17 (2009), 27-39.

95. Rezaiee-Pajand, M. and Alamatian, J. *Automatic DR structural analysis of snap-through and snap-back using optimized load increments*, ASCE Journal of Structural Engineering 137(1) (2011), 109-116.

96. Rezaiee-Pajand, M. and Estiri, H. *Mixing dynamic relaxation method with load factor and displacement increments*, Computers and Structures 168 (2016), 78-91.

97. Rezaiee-Pajand, M. and Estiri, H. *Computing the structural buckling limit load by using dynamic relaxation method*, International Journal of Non-Linear Mechanics 81 (2016), 245-260.

98. Rezaiee-Pajand, M. and Estiri, H. *A comparison of large deflection analysis of bending plates by dynamic relaxation*, Periodica Polytechnica Civil Engineering 60(4) (2016), 619-645.

99. Rezaiee-Pajand, M. and Estiri, H. *Finding equilibrium paths by minimizing external work in dynamic relaxation method*, Applied Mathematical Modelling 40 (2016), 10300-10322.

100. Rossikhin, Yu, A., Shitikova, M.V. and Shcheglova, T.A. *Analysis of free vibrations of a viscoelastic oscillator via the models involving several fractional parameters and relaxation/retardation times*, Computers and Mathematics with Applications 59(5) (2010), 1727-1744.

101. Rushton, K.R. *Large deflection of variable-thickness plates*, International Journal of Mechanical Sciences 10 (1968-a), 723-735.

102. Rushton, K.R. *Dynamic Relaxation method used for stress analysis*, Conf. Recent Advances in Stress Analysis, Royal Aeronautical Society, London, UK (1968-b), 41-46.

103. Rushton, K.R. *Postbuckling of tapered plates*, International Journal of Mechanical Sciences 11(5) (1969-a), 461-480.

104. Rushton, K.R. *Simply supported plates with corners free to lift*, Journal of Strain Analysis 4(4) (1969-b), 306-311.

105. Rushton, K.R. *Postbuckling of rectangular plates with various boundary conditions*, Aeron Quart 21(1970-a), 163-181.

106. Rushton, K.R. *Large deflexion of plates with initial curvature*, International Journal of Mechanical Sciences 12(12) (1970-b), 1037-1051.

107. Rushton, K.R. *Large deflection of plates with unsupported edges*, Journal of Strain Analysis 7(1) (1972-a), 44-53.

108. Rushton, K.R. *Buckling of laterally loaded plates having initial curvature*, International Journal of Mechanical Sciences 14(10) (1972-b), 667-680.

109. Rushton, K.R. and Hook, P.M. *Large deflection of plates and beams obeying non-linear stress-strain laws*, Journal of Strain Analysis 9(3) (1974), 178-184.

110. Salehi, M. and Aghaei, H. *Dynamic Relaxation large deflection analysis of non-axisymmetric circular viscoelastic plates*, Computers and Structures 83(23-24) (2005), 1878-1890.

111. Salehi, M. and Shahidi, A. *Transverse shear deformability of sector plates: New results*, American Society of Mechanical Engineers, Petroleum Division (Publication) 64(8-3) (1994-a), 545-552.

112. Salehi, M. and Shahidi, A. *Large deflection analysis of elastic sector Mindlin plates*, Computers and Structures 52(5) (1994-b), 987-998.

113. Salehi, M. and Sobhani, A.R. *Elastic linear and non-linear analysis of fiber-reinforced symmetrically laminated sector Mindlin plate*, Composite Structures 65(1) (2004), 65-79.

114. Salehi, M. and Turvey, G.J. *Elastic large deflection response of annular sector plates-a comparison of DR finite-difference, finite element and other numerical solutions*, Computers and Structures 40(5) (1991), 1267-1278.

115. Sarafrazi, S.R. *Numerical integration for structural dynamic analysis*, PhD Dissertation, Department of Civil Engineering, Ferdowsi University, Mashhad, Iran, 2010.

116. Sauve, R.G. and Badie, N. *Non-linear shell formulation for time-dependent deformation*, ASME Pressure Vessels and Piping Division (Publication) 265(1993), 269-275.

117. Shan, J., Yi, J. and Zheng, Q. *Investigation into the behavior of load relieving systems under loading*, Gong Cheng Li Xue/Engineering Mechanics 16(3) (1999), 38-42.

118. Shawi, F.A.N. and Mardirosion, A.H. *An improved Dynamic Relaxation method for the analysis of plate bending problems*, Computers and Structures 27 (1987), 237-240.

119. Sherbourne, A.N. and Murthy, D.N.S. *Stresses in disks with variable profile*, International Journal of Mechanical Sciences 16(7) (1974), 449-459.

120. Sherbourne, A.N. and Murthy, D.N.S. *Bending of circular plates with variable profile*, Computers and Structures 11(4) (1980), 355-361.

121. Shmuely, M. and Alterman, Z.S. *Three dimensional numerical analysis of stress distribution in the vicinity of a crack tip*, Israel Journal of Technology, 9(5) (1971), 523-530.

122. Shoukry, S.N., William, G.W., Riad, M.Y. and McBride, K.C. *Dynamic Relaxation: A technique for detailed thermo-elastic structural analysis of transportation structures*, International Journal of Computational Methods in Engineering Sciences and Mechanics 7(4) (2006), 303-311.

123. Shugar, T.A. *Automated dynamic relaxation solution method for compliant structures*, ASME Computer Engineering Division 4 (1991), 1-12.

124. Swan, G. *The numerical solution of certain dynamic crack propagation problems*, International Journal of Rock Mechanics and Mining Sciences 12(10) (1975), 295-302.

125. Topping, B.H.V. *Intuitive form-finding of truss structures*, Civil Engineering for Practicing and Design Engineers 3(5) (1984), 491-509.

126. Topping, B.H.V. and Khan, A.I. *Parallel computation schemes for Dynamic Relaxation*, Engineering computations 11(6) (1994), 513-548.

127. Tsotsos, S. and Hatzigogos, T. *Dynamic Relaxation analysis of the foundations of dams and embankments*, Bulletin of the International Association of Engineering Geology 20 (1979), 237-239.

128. Tuma, F.Y. and Galletly, G.D. *Large-deflection of elastic plates using Dynamic Relaxation*, Transactions of the Canadian Society for Mechanical Engineering 2(3) (1973), 121-128.

129. Turvey, G.J. *Study of the behavior of square plates at large deflections according to the theories of FOEPPL and Von Karman*, Journal of Strain Analysis in Engineering Design 13(1) (1978-a), 11-16.

130. Turvey, G.J. *Large deflections of tapered annular plates by Dynamic Relaxation*, ASCE Journal of Engineering Mechanics Division 104(2) (1978-b), 351-366.

131. Turvey, G.J. *Large deflection of circular plates with affine imperfections*, International Journal of Solids and Structures 14(7) (1978-c), 559-569.

132. Turvey, G.J. *Axisymmetric elasto-plastic flexure of circular plates in the large deflexion regime*, Institute of Civil Engineers, ICE proceedings Journal, USA 67 (1979-a), 81-92.

133. Turvey, G.J. *Thickness-tapered circular plates–an elastoplastic large deflection analysis*, Journal of structural mechanics 7(3) (1979-b), 247-271.

134. Turvey, G.J. *Large deflecion of prestressed/prestrained circular membranes*, Institute of Civil Engineers. Part 1 - Design & Construction, ICE proceedings Journal, USA 67 (1979-c), 1121-1126.

135. Turvey, G.J. *Study of the effects of imperfections and lay-up antisymmetry on the initial flexural failure response of cross-ply strips*, Economic Computation and Economic Cybernetics Studies and Research 1 (1980), 291-304.

136. Turvey, G.J. *Large deflection cylindrical bending analysis of cross-ply laminated strips*, Journal of Mechanical Engineering Science 23(1) (1981), 21-29.

137. Turvey, G.J. *Axisymmetric elastic large deflection analysis of composite circular plates*, Fibre Science and Technology 16(3) (1982-a), 191-217.

138. Turvey, G.J. *Axisymmetric flexure of variable thickness circular mindlin plates*, International Journal of Structures 2 (1982-b), 81-88.

139. Turvey, G.J. *Study of the nonlinear elastic flexure of bimodular composite strips*, Fibre Science and Technology 16(2) (1982-c), 121-147.

140. Turvey, G.J. and Der Avanessian, N.G.V. *Elastic large deflection analysis of ring-stiffened circular plates using graded finite-difference*, International Conference on Numerical Methods in Engineering: Theory and Applications Swansea. Wales,UK 7–11 January, 3 (1985), 875-884.

141. Turvey, G.J. and Der Avanessian, N.G.V. *Elastic large deflection of circular plates using graded finite-differences*, Computers and Structures 23(6) (1986-a), 763-774.

142. Turvey, G.J. and Der Avanessian, N.G.V. *DR analysis of beams using graded finite differences*, Computers and Structures 22(5) (1986-b), 737-742.

143. Turvey, G.J. and Der Avanessian, N.G.V. *Axisymmetric elasto-plastic large deflection response of ring stiffened circular plates*, International Journal of Mechanical Sciences 31(11-12) (1989), 905-924.

144. Turvey, G.J. and Der Avanessian, N.G.V. *Full-range response of clamped ring-stiffened circular steel plates-comparisons between experiment and theory*, Computers and Structures 37(1) (1990), 55-70.

145. Turvey, G.J. and Drinali, H. *Elastic postbuckling of orthotropic circular and annular plates with imperfections*, The Third Conference of Composite Structures, Paisley, Scotland, Elsevier Applied Science, London, England (1985), 315-335.

146. Turvey, G.J. and Drinali, H. *Nonlinear first yield analysis of circular plates subjected to combined uniform pressure and edge compression*, Computers and Structures 63(4) (1997), 769-773.

147. Turvey, G.J. and Lim, G.T. *Axisymmetric full-range analysis of transverse pressure-loaded circular plates*, International Journal of Mechanical Sciences 26(9-10) (1984-a), 489-502.

148. Turvey, G.J. and Lim, G.T. *On the degradation of elastic integrity in transverse pressure loaded circular steel plates*, 20th Annual British Society for Strain Measurement Conference on Structural Integrity, Lancaster University, Lancaster, UK (1984-b).

149. Turvey, G.J. and Lim, G.T. *A parametric study of the axisymmetric full-range response of thickness-tapered circular steel plates*, Computers and Structures 22(3) (1986), 459-468.

150. Turvey, G.J. and Osman, M.Y. *Large deflection analysis of orthotropic Mindlin plates*, ASME, Petroleum Division (Publication) 24(1988), 163-172.

151. Turvey, G.J. and Osman, M.Y. *Large deflection initial failure analysis of angle-ply laminated plates*, Composite Structures 25(1-4) (1993), 529-539.

152. Turvey, G.J. and Osman, M.Y. *Elastic and initial flexural failure analysis of unsymmetrically laminated cross-ply strips*, Composites Part B: Engineering 7(5) (1996), 505-518.

153. Turvey, G.J. and Salehi, M. *DR large deflection analysis of sector plates*, Computers and Structures 34(1) (1990), 101-112.

154. Turvey, G.J. and Salehi, M. *Circular plates with one diametral stiffener - An elastic large deflection analysis*, Computers and Structures 63(4) (1997), 775-783.

155. Turvey, G.J. and Salehi, M. *Large deflection analysis of eccentrically stiffened sector plates*, Computers and Structures 68(1-3) (1998), 191-205.

156. Turvey, G.J. and Salehi, M. *Elasto-plastic response of uniformly loaded sector plates: Full-section yield model predictions and spread of plasticity*, Computers and Structures 79(26-28) (2001), 2335-2348.

157. Turvey, G.J. and Salehi, M. *Annular sector plates: Comparison of full-section and layer yield predictions*, Computers and Structures 83(28-30) (2005), 2431-2441.

158. Turvey, G.J. and Wittrick, W.H. *Large deflection and post-buckling behavior of some laminated plates*, Aeron Quart 24(2) (1973), 77-86.

159. Wakefield, D.S. *Engineering analysis of tension structures: Theory and practice*, Engineering Structures 21(8) (1999), 680-690.

160. Wan-lin, D. and Xiao-qing, H. *A study of the post-buckling path of cylindrically curved panels of laminated composite materials during loading and unloading*, Applied Mathematics and Mechanics 11(7) (1990), 651-657.

161. Webb, S.E. and Dowling, P.J. *Large-deflection elasto-plastic behavior of discretely stiffened plates*, Institute of Civil Engineers. Part 1 - Design & Construction, ICE proceedings Journal, USA 69(2) (1980), 375-401.

162. Wu, X.S. and Deng, H. *Form finding of slack cable-bar assembly by Dynamic Relaxation method*, Jisuan Lixue Xuebao/Chinese Journal of Computational Mechanics 25(2) (2008), 229-236.

163. Xiao-qing, H. and Hong, Z. *Influence of compression-bending coupling on the stability behavior of anisotropic laminated panels*, Applied Mathematics and Mechanics 20(1) (1990), 18-26.

164. Xiao-qing, H. and Wan-lin, D. *Effects of transverse shear on the nonlinear bending of rectangular plates laminated of bimodular composite materials*, Applied Mathematics and Mechanics 8(1) (1987), 81-88.

165. Ye, J.H. and Zhou, S.L. *The modified Dynamic Relaxation method for form-finding of membrane structures*, Gongcheng Lixue/Engineering Mechanics 25(12) (2008), 194-201.

166. Zhang, H. and Shan, J. *Form-finding of prestressed cable and membrane structures by Dynamic Relaxation*, Gongcheng Lixue/Engineering Mechanics 19(2) (2002), 41-44.

167. Zhang, L., Maurin, B. and Motro, R. *Form-finding of nonregular tensegrity systems*, Journal of Structural Engineering 132(9) (2006), 1435-1440.

168. Zhang, L.C. *Numerical analysis of the shape effect on the tensile strength evaluation of axisymmetric specimens*, International Journal of Numerical Analysis Methods in Geomechanics 15(4) (1991), 241-250.

169. Zhang, L.C., Yu, T.X. and Wang, R. *A new approach of predicting bifurcation points of elastic-plastic buckling of plates and shells*, Acta Mechanica Sinica 5(2) (1989-a), 145-151.

170. Zhang, L.C., Yu, T.X. and Wang, R. *Investigation of sheet metal forming by bending-Part I. Axisymmetric elastic-plastic bending of circular sheets pressed by cylindrical punches*, International Journal of Mechanical Sciences 31(4) (1989-b), 285-300.

171. Zhao, C.B., Peng, S.L., Liu, L.M., Hobbs, B.E. and Ord, A. *Effective loading algorithm associated with explicit Dynamic Relaxation method for simulating static problems*, Journal of Central South University of Technology 16(1) (2009), 125-130.

172. Zienkiewicz, O.C. and Lohner, R. *Accelerated Relaxation or direct solution future prospects for FEM*, International Journal of Numerical Methods Engineering 21(1) (1985), 1-11.

Iranian Journal of Numerical Analysis and Optimization
Vol. 7, No. 2, (2017), pp 115–135
DOI:10.22067/ijnao.v7i2.62042

Using a LDG method for solving an inverse source problem of the time-fractional diffusion equation

S. Yeganeh, R. Mokhtari* and S. Fouladi

Abstract

In this paper, we apply a local discontinuous Galerkin (LDG) method to solve some fractional inverse problems. In fact, we determine a time-dependent source term in an inverse problem of the time-fractional diffusion equation. The method is based on a finite difference scheme in time and a LDG method in space. A numerical stability theorem as well as an error estimate is provided. Finally, some numerical examples are tested to confirm theoretical results and to illustrate effectiveness of the method. It must be pointed out that proposed method generates stable and accurate numerical approximations without using any regularization methods which are necessary for other numerical methods for solving such ill-posed inverse problems.

Keywords: Local discontinuous Galerkin method; Inverse source problem; Time-fractional diffusion equation.

1 Introduction

Recently, studying problems involving fractional order partial differential equations (PDEs) has attracted a lot of interests of scientists and engineers, see e.g. [1, 5–12, 15, 18–20, 22, 24–30, 33–35]. One of the fractional

*Corresponding author
Received 22 January 2017; revised 29 March 2017; accepted 23 April 2017
S. Yeganeh
Department of Mathematical Sciences, Isfahan University of Technology, Isfahan 84156-83111, Iran. e-mail: s.yeganeh@math.iut.ac.ir

R. Mokhtari
Department of Mathematical Sciences, Isfahan University of Technology, Isfahan 84156-83111, Iran. e-mail: mokhtari@cc.iut.ac.ir

S. Fouladi
Department of Mathematical Sciences, Isfahan University of Technology, Isfahan 84156-83111, Iran.

PDEs which has been very popular is the fractional diffusion equation (FDE), see e.g. [1, 6–12, 15, 18–20, 22, 24–30, 33–35]. Nowadays instead of the classical diffusion equations, FDEs have attracted wide attentions since a FDE is a generalization of a diffusion equation which can be used to describe an anomalous diffusion phenomenon such as super-diffusion or sub-diffusion. By replacing the standard time derivative with a time fractional derivative in a diffusion equation, a time-fractional diffusion equation is obtained. FDEs can be applied in modelling of some problems in porous flows, rheology and mechanical systems, models of a variety of biological processes, control and robotics, transport in fusion plasmas, and many other areas of applications. Analytical or numerical studying of the direct problems corresponding to the time-fractional diffusion equations have been carried out extensively in the recent years, see e.g. [6, 7, 9, 11, 12, 15, 30] as well as references cited therein [27, 28] for some subjects related to the obtaining some uniqueness and existence results, establishing maximum principle, finding analytical solutions, applying some numerical methods such as finite element methods or finite difference methods.

If in an initial or initial-boundary value problem some parts of data such as boundary data, or initial data, or source term or even some coefficients of the main equation may not be given, we have encountered an inverse problem. Inverse problems are appeared in many practical situations, and for solving them we need to some additional measured data, see e.g. [1,8,10,16–25,27–29, 32–35] and references cited therein. In some inverse problems, we need to find space-dependent source term [27, 32] or time-dependent source term [28] or even space- and time-dependent source term [23]. In this paper, we focus our attention on finding the time-dependent source term in a fractional inverse problem which is one of the interesting and novel inverse problems. One of the pioneering scientists in this subject is Murio [18–20]. In the following we mention some of works which have been published after that. An inverse problem for determining the order of fractional derivative and the diffusion coefficient in a FDE has been considered in [1] where a uniqueness result has been also obtained. A backward problem for the time-fractional diffusion equation has been solved by a quasi-reversibility regularization method in [13]. In [34, 35] some Cauchy problems based on the time-fractional diffusion equation have been investigated on a bounded domain and on a strip domain, respectively. Qian [22] has investigated a modified kernel method for solving an inverse fractional diffusion equation. An inverse source problem for a FDE has been solved in [33]. Rundell et al. [10] have been investigated some nonlinear fractional inverse problems. Recently, some interesting works have been carried out by Wei et al., see e.g. [27–29]. In [10] known theoretical results and computational techniques for FDEs have been provided.

In [28] the following initial-boundary value problem for the time-fractional diffusion equation has been considered

$$\begin{cases} D_t^\alpha u = u_{xx} + f(x)p(t),\ 0 < x < 1,\ 0 < t < T, \\ u(0,t) = k_0(t), \qquad\qquad\qquad 0 \leqslant t \leqslant T, \\ u(1,t) = k_1(t), \qquad\qquad\qquad 0 \leqslant t \leqslant T, \\ u(x,0) = \phi(x), \qquad\quad 0 \leqslant x \leqslant 1, \end{cases} \tag{1}$$

where D_t^α is the Caputo fractional derivative of order α, i.e.,

$$D_t^\alpha u = \frac{1}{\Gamma(1-\alpha)} \int_0^t \frac{\partial u(x,s)}{\partial s} \frac{ds}{(t-s)^\alpha}, \qquad 0 < \alpha < 1, \tag{2}$$

in which Γ is the Gamma function. For $\alpha = 1$, we have $D_t^\alpha u = u_t$. We assume that k_0, k_1 and ϕ are given functions. Problem (1) will be a direct (forward) problem whenever f and p are known functions. Based on the availability of f or p, there are some inverse problems. If p is known and f is unknown we need to an extra condition such as

$$u(x,T) = g(x), \qquad 0 \leq x \leq 1.$$

We have investigated numerical solution of this inverse problem in [32]. In another inverse problem, f is known but p is unknown and an over-determination condition such as

$$u(x^*,t) = g(t), \qquad 0 \leq t \leq T, \tag{3}$$

will be needed where $x^* \in (0,1)$ is an interior measurement location. It must be pointed out that although these two inverse problems are very similar they are completely different. The inverse source problem which we consider here is to determine (p,u) based on problem (1) and condition (3). Using the main equation in (1) and Eq. (3), we have

$$p(t) = \frac{1}{f(x^*)} \left(D_t^\alpha g(t) - \frac{\partial^2 u(x^*,t)}{\partial x^2} \right). \tag{4}$$

We need (4) just for theoretical purposes.

The above mentioned inverse source problem is an ill-posed problem [28]. Sakamoto et al. [24] have given a stability estimate for the inverse source problem and mentioned that the uniqueness of p is guaranteed if $f \neq 0$, but they did not present any numerical method. This inverse source problem has been solved numerically by Wei et al. [28] using a regularized method based on the boundary element discretization for recovering a stable approximation to p. In [28], a numerical method has been applied to various examples in particular some examples with none-smooth data which lead to the none-smooth solutions. Therefore, we decided to apply the discontinuous Galerkin method to the above mentioned inverse source problem. To the best of our knowledge, for the inverse source problem with or without fractional operators, the development of the DG methods remains limited and there are a few results, see e.g. [32] where a space-dependent source term is determined in a time-fractional diffusion equation by using a local discontinuous Galerkin method. Of course, some DG methods have been applied successfully for the forward fractional diffusion equation. For example, Hesthaven et al. [6, 30] have been solved some space-fractional diffusion equations using a local discontinuous Galerkin method in a semi-discrete regime and Yang Liu et al. [14] have developed a LDG methos combined with WSGD approximation for a time fractional subdiffusion equation.

In the present paper, we aim to extend application of the discontinuous Galerkin method to some inverse source problems and for this purpose, we present a fully-discrete local discontinuous Galerkin method for solving the inverse source problem of the time-fractional diffusion equation. In the proposed fully-discrete method, we apply a LDG method for the space variable and the time-fractional derivative is discretized by using a backward difference scheme. The rest of the paper is organized as follows. In Section 2, some preliminaries are prepared. Construction of the proposed method for the inverse source problem (1)-(3) as well as stability and convergence theorems are dealt with in Section 3. Section 4 is devoted to some numerical experiments to illustrate the accuracy and capability of the method. Finally, the paper is concluded with a brief conclusion.

2 Preliminaries

In this section, some notations are defined and some auxiliary results are prepared. At first, we decompose interval $[0, 1]$ to some cells (subintervals) as follows

$$0 = x_{\frac{1}{2}} < x_{\frac{3}{2}} < \cdots < x_{N+\frac{1}{2}} = 1,$$

and set $I_j = [x_{j-\frac{1}{2}}, x_{j+\frac{1}{2}}]$, with the cell lengths $\Delta x_j = x_{j+\frac{1}{2}} - x_{j-\frac{1}{2}}$, for $j = 1, \ldots, N$ and $h = \max_{1\leq j\leq N} \Delta x_j$. We denote by $u^+_{j+\frac{1}{2}}$ and $u^-_{j+\frac{1}{2}}$ the values of u at $x_{j+\frac{1}{2}}$, from the right cell I_{j+1} and from the left cell I_j. $[u]_{j+\frac{1}{2}}$ is used to denote $u^+_{j+\frac{1}{2}} - u^-_{j+\frac{1}{2}}$, that is the jump of u at the cell interfaces. For any integer k, we define the piecewise-polynomial space V_h^k as the space of polynomials of degree up to k in each cell I_j, thus

$$V_h^k = \left\{ v \in L^2[0, 1] : \ v|_{I_j} \in \mathbb{P}^k(I_j), \ j = 1, \ldots, N \right\}.$$

In order to investigate the convergence of the method, we need to define projections $\mathbf{P}$ and $\mathbf{P}^{\pm}$ as follows

$$\int_{I_j} (\mathbf{P}\omega(x) - \omega(x))v(x)dx = 0, \quad \forall v \in \mathbb{P}^k(I_j), \quad \forall j,$$

$$\int_{I_j}(\mathbf{P}^{\pm}\omega(x)-\omega(x))v(x)dx=0, \quad \forall v\in\mathbb{P}^{k-1}(I_j), \quad \forall j,$$

$$\mathbf{P}^{\pm}\omega(x^{+}_{j\mp\frac{1}{2}})=\omega(x_{j\mp\frac{1}{2}}).$$

It is well-known that these projections satisfy the following inequality [2,31]

$$\| \omega^e \| + h \| \omega^e \|_\infty + h^{\frac{1}{2}} \| \omega^e \|_{\tau_h} \leq Ch^{k+1},$$

where $\omega^e = \mathbf{P}\omega - \omega$ or $\omega^e = \mathbf{P}^{\pm}\omega - \omega$, the positive constant C, solely depending on ω, is independent of h, and τ_h denotes the set of boundary points of all cells I_j. In the following, we use C to denote a positive constant which is independent of h and may have a different value in each occurrence. v_x denotes the piecewise derivative with respect to x, and the norm $\| \cdot \|$ denotes the usual norm of the space $L^2[0,1]$.

3 Construction of the method

In this section, we construct a numerical scheme for solving problem (1)-(3). Let M be a positive integer, $\Delta t = T/M$ be the time step size, and $t_n = n\Delta t,\ n = 0,1,\ldots,M$ denote the time mesh points. An approximation to time-fractional derivative (2) can be obtained by a simple quadrature formula given as [9,11,12],

$$D_t^{\alpha}u(x,t_n)=\frac{(\Delta t)^{1-\alpha}}{\Gamma(2-\alpha)}\sum_{i=0}^{n-1}b_i\frac{u(x,t_{n-i})-u(x,t_{n-i-1})}{\Delta t}+O((\Delta t)^{2-\alpha}), \quad (5)$$

where $b_i = (i+1)^{1-\alpha} - i^{1-\alpha}$.
Following the LDG regime [6,30], we must rewrite (1) as the following first-order system of equations

$$q = u_x, \qquad D_t^{\alpha}u(x,t) - q_x = f(x)p(t). \quad (6)$$

Let $u_h^n, q_h^n \in V_h^k$ be the approximation of $u(\cdot,t_n), q(\cdot,t_n)$ respectively, and $p^n = p(t_n), g^n = g(t_n)$. Using (5), we establish the necessary weak forms corresponding to (6) and then define a fully-discrete local discontinuous Galerkin scheme as follows: find $u_h^n, q_h^n \in V_h^k$, such that for all test functions $v, w \in V_h^k$,

$$\begin{cases} \int_\Omega u_h^n v dx + \beta \left(\int_\Omega q_h^n v_x dx - \sum_{j=1}^{N} ((\hat{q}_h^n v^-)_{j+\frac{1}{2}} - (\hat{q}_h^n v^+)_{j-\frac{1}{2}}) \right) = \\ \qquad \beta p^n \int_\Omega f(x) v dx + \sum_{i=1}^{n-1} (b_{i-1} - b_i) \int_\Omega u_h^{n-i} v + b_{n-1} \int_\Omega u_h^0 v dx, \\ \int_\Omega q_h^n w dx + \int_\Omega u_h^n w_x dx - \sum_{j=1}^{N} ((\hat{u}_h^n w^-)_{j+\frac{1}{2}} - (\hat{u}_h^n w^+)_{j-\frac{1}{2}}) = 0, \\ u_h^n(x^*) = g^n, \end{cases} \tag{7}$$

where $\Omega = [0,1]$ and $\beta = (\Delta t)^\alpha \Gamma(2-\alpha)$ and without lose of generality we assume that x^* is a grid point. The "hat" terms in (7) in the cell boundary terms from integration by parts are the so-called "numerical fluxes", which are single valued functions defined on the interfaces and should be selected carefully for ensuring the numerical stability of the scheme. The choice for the numerical fluxes is not unique and among several choices, we can take $\hat{u}_h^n = (u_h^n)^-$ and $\hat{q}_h^n = (q_h^n)^+$ or $\hat{u}_h^n = (u_h^n)^+$ and $\hat{q}_h^n = (q_h^n)^-$. In fact, it is important to take $\hat{u}_h^n$ and $\hat{q}_h^n$ from opposite sides [3, 4].

Before investigating theoretical aspects of the method, we are going to explain details of the method somewhat more. We set

$$u_h^n(x) = u_h(x, n\Delta t) = \sum_{i=1}^{N_p} \delta_i^n \Phi_i(x), \qquad q_h^n(x) = q_h(x, n\Delta t) = \sum_{i=1}^{N_p} \gamma_i^n \Phi_i(x),$$

where N_p is the total number of basis functions and

$$F = \left(\int_\Omega f_h(x)\Phi_1(x)dx \ \cdots \ \int_\Omega f_h(x)\Phi_{N_p}(x)dx \right)^T,$$

$$\Phi = \left(\Phi_1(x^*) \ \cdots \ \Phi_{N_p}(x^*) \right), \quad Z = (0 \ \cdots \ 0).$$

Setting $\delta^n = (\delta_1^n \ \cdots \ \delta_{N_p}^n)^T$ and $\gamma^n = (\gamma_1^n \ \cdots \ \gamma_{N_p}^n)^T$, scheme (7) leads to the following iteration scheme

$$\begin{cases} K_{11}\delta^n + K_{12}\gamma^n = \beta p^n F + \sum_{i=1}^{n-1} (b_{i-1} - b_i) K_{22} \delta^{n-i}, \\ K_{21}\delta^n + K_{22}\gamma^n = 0, \\ \Phi\delta^n = g^n, \end{cases}$$

where $n = 1, \ldots, M$ and

$$(K_{11})_{lr} = \int_\Omega \Phi_l(x)\Phi_r(x)dx, \qquad K_{22} = K_{11},$$

$$(K_{12})_{lr} = \beta \int_\Omega \Phi_l(x)(\Phi_r(x))_x dx - \beta \sum_{j=1}^{N} \Big(\Phi_l(x^-_{j+\frac{1}{2}})\Phi_r(x^-_{j+\frac{1}{2}}) - \Phi_l(x^-_{j-\frac{1}{2}})\Phi_r(x^+_{j-\frac{1}{2}}) \Big),$$

$$(K_{21})_{lr} = \int_\Omega \Phi_l(x)(\Phi_r(x))_x dx - \sum_{j=1}^{N} \Big(\Phi_l(x^+_{j+\frac{1}{2}})\Phi_r(x^-_{j+\frac{1}{2}}) - \Phi_l(x^+_{j-\frac{1}{2}})\Phi_r(x^+_{j-\frac{1}{2}}) \Big).$$

For solving the direct problem, we have

$$M \begin{pmatrix} \delta^n \\ \gamma^n \end{pmatrix} = \begin{pmatrix} \beta p^n F + \sum_{i=1}^{n-1} (b_{i-1} - b_i) K_{11} \delta^{n-i} \\ 0 \end{pmatrix}, \quad M = \begin{pmatrix} K_{11} & K_{12} \\ K_{21} & K_{11} \end{pmatrix}, \tag{8}$$

where matrix K_{11} is nonsingular and block diagonal which every block is a $k \times k$ (k is degree of basis polynomials) matrix. Using the Schur complement, linear system (8) has a unique solution iff $\det(K_{11} - K_{12}K_{11}^{-1}K_{21}) \neq 0$. For solving the inverse problem, we have

$$\begin{pmatrix} K_{11} & K_{12} & -\beta F \\ K_{21} & K_{11} & Z^T \\ \Phi & Z & 0 \end{pmatrix} \begin{pmatrix} \delta^n \\ \gamma^n \\ p^n \end{pmatrix} = \begin{pmatrix} \sum_{i=1}^{n-1} (b_{i-1} - b_i) K_{11} \delta^{n-i} \\ 0 \\ g^n \end{pmatrix}, \tag{9}$$

where we put g^n_δ instead of g^n since data are usually obtained by measurement tools and have some noises. By solving the nonsymmetric linear system (9) using the BiCGStab method, we can obtain u^n_h and p^n.

Just for convenience and without lose of generality, we deal with the case $g = 0$ in the theoretical analysis. In order to examine the stability property of the scheme (7), we express following result.

Theorem 3. *Assume that the second derivative of u at $x = x^*$ is bounded and f is a continuous function on $[0, 1]$. For periodic or compactly supported boundary conditions, fully-discrete LDG scheme (7) is unconditionally stable, and the numerical solution u^n_h satisfies*

$$\|u^n_h\| \leq \|u^0_h\| + \kappa, \quad n = 1, \ldots, M,$$

where κ is a constant depending on β, f and u_{xx} at $x = x^*$.

Proof. We can rewrite scheme (7) as follows

$$\begin{aligned}
&\int_\Omega u_h^n v dx + \beta\left(\int_\Omega q_h^n v_x dx - \sum_{j=1}^{N}((\hat{q}_h^n v^-)_{j+\frac{1}{2}} - (\hat{q}_h^n v^+)_{j-\frac{1}{2}})\right)\\
&-\sum_{j=1}^{N}((\hat{u}_h^n w^-)_{j+\frac{1}{2}} - (\hat{u}_h^n w^+)_{j-\frac{1}{2}}) + \int_\Omega q_h^n w dx + \int_\Omega u_h^n w_x dx\\
&= \beta p^n \int_\Omega f(x) v dx + \sum_{i=1}^{n-1}(b_{i-1}-b_i)\int_\Omega u_h^{n-i} v dx + b_{n-1}\int_\Omega u_h^0 v dx,
\end{aligned}$$

With taking test functions $v = u_h^n$, $w = \beta q_h^n$, for periodic or compactly supported boundary conditions, we can obtain

$$\begin{aligned}
&\beta\left(\int_\Omega q_h^n v_x dx - \sum_{j=1}^{N}((\hat{q}_h^n v^-)_{j+\frac{1}{2}} - (\hat{q}_h^n v^+)_{j-\frac{1}{2}})\right) + \int_\Omega u_h^n w_x dx\\
&-\sum_{j=1}^{N}((\hat{u}_h^n w^-)_{j+\frac{1}{2}} - (\hat{u}_h^n w^+)_{j-\frac{1}{2}}) = \beta\int_\Omega q_h^n (u_h^n)_x dx\\
&-\beta\sum_{j=1}^{N}\left(((q_h^n)^+(u_h^n)^-)_{j+\frac{1}{2}} - ((q_h^n)^+(u_h^n)^+)_{j-\frac{1}{2}}\right) + \beta\int_\Omega u_h^n (q_h^n)_x dx\\
&-\beta\sum_{j=1}^{N}\left(((u_h^n)^-(q_h^n)^-)_{j+\frac{1}{2}} - ((u_h^n)^-(q_h^n)^+)_{j-\frac{1}{2}}\right) = 0,
\end{aligned}$$

then

$$\begin{aligned}
\int_\Omega u_h^n v dx + \int_\Omega q_h^n w dx = \sum_{i=1}^{n-1}(b_{i-1}-b_i)\int_\Omega u_h^{n-i} u_h^n dx + b_{n-1}\int_\Omega u_h^0 u_h^n dx\\
+ \beta p^n \int_\Omega f(x) u_h^n dx.
\end{aligned} \tag{10}$$

For $n = 1$ and using Eq. (4), we can get

$$\begin{aligned}
\| u_h^1 \|^2 + \beta \| q_h^1 \|^2 &= \int_\Omega u_h^0 u_h^1 dx + \beta p^1 \int_\Omega f(x) u_h^1 dx\\
&= \int_\Omega u_h^0 u_h^1 dx - \beta\int_\Omega \frac{f}{f^*}\left(u_h^1\right)^*_{xx} u_h^1 dx\\
&= \int_\Omega \left(u_h^0 - \beta\frac{f}{f^*}\left(u_h^1\right)^*_{xx}\right) u_h^1 dx\\
&\le \frac{1}{2}\left(\| u_h^0 - \beta\frac{f}{f^*}\left(u_h^1\right)^*_{xx} \|^2 + \| u_h^1 \|^2\right)\\
&\le \frac{1}{2}\left(\left(\| u_h^0 \| + \beta \| \frac{f}{f^*}\left(u_h^1\right)^*_{xx} \|\right)^2 + \| u_h^1 \|^2\right),\\
&\le \frac{1}{2}\left(\left(\| u_h^0 \| + \kappa\right)^2 + \| u_h^1 \|^2\right),
\end{aligned}$$

therefore

$$\| u_h^1 \| \leq \| u_h^0 \| + \kappa.$$

Next, we suppose the following inequalities hold

$$\| u_h^m \| \leq \| u_h^0 \| + \kappa, \qquad m = 1, \ldots, K.$$

For $n = K + 1$, in Eq. (10), and using

$$\sum_{i=1}^{l} (b_{i-1} - b_i) + b_l = 1,$$

we can obtain

$$\| u_h^{l+1} \| \leq \| u_h^0 \| + \kappa.$$

□

In order to examine the convergence of the scheme (7), we express following result.

Theorem 4. *Let $u(\cdot, t_n)$ be the exact solution of the problem (1)-(3), which is sufficiently smooth with bounded derivatives, and u_h^n be the numerical solution of the fully-discrete LDG scheme (7). There holds the following error estimate*

$$\|u(\cdot, t_n) - u_h^n\| \leq C(h^{k+1} + (\Delta t)^2 + (\Delta t)^{\frac{\alpha}{2}} h^{k+\frac{1}{2}} + c(\Delta t)^{\alpha}),$$

where C is a constant depending on α, u, and T, and c is a constant depending on f and u_{xx} at $x = x^*$.

Proof. Obviously for all test functions $v, w \in V_h^k$, we have

$$\begin{aligned}
&\int_\Omega u(x,t_n) v dx + \int_\Omega u(x,t_n) w_x dx - \sum_{j=1}^{N} ((u(x,t_n) w^-)_{j+\frac{1}{2}} - (u(x,t_n) w^+)_{j-\frac{1}{2}}) \\
&\quad + \beta \left(\int_\Omega q(x,t_n) v_x dx - \sum_{j=1}^{N} ((q(x,t_n) v^-)_{j+\frac{1}{2}} - (q(x,t_n) v^+)_{j-\frac{1}{2}}) \right) \\
&\quad - \sum_{i=1}^{n-1} (b_{i-1} - b_i) \int_\Omega u(x, t_{n-i}) v dx - b_{n-1} \int_\Omega u(x, t_0) v dx \\
&\quad + \int_\Omega q(x,t_n) w dx + \beta \int_\Omega \gamma^n(x) v dx - \beta p(x,t_n) \int_\Omega f(x) v dx = 0.
\end{aligned} \tag{11}$$

Subtracting equation (7) from (11), we can obtain the error equation

$$\begin{aligned}
&\int_\Omega e_u^n v dx + \beta\left(\int_\Omega e_q^n v_x dx - \sum_{j=1}^{N}(((e_q^n)^+ v^-)_{j+\frac{1}{2}} - ((e_q^n)^+ v^+)_{j-\frac{1}{2}})\right)\\
&+\int_\Omega e_q^n w dx + \int_\Omega e_u^n w_x dx - \sum_{j=1}^{N}(((e_u^n)^- w^-)_{j+\frac{1}{2}} - ((e_u^n)^- w^+)_{j-\frac{1}{2}})\\
&-b_{n-1}\int_\Omega e_u^0 v dx - \sum_{i=1}^{n-1}(b_{i-1}-b_i)\int_\Omega e_u^{n-i} v dx + \beta\int_\Omega \gamma^n(x) v dx\\
&-\beta p(x,t_n)\int_\Omega f(x) v dx = 0.
\end{aligned}$$

where

$$\begin{aligned}
e_u^n &= u(x,t_n) - u_h^n = \mathbf{P}^- e_u^n - (\mathbf{P}^- u(x,t_n) - u(x,t_n)),\\
e_q^n &= q(x,t_n) - q_h^n = \mathbf{P} e_q^n - (\mathbf{P} q(x,t_n) - q(x,t_n)).
\end{aligned} \tag{12}$$

Using Eq. (4), we have

$$\begin{aligned}
&\int_\Omega e_u^n v dx + \beta\left(\int_\Omega e_q^n v_x dx - \sum_{j=1}^{N}(((e_q^n)^+ v^-)_{j+\frac{1}{2}} - ((e_q^n)^+ v^+)_{j-\frac{1}{2}})\right)\\
&+\int_\Omega e_q^n w dx + \int_\Omega e_u^n w_x dx - \sum_{j=1}^{N}(((e_u^n)^- w^-)_{j+\frac{1}{2}} - ((e_u^n)^- w^+)_{j-\frac{1}{2}})\\
&-b_{n-1}\int_\Omega e_u^0 v dx - \sum_{i=1}^{n-1}(b_{i-1}-b_i)\int_\Omega e_u^{n-i} v dx + \beta\int_\Omega \gamma^n(x) v dx\\
&+\beta\int_\Omega \frac{f}{f^*} u_{xx}(x^*,t_n) v dx = 0.
\end{aligned} \tag{13}$$

Using Eq. (12), the error equation (13) can be rewritten as follows

$$\begin{aligned}
&\int_\Omega \mathbf{P}^- e_u^n v dx + \beta\left(\int_\Omega \mathbf{P} e_q^n v_x dx - \sum_{j=1}^{N}(((\mathbf{P} e_q^n)^+ v^-)_{j+\frac{1}{2}} - ((\mathbf{P} e_q^n)^+ v^+)_{j-\frac{1}{2}})\right)\\
&+\int_\Omega \mathbf{P} e_q^n w dx + \int_\Omega \mathbf{P}^- e_u^n w_x dx - \sum_{j=1}^{N}(((\mathbf{P}^- e_u^n)^- w^-)_{j+\frac{1}{2}} - ((\mathbf{P}^- e_u^n)^- w^+)_{j-\frac{1}{2}})\\
&+\beta\int_\Omega \frac{f}{f^*} u_{xx}(x^*,t_n) v dx = b_{n-1}\int_\Omega \mathbf{P}^- e_u^0 v dx + \sum_{i=1}^{n-1}(b_{i-1}-b_i)\int_\Omega \mathbf{P}^- e_u^{n-i} v dx\\
&+\int_\Omega (\mathbf{P}^- u(x,t_n) - u(x,t_n)) v dx + \beta\left(\int_\Omega (\mathbf{P} q(x,t_n) - q(x,t_n)) v_x dx\right.\\
&\left.-\sum_{j=1}^{N}(((\mathbf{P} q(x,t_n) - q(x,t_n))^+ v^-)_{j+\frac{1}{2}} - ((\mathbf{P} q(x,t_n) - q(x,t_n))^+ v^+)_{j-\frac{1}{2}})\right)\\
&+\int_\Omega (\mathbf{P} q(x,t_n) - q(x,t_n)) w dx + \int_\Omega (\mathbf{P}^- u(x,t_n) - u(x,t_n)) w_x dx
\end{aligned}$$

$$-\sum_{j=1}^{N}(((\mathbf{P}^{-}u(x,t_n)-u(x,t_n))^{-}w^{-})_{j+\frac{1}{2}}-((\mathbf{P}^{-}u(x,t_n)-u(x,t_n))^{-}w^{+})_{j-\frac{1}{2}})$$
$$-\beta\int_{\Omega}\gamma^{n}(x)vdx-b_{n-1}\int_{\Omega}(\mathbf{P}^{-}u(x,t_0)-u(x,t_0))vdx$$
$$-\sum_{i=1}^{n-1}(b_{i-1}-b_i)\int_{\Omega}(\mathbf{P}^{-}u(x,t_{n-i})-u(x,t_{n-i}))vdx.$$

With taking the test functions $v=u_h^n$, $w=\beta q_h^n$, for periodic or compactly supported boundary conditions, we derive

$$\int_{\Omega}\left(\mathbf{P}^{-}e_u^n\right)^2dx+\beta\int_{\Omega}\left(\mathbf{P}e_q^n\right)^2dx+\beta\int_{\Omega}\frac{f}{f^*}u_{xx}(x^*,t_n)\mathbf{P}^{-}e_u^ndx$$
$$=b_{n-1}\int_{\Omega}\mathbf{P}^{-}e_u^0\mathbf{P}^{-}e_u^ndx+\sum_{i=1}^{n-1}(b_{i-1}-b_i)\int_{\Omega}\mathbf{P}^{-}e_u^{n-i}\mathbf{P}^{-}e_u^ndx$$
$$-\beta\int_{\Omega}\gamma^{n}(x)\mathbf{P}^{-}e_u^ndx+\beta\sum_{j=1}^{N}\left(((\mathbf{P}q(x,t_n)-q(x,t_n))^{+}\left[\mathbf{P}^{-}e_u^n\right]\right)_{j-\frac{1}{2}}$$
$$+\int_{\Omega}(\mathbf{P}^{-}u(x,t_n)-u(x,t_n))\mathbf{P}^{-}e_u^ndx-b_{n-1}\int_{\Omega}(\mathbf{P}^{-}u(x,t_0)-u(x,t_0))\mathbf{P}^{-}e_u^ndx$$
$$-\sum_{i=1}^{n-1}(b_{i-1}-b_i)\int_{\Omega}(\mathbf{P}^{-}u(x,t_{n-i})-u(x,t_{n-i}))\mathbf{P}^{-}e_u^ndx.$$

For $n=1$, we have

$$\begin{aligned}&\int_{\Omega}\left(\mathbf{P}^{-}e_u^1\right)^2dx+\beta\int_{\Omega}\left(\mathbf{P}e_q^1\right)^2dx+\beta\int_{\Omega}\frac{f}{f^*}u_{xx}(x^*,t_1)\mathbf{P}^{-}e_u^1dx\\&=\int_{\Omega}\mathbf{P}^{-}e_u^0\mathbf{P}^{-}e_u^1dx+\int_{\Omega}(\mathbf{P}^{-}u(x,t_0)-u(x,t_0))\mathbf{P}^{-}e_u^1dx\\&-\beta\int_{\Omega}\gamma^{1}(x)\mathbf{P}^{-}e_u^1dx+\beta\sum_{j=1}^{N}\left(((\mathbf{P}q(x,t_1)-q(x,t_1))^{+}\left[\mathbf{P}^{-}e_u^1\right]\right)_{j-\frac{1}{2}}\\&-\int_{\Omega}(\mathbf{P}^{-}u(x,t_1)-u(x,t_1))\mathbf{P}^{-}e_u^1dx.\end{aligned}$$

Using the following facts

$$\| P^{-}e_u^0\|\leq Ch^{k+1},\quad ab\leq\varepsilon a^2+\frac{1}{4\varepsilon}b^2, \tag{14}$$

we obtain

$$\begin{aligned}\|\mathbf{P}^{-}e_u^1\|^2+\beta\|\mathbf{P}e_q^1\|^2\leq{}&(\|\mathbf{P}^{-}e_u^0\|+\beta\|\gamma^1(x)\|+\|\mathbf{P}^{-}u(x,t_1)-u(x,t_1)\|\\&+\|\mathbf{P}^{-}u(x,t_0)-u(x,t_0)\|+c\beta)\|\mathbf{P}^{-}e_u^1\|\\&+\frac{\beta}{4\varepsilon}\sum_{j=1}^{N}\left((\mathbf{P}q(x,t_1)-q(x,t_1))^{+}\right)^2_{j-\frac{1}{2}}+\beta\varepsilon\sum_{j=1}^{N}\left[\mathbf{P}^{-}e_u^1\right]^2_{j-\frac{1}{2}}\end{aligned}$$

$$\leq C(h^{k+1}+(\Delta t)^2+(\Delta t)^{\frac{\alpha}{2}}h^{k+\frac{1}{2}}+c(\Delta t)^{\alpha})^2+\varepsilon \parallel \mathbf{P}^{-}e_u^1 \parallel^2$$
$$+\beta\varepsilon\sum_{j=1}^{N}\left[\mathbf{P}^{-}e_u^1\right]_{j-\frac{1}{2}}^2.$$

If we choose ε very small, we conclude that

$$\parallel \mathbf{P}^{-}e_u^1 \parallel^2 +\beta \parallel \mathbf{P}e_q^1 \parallel^2 \leq C(h^{k+1}+(\Delta t)^2+(\Delta t)^{\frac{\alpha}{2}}h^{k+\frac{1}{2}}+c(\Delta t)^{\alpha})^2.$$

Now, we suppose the following inequalities hold

$$\|\mathbf{P}^{-}e_u^m\| \leq C(h^{k+1}+(\Delta t)^2+(\Delta t)^{\frac{\alpha}{2}}h^{k+\frac{1}{2}}+c(\Delta t)^{\alpha}), \quad m=1,2,\ldots,l.$$

We need to prove $\|\mathbf{P}^{-}e_u^{l+1}\| \leq C(h^{k+1}+(\Delta t)^2+(\Delta t)^{\frac{\alpha}{2}}h^{k+\frac{1}{2}}+c(\Delta t)^{\alpha})$. Letting $n=l+1$, we have

$$\int_\Omega \left(\mathbf{P}^{-}e_u^{l+1}\right)^2 dx+\beta\int_\Omega \left(\mathbf{P}e_q^{l+1}\right)^2 dx+\beta\int_\Omega \frac{f}{f^*}u_{xx}(x^*,t_{l+1})\mathbf{P}^{-}e_u^{l+1}dx$$
$$=b_l\int_\Omega \mathbf{P}^{-}e_u^0\mathbf{P}^{-}e_u^{l+1}dx+\sum_{i=1}^{l}(b_{i-1}-b_i)\int_\Omega \mathbf{P}^{-}e_u^{l+1-i}\mathbf{P}^{-}e_u^{l+1}dx$$
$$-\beta\int_\Omega \gamma^{l+1}(x)\mathbf{P}^{-}e_u^{l+1}dx+\beta\sum_{j=1}^{N}\left(((\mathbf{P}q(x,t_{l+1})-q(x,t_{l+1}))^{+}\left[\mathbf{P}^{-}e_u^{l+1}\right]\right)_{j-\frac{1}{2}}$$
$$+\int_\Omega(\mathbf{P}^{-}u(x,t_{l+1})-u(x,t_{l+1}))\mathbf{P}^{-}e_u^{l+1}dx$$
$$-b_l\int_\Omega(\mathbf{P}^{-}u(x,t_0)-u(x,t_0))\mathbf{P}^{-}e_u^{l+1}dx$$
$$-\sum_{i=1}^{l}(b_{i-1}-b_i)\int_\Omega(\mathbf{P}^{-}u(x,t_{l+1-i})-u(x,t_{l+1-i}))\mathbf{P}^{-}e_u^{l+1}dx.$$

Then by using (14) and

$$\sum_{i=1}^{l}(b_{i-1}-b_i)+b_l=1,$$

we can obtain

$$\parallel \mathbf{P}^{-}e_u^{l+1} \parallel^2 +\beta \parallel \mathbf{P}e_q^{l+1} \parallel^2 \leq (b_l \parallel \mathbf{P}^{-}e_u^0 \parallel + \parallel \mathbf{P}^{-}u(x,t_{l+1})-u(x,t_{l+1}) \parallel$$
$$+\beta \parallel \gamma^1(x) \parallel +b_l \parallel \mathbf{P}^{-}u(x,t_0)-u(x,t_0) \parallel +c\beta) \parallel \mathbf{P}^{-}e_u^{l+1} \parallel$$
$$+\sum_{i=1}^{l}(b_{i-1}-b_i) \parallel \mathbf{P}^{-}e_u^{l+1-i} \parallel\parallel \mathbf{P}^{-}e_u^{l+1} \parallel +\beta\varepsilon\sum_{j=1}^{N}\left[\mathbf{P}^{-}e_u^{l+1}\right]_{j-\frac{1}{2}}^2$$
$$+\frac{\beta}{4\varepsilon}\sum_{j=1}^{N}\left((\mathbf{P}q(x,t_{l+1})-q(x,t_{l+1}))^{+}\right)_{j-\frac{1}{2}}^2$$

$$
\begin{aligned}
&\leq C_1 b_l (h^{k+1} + (\Delta t)^2 + (\Delta t)^{\frac{\alpha}{2}} h^{k+\frac{1}{2}} + c(\Delta t)^{\alpha}) \parallel \mathbf{P}^- e_u^{l+1} \parallel \\
&+\beta\varepsilon \sum_{j=1}^{N} \left[\mathbf{P}^- e_u^{l+1}\right]_{j-\frac{1}{2}}^2 + \sum_{i=1}^{l} (b_{i-1} - b_i) C_2 (h^{k+1} + (\Delta t)^2 + (\Delta t)^{\frac{\alpha}{2}} h^{k+\frac{1}{2}} \\
&+c(\Delta t)^{\alpha}) \parallel \mathbf{P}^- e_u^{l+1} \parallel \leq C(h^{k+1} + (\Delta t)^2 + (\Delta t)^{\frac{\alpha}{2}} h^{k+\frac{1}{2}} + c(\Delta t)^{\alpha})^2 \\
&+\varepsilon \parallel \mathbf{P}^- e_u^{l+1} \parallel^2 + \beta\varepsilon \sum_{j=1}^{N} \left[\mathbf{P}^- e_u^{l+1}\right]_{j-\frac{1}{2}}^2 .
\end{aligned}
$$

Choosing a small ε, we derive

$$
\|\mathbf{P}^- e_u^{l+1}\| \leq C(h^{k+1} + (\Delta t)^2 + (\Delta t)^{\frac{\alpha}{2}} h^{k+\frac{1}{2}} + c(\Delta t)^{\alpha}).
$$

□

4 Numerical examples

In this section, we carry out some numerical tests to confirm theoretical results and to investigate the efficiency of the proposed method. The maximum time is $T = 1$ otherwise it will be specified. The space and time step sizes are $h = 1/N$ and $\Delta t = T/M$, respectively. We use the relative root mean square error, i.e.,

$$
\varepsilon(p) = \left(\sum_{n=1}^{M} (p_h^n - p(t_n))^2 / \sum_{n=1}^{M} p(t_n)^2 \right)^{1/2}, \tag{15}
$$

for checking the accuracy of the numerical solutions. In all of tests, we take $k = 2$, i.e., we consider piecewise polynomials of degree two as the basis functions in the LDG regime. For dealing with the sensitivity of the solution with respect to the data, we use the following noisy data

$$
g^{\delta}(t_n) = g(t_n)(1 + \delta \, \mathrm{rnd}(n)), \quad n = 0, 1, \ldots,
$$

where g is the exact data and $\mathrm{rnd}(n)$ is a random number uniformly distributed in $[-1, 1]$ and the magnitude δ indicates a relative noise level.

Example 1 We consider the inverse source problem of the time-fractional diffusion equation (1)-(3) with the exact solution $u(x,t) = e^{-t}\cos(2\pi x)$. Setting Δt very small and using the usual L^2 and L^∞ error norms, we show in Table 1 that the order of convergence of the proposed method is about three as we expected (according to the obtained error estimate since $k = 2$). Since the exact p of this problem is not accessible, in Fig 1. we show p_h^n for $\alpha = 0.5, x^\star = 0.75$ and $N = 8, 16$. The errors in L^2-norm and L^∞-norm for piecewise $P^k, k = 1, 2, 3$ polynomials for $\alpha = 0.1, x^\star = 0.25$ are presented in Fig 2.

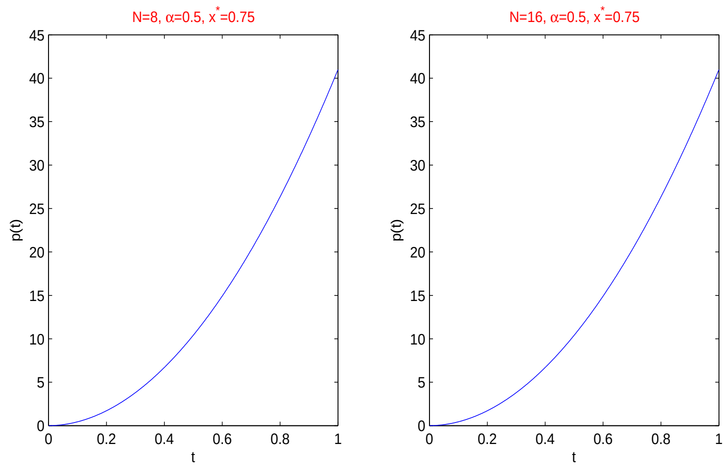

Figure 1: Numerical approximations to p for Example 1 for $N = 8$ (left) and $N = 16$ (right).

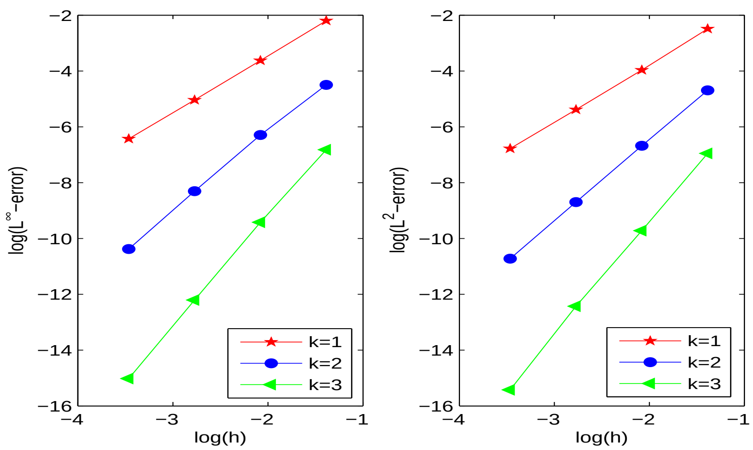

Figure 2: log(error) as a function of log(h) for $\alpha = 0.1, x^\star = 0.25$ when using piecewise $P^k, k = 1, 2, 3$ polynomials for Example 1.

Example 2. Let the exact solution for problem (1)-(3) be $u(x,t) = t^2 \sin\left(\frac{\pi}{2}x\right)$. Therefore, $\phi(x) = u(x,0) = 0$, $k_0(t) = u(0,t) = 0$, $k_1(t) = u(1,t) = t^2$, $f(x) = \sin\left(\frac{\pi}{2}x\right)$, and $p(t) = \frac{2}{\Gamma(3-\alpha)}t^{2-\alpha} + \frac{\pi^2}{4}t^2$. We take

Table 1: Accuracy test for Example 1 for different α with $x^* = 0.5$.

	N	L^2 error	Order	L^∞ error	Order
$\alpha = 0.3$	5	0.002067	-	0.002780	-
	10	0.000280	2.9	0.000376	2.9
	15	0.000079	3.1	0.000112	3.0
	20	0.000034	2.9	0.000047	3.0
$\alpha = 0.5$	5	0.002068	-	0.002781	-
	10	0.000280	2.9	0.000376	2.9
	15	0.000079	3.1	0.000112	3.0
	20	0.000034	2.9	0.000047	3.0
$\alpha = 0.7$	5	0.002069	-	0.002783	-
	10	0.000280	2.9	0.000377	2.9
	15	0.000079	3.1	0.000112	3.0
	20	0.000034	2.9	0.000047	3.0
$\alpha = 1$	5	0.002070	-	0.002784	-
	10	0.000281	2.9	0.000377	2.9
	15	0.000079	3.1	0.000112	3.0
	20	0.000034	2.9	0.000047	3.0

$x^* = 0.5$, then $g(t) = \sin(\frac{\pi}{4})t^2$. p_h^n for $\alpha = 0.5$ and $\alpha = 0.95$ with various noise levels $\delta = 5\%,\ 10\%,\ 15\%$ are plotted in Fig. 3. Corresponding relative root mean square errors are $\varepsilon(p) = 8.5762 \times 10^{-5},\ 8.6406 \times 10^{-5},\ 8.7104 \times 10^{-5}$ for $\alpha = 0.5$ and $\varepsilon(p) = 2.030156 \times 10^{-3},\ 3.077799 \times 10^{-3},\ 4.153917 \times 10^{-3}$ for $\alpha = 0.95$. In Table 2, we compare the relative root mean square errors for the

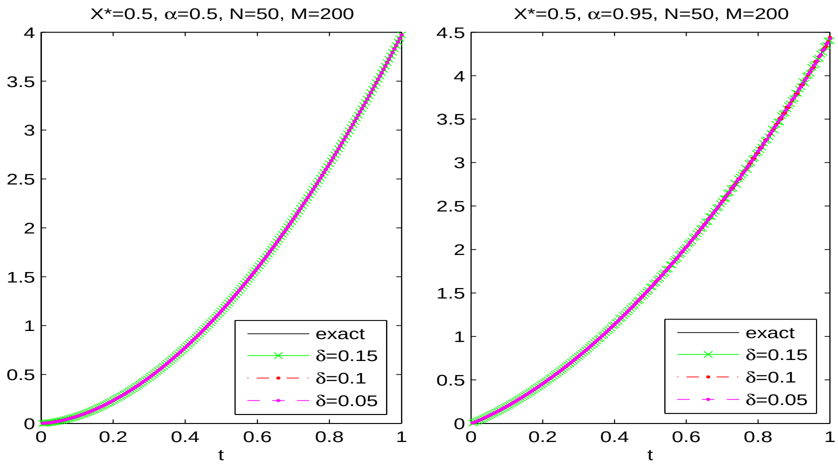

Figure 3: Numerical approximations to p for Example 2.

proposed method in [28] ($\varepsilon_1(p)$ for no regularization method and $\varepsilon_2(p)$ with a regularization method) with the proposed LDG method ($\varepsilon_3(p)$). In Table 3 the relative errors for different x^* with $N = 50$ are compared. The proposed method could generate more satisfactory results without any regularization method. To verify the role of the final time T, we depict p_h^n for $\alpha = 0.95$ with $T = 100, 10000$ and $\delta = 5\%,\ 10\%,\ 15\%$ in Fig. 4. We can see that the dependency of the results to final time T is almost unimportant, even when T is very large, i.e., $T = 10000$. Without any regularization method, the trace of the loss of stability does not appear.

Table 2: Comparison approximation solutions of Example 2 with the literature for various α.

		$\alpha = 0.1$	$\alpha = 0.3$	$\alpha = 0.5$	$\alpha = 0.7$	$\alpha = 0.9$
$\delta = 5\%$	$\varepsilon_1(p)$	0.0773	0.0880	0.1230	0.2651	0.8079
	$\varepsilon_2(p)$	0.0331	0.0362	0.0393	0.0413	0.0431
	$\varepsilon_3(p)$	2.162×10^{-6}	1.9319×10^{-5}	8.5698×10^{-5}	3.33882×10^{-4}	0.001419157
$\delta = 10\%$	$\varepsilon_1(p)$	0.1545	0.1738	0.2436	0.5296	1.6159
	$\varepsilon_2(p)$	0.0634	0.0633	0.0662	0.0721	0.0812
	$\varepsilon_3(p)$	2.1600×10^{-6}	1.9334×10^{-5}	8.6232×10^{-5}	3.51023×10^{-4}	0.002105562
$\delta = 15\%$	$\varepsilon_1(p)$	0.2322	0.2611	0.3658	0.7948	2.4241
	$\varepsilon_2(p)$	0.0952	0.0943	0.0948	0.0721	0.1248
	$\varepsilon_3(p)$	2.1660×10^{-6}	1.9356×10^{-5}	8.6557×10^{-5}	3.96662×10^{-4}	0.002444287

Table 3: Comparison approximation solutions of Example 2 with the literature for various x^*.

x^*	$\varepsilon_1(p)$	$\varepsilon_2(p)$	$\varepsilon_3(p)$
0.1	1.0010	0.1801	1.024501×10^{-3}
0.2	0.9047	0.0661	8.97953×10^{-4}
0.3	0.9197	0.0767	8.03529×10^{-4}
0.4	0.9323	0.0694	7.96885×10^{-4}
0.5	0.9222	0.0839	7.50627×10^{-4}
0.6	0.9071	0.0761	7.92723×10^{-4}
0.7	0.9147	0.1026	7.78528×10^{-4}
0.8	0.9256	0.0974	7.55676×10^{-4}

Example 3. We test a none-smooth problem corresponding to (1)-(3), with $\phi(x) = u(x,0) = \sin(2\pi x)$, $k_0(t) = u(0,t) = 0$, $k_1(t) = u(1,t) = 0$, $f(x) = x^2$, and

$$p(t) = \begin{cases} 2t + \alpha, & t \in [0, 0.5], \\ -2t + 2 + \alpha, & t \in (0.5, 1]. \end{cases}$$

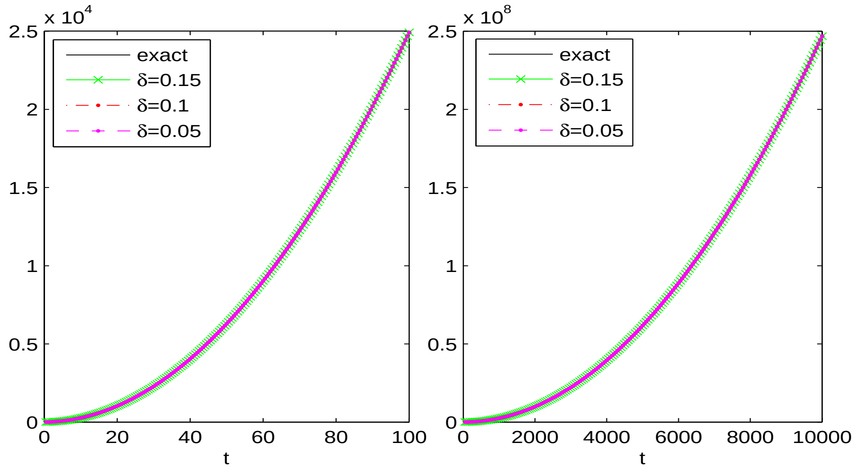

Figure 4: Numerical approximations to p for Example 2 for $T = 100$ (left) and $T = 10000$ (right).

Since the exact solution of this problem is not accessible, we first solve a direct problem using a suitable LDG method to obtain the input data g then we solve the inverse problem using our method. In [28], the direct problem has been solved by using an implicit finite difference (FD) method but since p is not a smooth function we expect to have a none-smooth solution and we decided to solve the direct problem using a LDG method too. We have to point out that since in our method we face the sparse systems, the computational complexity of both methods, i.e., FD and LDG is almost equal. p_h^n for $\alpha = 0.5,\ 0.95$ with noise levels $\delta = 5\%,\ 10\%,\ 15\%$ are presented in Fig 5. Without applying any regularization methods, our results are in good agreement with the results of [28]. The corresponding relative root mean square errors are $\varepsilon(p) = 3.8300 \times 10^{-7},\ 6.2300 \times 10^{-7},\ 9.4800 \times 10^{-7}$ for $\alpha = 0.5$ and $\varepsilon(p) = 1.03320 \times 10^{-4},\ 2.33279 \times 10^{-4},\ 1.03320 \times 10^{-4}$ for $\alpha = 0.95$, which are considerably better than reported in [28].

Example 4. We test a discontinuous problem corresponding to (1)-(3), with $\phi(x) = u(x, 0) = \sin(2\pi x)$, $k_0(t) = u(0, t) = 0$, $k_1(t) = u(1, t) = 0$, $f(x) = x^2$, and

$$p(t) = \begin{cases} 1,\ t \in [0.25, 0.75], \\ 0,\ t \in [0, 0.25) \cup (0.75, 1]. \end{cases}$$

Since the exact solution of this problem is not accessible, we first solve a direct problem using a suitable LDG method to obtain the input data g then we solve the inverse problem using our method. In [28], the direct problem has been solved by using an implicit finite difference method but since p is not a continuous function we expect to have a discontinuous solution and we decided to solve the direct problem using a LDG method too. We

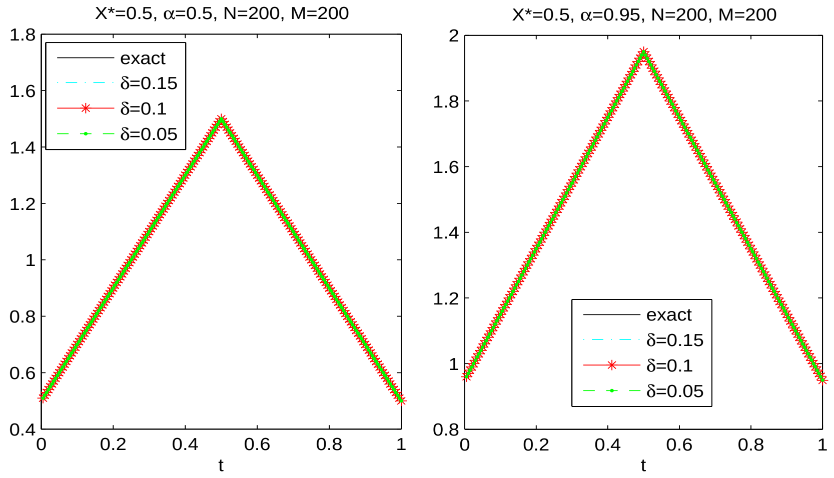

Figure 5: Numerical approximations to p for Example 3 with various α.

have to point out that since in our method we face the sparse systems, the computational complexity of both methods, i.e., FD and LDG is almost equal. p_h^n for $\alpha = 0.5,\ 0.95$ with noise levels $\delta = 5\%,\ 10\%,\ 15\%$ are plotted in Fig 6. Without applying any regularization methods, our results are in good agreement with the results of [28]. The corresponding relative root mean square errors are $\varepsilon(p) = 4.1200 \times 10^{-7},\ 6.2300 \times 10^{-7},\ 8.2700 \times 10^{-7}$ for $\alpha = 0.5$ and $\varepsilon(p) = 8.8388 \times 10^{-5},\ 1.61535 \times 10^{-4},\ 2.58527 \times 10^{-4}$ for $\alpha = 0.95$, which are considerably better than reported in [28].

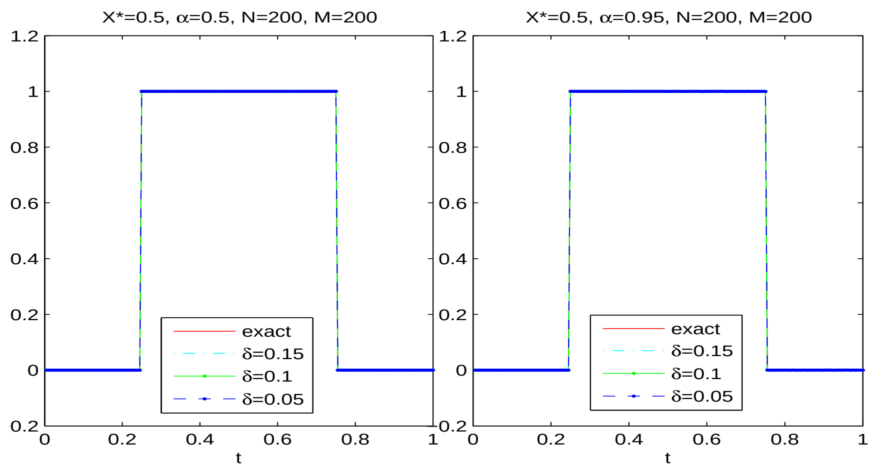

Figure 6: Numerical approximations to p for Example 4 with various α.

5 Conclusion

In this paper, an inverse source problem for the time-fractional diffusion equation was solved numerically by using a local discontinuous Galerkin method. In fact, we could extend a fully-discrete LDG finite element method for solving a class of time-fractional inverse problem. By applying this method without using any regularization methods, we could obtain stable and accurate numerical approximations to the time-dependent source term using an additional data in an interior measurement location. The numerical stability and convergence of the proposed method have been investigated and theoretically proven. Various numerical examples with smooth or none-smooth data and maybe solutions have been verified to demonstrate the effectiveness and robustness of the proposed method. This outstanding and promising method can be further applied to another one-dimensional or higher dimensional inverse problems which can be considered for the future works.

References

1. Cheng, J., Nakagawa, J., Yamamoto, M. and Yamazaki, T. *Uniqueness in an inverse problem for a one-dimensional fractional diffusion equation*, Inverse Probl, 25 (11) (2009), 115002.

2. Cockburn, B., Kanschat, G., Perugia, I. and Schotzau, D. *Superconvergence of the local discontinuous Galerkin method for elliptic problems on cartesian grids*, SIAM J. Numer. Anal, 39 (2001), 264-285.

3. Cockburn, B. and Shu, C.W. *The Runge-Kutta discontinuous Galerkin method for conservation laws, V: multidimensional systems*, J. Comput. Phys, 141 (1998), 199-224.

4. Cockburn, B. and Shu, C.W. *The local discontinuous Galerkin method for time-dependent convection-diffusion systems*, SIAM J. Numer. Anal, 35 (1998), 2440-2463.

5. Deng, W.H. *Finite element method for the space and time fractional Fokker-Planck equation*, SIAM J. Numer. Anal, 47 (2008), 204-226.

6. Deng, W.H. and Hesthaven, J.S. *Local discontinuous Galerkin methods for fractional diffusion equations*, Math. Modelling Numer. Anal, 47 (2013), 1845-1864.

7. Dou, F.F. and Hon, Y.C. *Kernel-based approximation for Cauchy problem of the time-fractional diffusion equation*, Eng. Anal. Boundary Elem, 36 (2012), 1344-1352.

8. Dou, F.F. and Hon, Y.C. *Numerical computation for backward time-fractional diffusion equation*, Eng. Anal. Boundary Elem, 40 (2014), 138-146.

9. Jiang, Y.J. and Ma, J.T. *High-order finite element methods for time-fractional partial differential equations*, J. Comput. Appl. Math, 235 (2011), 3285-3290.

10. Jin, B.T. and Rundell, W. *An inverse problem for a one-dimensional time-fractional diffusion problem*, Inverse Probl, 28 (7) (2012), 075010.

11. Li, C.Z. and Chen, Y. *Numerical approximation of nonlinear fractional differential equations with subdiffusion and superdiffusion*, Comput. Math. Appl, 62 (2011), 855-875.

12. Lin, Y.M. and Xu, C.J. *Finite difference/spectral approximations for the time-fractional diffusion equation*, J. Comput. Phys, 225 (2007), 1533-1552.

13. Liu, J.J. and Yamamoto, M. *A backward problem for the time-fractional diffusion equation*, Appl. Anal, 89 (2010), 1769-1788.

14. Liu, Y., Zhang, M., Li, H., Li, J. *High-order local discontinuous Galerkin method combined with WSGD-approximation for a fractional subdiffusion equation*, Comput. Math. Appl, 73 (2017), 1298-1314.

15. Metzler, R., Glöckle, W.G. and Nonnenmacher, T.F. *Fractional model equation for anomalous diffusion*, Physica A, 211 (1994), 13-24.

16. Mohammadi, M., Mokhtari, R. and Panahipour, H. *Solving two parabolic inverse problems with a nonlocal boundary condition in the reproducing kernel space*, Appl. Comput. Math, 13 (2014), 91-106.

17. Mohammadi, M., Mokhtari, R. and Toutian, F. *Solving an inverse problem for a parabolic equation with a nonlocal boundary condition in the reproducing kernel space*, Iranian J. Numer. Anal. Optimization, 4 (2014), 57-76.

18. Murio, D.A. *Stable numerical solution of a fractional-diffusion inverse heat conduction problem*, Comput. Math. Appl, 53 (2007), 1492-1501.

19. Murio, D.A. *Time fractional IHCP with Caputo fractional derivatives*, Comput. Math. Appl, 56 (2008), 2371-2381.

20. Murio, D.A. *Stable numerical evaluation of Grünwald-Letnikov fractional derivatives applied to a fractional IHCP*, Inverse Probl. Sci. Eng, 17 (2009), 229-243.

21. Pourgholi, R. , Esfahani, A., Abtahi, M. *A numerical solution of a two-dimensional IHCP*, J. Appl. Math. Comput, 41 (2013), 61-79.

22. Qian, Z. *Optimal modified method for a fractional-diffusion inverse heat conduction problem*, Inverse Probl. Sci. Eng, 18 (2010), 521-533.

23. Rashedi, K., Adibi, H., Dehghan. M. *Determination of space-time-dependent heat source in a parabolic inverse problem via the Ritz-Galerkin technique*, Inverse Probl. Sci. Eng, 22 (2014), 1077-1108.

24. Sakamoto, K. and Yamamoto, M. *Initial value/boundary value problems for fractional diffusion-wave equations and applications to some inverse problems*, J. Math. Anal. Appl, 382 (2011), 426-447.

25. Tuan, V.K. *Inverse problem for fractional diffusion equation*, Fractional Calculus Appl. Anal, 14 (2011), 31-55.

26. Wang, T., Wang, Y.M. *A modified compact ADI method and its extrapolation for two-dimensional fractional subdiffusion equations*, J. Appl. Math. Comput, 52 (2016), 439-476.

27. Wei, T. and Wang, J.G. *A modified quasi-boundary value method for an inverse source problem of the time-fractional diffusion equation*, Appl. Numer. Math, 78 (2014), 95-111.

28. Wei, T. and Zhang, Z.Q. *Reconstruction of a time-dependent source term in a time-fractional diffusion equation*, Eng. Anal. Boundary Elem, 37 (2013), 23-31.

29. Wei, T., Zhang, Z.Q. *Stable numerical solution to a Cauchy problem for a time fractional diffusion equation*, Eng. Anal. Boundary Elem, 40 (2014), 128-137.

30. Xu, Q. and Hesthaven, J.S. *Discontinuous Galerkin method for fractional convection-diffusion equations*, To appear in SIAM J. Numer. Anal

31. Xu, Y. and Shu, C.W. *Local Discontinuous Galerkin method for the Camassa-Holm equation*, 46 (2008), 1998-2021.

32. Yeganeh, S., Mokhtari, R., Hesthaven, J.S. *Space-dependent source determination in a time-fractional diffusion equation using a local discontinuous Galerkin method*, BIT Numer Math, DOI 10.1007/s10543-017-0648-y.

33. Zhang, Y. and Xu, X. *Inverse source problem for a fractional diffusion equation*, Inverse Probl, 27 (3) (2011), 035010.

34. Zheng, G.H. and Wei, T. *Spectral regularization method for a Cauchy problem of the time fractional advection-dispersion equation*, J. Comput. Appl. Math, 233 (2010), 2631-2640.

35. Zheng, G.H. and Wei, T. *A new regularization method for Cauchy problem of the fractional diffusion equation*, Adv. Comput. Math, 36 (2012), 377-398.

Persian Translation of Abstracts

بزرگ نمایی تصویر توسط رویه‌های کم‌ترین مربعات

علی‌محمد اسمعیلی‌زینی[۱] ، *قاسم برید لقمانی*[۲] و *علی‌محمد لطیف*[۳]

[۱] دانشگاه یزد، پردیس علوم، دانشکده علوم ریاضی
[۲] دانشگاه یزد، پردیس علوم، دانشکده علوم ریاضی
[۳] دانشگاه یزد، پردیس فنی و مهندسی، گروه مهندسی کامپیوتر

دریافت مقاله ۱۶ دی ۱۳۹۴، دریافت مقاله اصلاح شده ۲۴ مرداد ۱۳۹۵، پذیرش مقاله ۲۸ مهر ۱۳۹۵

چکیده : بزرگ نمایی تصویر یکی از مسائل موجود در زمینه پردازش تصویر است که مسئله اصلی در آن، حفظ کیفیت و ساختار تصویر بزرگ نمایی شده می‌باشد. در بزرگ نمایی لازم است که پیکسل های اضافی در اطلاعات تصویر قرار داده شود. اضافه کردن اطلاعات به تصویر باید با بافت موجود در تصویر سازگار باشد و بلوک های مصنوعی ایجاد نکند. در این پژوهش با استفاده از روش رویه‌های کم‌ترین مربعات، پیکسل های مورد نیاز تخمین زده می شوند و بر اساس الگوریتم پیشنهادی بهبود لبه، مجددا تمام پیکسل‌ها مورد بازنگری قرار می‌گیرند. روش پیشنهادی لبه‌ها را حفظ می‌کند و ماتی و مصنوعات بلوکی تصویر بزرگ‌نمایی‌شده را به حداقل می‌رساند. جهت سنجش توانایی این روش، نتایج حاصل بر روی چند تصویر با روش های دیگر توسط معیار PSNR و SSIM مورد مقایسه و ارزیابی قرار گرفته است. میانگین PSNR مربوط به تصویر اصلی و بزرگ‌نمایی شده ۷۹/۳۲ می‌باشد که نشان می‌دهد تصویر بزرگ‌نمایی شده به تصویر اصلی شباهت زیادی دارد. نتایج آزمایشات نشان می‌دهد روش پیشنهادی از کارائی بهتری نسبت به دیگر روش‌ها برخوردار است و تصویر با کیفیت مطلوب فراهم می‌کند.

کلمات کلیدی : بزرگ نمایی تصویر؛ رویه کم‌ترین مربعات؛ درونیابی.

روش توابع پایه شعاعی برای حل معادلات انتگرال فردهلم خطی سه بعدی روی دامنه های مکعبی

محسن اسماعیل بیگی، فرشید میرزایی و داود معظمی

دانشگاه ملایر، دانشکده علوم ریاضی و آمار، گروه ریاضی

دریافت مقاله ۱۸ آذر ۱۳۹۴، دریافت مقاله اصلاح شده ۱۴ شهریور ۱۳۹۵، پذیرش مقاله ۲۶ آبان ۱۳۹۵

چکیده : هدف اصلی این مقاله ارایه یک روش عددی کارآمد برای حل معادلات انتگرال فردهلم خطی از نوع دوم روی دامنه های سه بعدی مکعبی می باشد. روش ارایه شده بر اساس درونیاب توابع پایه شعاعی مبتنی بر نقاط و وزنهای گاوس لژاندر طراحی شده است. آنالیز خطا برای روش مدنظر بیان شده است. به کمک مثالهای عددی متنوع قابلیت و کارایی روش، مورد سنجش و ارزیابی قرار گرفته است.

کلمات کلیدی : معادلات انتگرال سه بعدی؛ توابع پایه شعاعی؛ روش هم محلی؛ دامنه های مکعبی.

فشرده‌سازی پروژه در مسئله زمانبندی پرداخت براساس پیشرفت پروژه

مرضیه مرتضوی نژاد ، حامد رضا طارقیان و زینب ساری

دانشگاه فردوسی مشهد، دانشکده علوم رياضي، گروه رياضي كاربردي

دریافت مقاله ۹ اردیبهشت ۱۳۹۴، دریافت مقاله اصلاح شده ۱۸ آبان ۱۳۹۴، پذیرش مقاله ۱۳ آذر ۱۳۹۵

چکیده : در این مقاله، دیدگاه جدیدی در زمینه زمانبندی پرداخت پروژه مطرح می‌شود. در این دیدگاه فعالیت‌های پروژه برای بیشینه کردن خالص ارزش جاری پیمانکار مجاز به فشرده‌سازی هستند. فرض می‌شود پرداخت به پیمانکار در پایان دوره‌های زمانی مشخص که به آن نقاط بازبینی گفته می‌شود، به ازای حجم کار انجام شده و هزینه‌ها در زمان اتمام فعالیت‌ها رخ دهند. دو رویکرد متفاوت برای تعیین حجم کار در نقاط بازبینی استفاده می‌شود. در رویکرد اول فعالیت‌هایی که در نقطه بازبینی به طور کامل تکمیل شده باشند، در نظر گرفته می‌شوند. در رویکرد دوم هر بخش از فعالیت‌هایی که اجرا شده‌اند، نیز در نظر گرفته می‌شوند. برای افزایش حجم کار در نقاط بازبینی، ممکن است پیمانکار تصمیم بگیرد برخی از فعالیت‌ها را برای افزایش خالص ارزش جاری خود فشرده کند. این در حالی است که هزینه‌های فشرده‌سازی توسط پیمانکار پرداخت می‌شود. براساس هر یك از رویکردها، دو مدل برنامه‌ریزی ریاضی یکی در حالتی که فعالیت‌ها در زمان عادی زمانبندی شوند و دیگری در حالتی که فعالیت‌ها امکان فشرده‌سازی داشته باشند، ارائه می‌شود. این مدل‌ها ابزاری برای تصمیم‌گیری بهتر پیمانکار درباره فشرده‌سازی فعالیت‌های پروژه هستند. نشان داده می‌شود که پیمانکار می‌تواند مقدارخالص ارزش جاری خود را با فشرده‌سازی فعالیت‌ها افزایش دهد حتی اگر هزینه‌های فشرده‌سازی را خود پیمانکار پرداخت کند. در پایان هر یك از مدل‌ها بر روی یك مثال پیاده‌سازی و نتایج حاصل تجزیه و تحلیل شده است.

کلمات کلیدی : زمانبندی پرداخت‌ها؛ پرداخت براساس پیشرفت پروژه؛ فشرده‌سازی پروژه؛ خالص ارزش جاری پیمانکار.

روش لاگرانژ بهبود یافته برای پیدا کردن جواب با کمترین نرم- ۱ دستگاه معادلات قدر مطلق

سعید کتابچی[۱] *و حسین موسایی*[۲]

[۱] دانشگاه گیلان، دانشکده علوم ریاضی، گروه ریاضی کاربردی
[۲] دانشگاه بجنورد، دانشکده علوم، گروه ریاضی

دریافت مقاله ۱۲ مرداد ۱۳۹۵، دریافت مقاله اصلاح شده ۸ دی ۱۳۹۵، پذیرش مقاله ۴ اسفند ۱۳۹۵

چکیده : دراین مقاله روش لاگرانژ بهبود یافته برای بدست آوردن جواب با کمترین نرم- ۱ دستگاه معادلات قدر مطلق (AEV) ارائه می شود. این روش منجر می شود به حل مساله مینیمم سازی نامقید با تابع هدفی که تنها یکبار مشتق پذیر است. روش شبه نیوتن را برای حل این مساله بهینه سازی نا مقید پیشنهاد می کنیم. محاسبات عددی، مبین دقت بالا در همگرایی با تعداد کم تکرار در اغلب محاسبات است.

کلمات کلیدی : دستگاه معادلات قدر مطلق؛ جواب کمترین نرم؛ روش نیوتن تعمیم یافته؛ روش لاگرانژ بهبود یافته.

مروری بر روش های رهایی پویا در سازه های مکانیکی
بخش اول : رابطه سازی ها

محمد رضایی پژند[۱] ، *جواد علامتیان*[۲] و *حسینه رضایی*[۳]

[۱] دانشگاه فردوسی مشهد، دانشکده مهندسی، گروه مهندسی عمران
[۲] دانشگاه آزاد اسلامی، واحد مشهد، گروه مهندسی عمران
[۲] دانشگاه فردوسی مشهد، دانشکده مهندسی، گروه مهندسی عمران

دریافت مقاله ۵ آذر ۱۳۹۵، دریافت مقاله اصلاح شده ۲۲ اسفند ۱۳۹۵، پذیرش مقاله ۳ اردیبهشت ۱۳۹۶

چکیده : در شصت سال گذشته، روش های رهایی پویا تحول های فراوانی یافته اند. در بیشتر زمان ها، این فرایند های صریح و تکراری برای حل معادله های خطی و ناخطی حاکم بر رفتار سازه ها به کار می روند. در بخش اول این مطالعه، رابطه سازی های معمول مرور می شوند. پایه های ریاضی و نیزمفهوم های فیزیکی به طور خلاصه شرح داده خواهند شد. سپس، شرح همه ی عامل های رهایی پویا، مانند: جرم ساختگی، میرایی ساختگی، گام زمانی ساختگی و حدس نخستین، می آیند. افزون بر این ها، به چگونگی حل مساله های سازه ها با شیوه های جنبشی و لزجی پرداخته می شود. سرانجام، روش های کنونی و راستاهای پژوهش آیندگان واکاوی می گردند. دربخش دوم، کاربردهای روش های رهایی پویا در رشته های مهندسی مرور خواهند شد. این موضوع، توانایی بالای فرایند رهایی پویا در حل مساله های مهندسی را آشکار می سازد.

کلمات کلیدی : روش های رهایی پویا؛ رابطه سازی؛ حل کننده؛ مرور؛ فن های تکراری.

مروری بر روش های رهایی پویا در سازه های مکانیکی
بخش دوم : کاربردها

محمد رضایی پژند[۱] ، *جواد علامتیان*[۲] و *حسینه رضایی*[۳]

[۱] دانشگاه فردوسی مشهد، دانشکده مهندسی، گروه مهندسی عمران
[۲] دانشگاه آزاد اسلامی، واحد مشهد، گروه مهندسی عمران
[۳] دانشگاه فردوسی مشهد، دانشکده مهندسی، گروه مهندسی عمران

دریافت مقاله ۵ آذر ۱۳۹۵، دریافت مقاله اصلاح شده ۲۲ اسفند ۱۳۹۵، پذیرش مقاله ۳ اردیبهشت ۱۳۹۶

چکیده : در این مقاله، پیشرفت های مهم در کاربردهای روش های رهایی پویا طی شصت سال گذشته در مهندسی سازه خلاصه می شوند. تاکید بر روی صفحه ها، شکل یابی، سازه های ریسمانی، واکاوی پویا و دیگرکاربردها خواهد بود. همچنین، نقش روش های رهایی پویا درتحلیل خطی و ناخطی آشکار می گردد. از سوی دیگر، این پژوهش به شرح شیوه های حل مساله های ایستایی، پویایی و پایداری می پردازد. به طور خلاصه، اثر این فن ها درتحلیل ماده های همگن، مرکب، سه سانگرد و لایه ای بررسی می گردند. افزون براین ها، پیرامون کاربردهای روش های رهایی پویا، تحلیل های کمانشی و پیشنهاد پژوهش های آیندگان سخن به میان می آید.

کلمات کلیدی : روش های رهایی پویا؛ کاربرد؛ مرور؛ حل کننده؛ فن های تکراری.

استفاده از یک روش LDG برای حل مساله منبع وارون از نوع معادله انتشار کسری-زمانی

سمیه یگانه، رضا مختاری و سمیه فولادی

دانشگاه صنعتی اصفهان، دانشکده علوم ریاضی

دریافت مقاله ۳ بهمن ۱۳۹۵، دریافت مقاله اصلاح شده ۹ فروردین ۱۳۹۶، پذیرش مقاله ۳ اردیبهشت ۱۳۹۵

چکیده : در این مقاله یك روش گالرکین ناپیوسته موضعی (LDG) را برای حل برخی مسائل وارون کسری به کار می بریم. در واقع جمله منبع وابسته به زمان را در یك مساله وارون از نوع معادله انتشار کسری-زمانی تعیین می‌کنیم. این روش بر اساس یك طرح تفاضل متناهی در زمان و یك روش (LDG) در مکان است. یک قضیه پایداری عددی به علاوه یك تخمین خطا مهیا می شود. در پایان، چند مثال عددی به منظور تائید نتایج نظری و نشان دادن اثربخشی روش، آزمایش می شوند. باید اشاره‌کرد‌که روش پیشنهادی بدون استفاده از روشهای منظم سازی‌که برای سایر روش های عددی در حل چنین مسائل وارون بدطرح ضروری هستند، تقریب های عددی پایدار و دقیقی را تولید می‌کند.

کلمات کلیدی : روش گالرکین ناپیوسته موضعی؛ مسئله منبع وارون؛ معادله انتشار کسری-زمانی.

Aims and scope

Iranian Journal of Numerical Analysis and Optimization (IJNAO) is published twice a year by the Department of Applied Mathematics, Faculty of Mathematical Sciences, Ferdowsi University of Mashhad. Papers dealing with different aspects of numerical analysis and optimization, theories and their applications in engineering and industry are considered for publication.

Journal Policy

After receiving an article, the editorial committee will assign referees. Refereeing process can be followed via the web site of the Journal.
The manuscripts are accepted for review with the understanding that the work has not been published and also it is not under consideration for publication by any other journal. All submissions should be accompanied by a written declaration signed by the author(s) that the paper has not been published before and has not been submitted for consideration elsewhere.

Instruction for Authors

The Journal publishes all papers in the fields of numerical analysis and optimization. Articles must be written in English.
All submitted papers will be refereed and the authors may be asked to revise their manuscripts according to the referee's reports. The Editorial Board of the Journal keeps the right to accept or reject the papers for publication.
The papers with more than one authors, should determine the corresponding author. The e-mail address of the corresponding author must appear at the end of the manuscript or as a footnote of the first page.
It is strongly recommended to set up the manuscript by Latex or Tex, using the template provided in the web site of the Journal. Manuscripts should be typed double-spaced with wide margins to provide enough room for editorial remarks.
References should be arranged in alphabetical order by the surname of the first author as examples below:
[1] Stoer, J. and Bulirsch, R. *Introduction to Numerical Analysis*, Springer-verlag, New York, 2002.
[2] Brunner, H. *A survey of recent advances in the numerical treatment of Volterra integral and integro-differential equations*, J. Comput. Appl. Math. 8 (1982), 213-229.

Submission of Manuscripts

Authors may submit their manuscripts by either of the following ways:

a) Online submission (pdf or dvi files) via the website of the Journal at:

http://ijnao.um.ac.ir

b) Via journal's email mjms@um.ac.ir

Copyright Agreement

Upon the acceptance of an article by the Journal, the corresponding author will be asked to sign a "Copyright Transfer Agreement" (see the web site) and send it to the Journal address. This will permit the publisher to publish and distribute the work.

Iranian Journal of Numerical Analysis and Optimization

Former : MRJMS

CONTENTS Vol. 7, No.2, pp 1-135, 2017

web site : http://ijnao.um.ac.ir

Email : mjms@um.ac.ir

ISSN : 2423-6977